

Doctoral dissertation

**Development of novel biochar adsorbent functionalized with
layered double hydroxides for phosphate removal
and its application potential as fertilizer**

リン除去のための層状複水酸化物を担持させたバイオ炭系
新規吸着材の開発とその肥料としての応用の可能性

September 2021

Jittrera Buates

Graduate School of Sciences and Technology for Innovation
Yamaguchi University

A dissertation submitted for the degree of Doctor of Engineering

Table of contents

List of figures.....	v
List of tables.....	vii
Acknowledgements.....	viii
Abstract.....	ix
Chapter 1 – Introduction.....	1
1.1 Background.....	1
1.2 Research objectives.....	3
1.3 Thesis structure.....	3
Chapter 2 – Literature review.....	5
2.1 The role and importance of phosphate.....	5
2.2 Sources of phosphate in wastewater.....	6
2.3 Phosphate treatment technologies.....	7
2.3.1 Biological phosphate removal.....	7
2.3.2 Chemical phosphate removal.....	10
2.3.3 Adsorption technique for phosphate removal.....	11
2.3.4 Cost comparison of phosphate treatment approaches.....	13
2.4 Biochar functionalized with layered double hydroxides for phosphate treatment.....	15
Chapter 3 – Biochar functionalized with layered double hydroxides composites prepared from different techniques and varying biochar quantities.....	20
3.1 Introduction.....	20
3.2 Materials and methods.....	21
3.2.1 Materials.....	21
3.2.2 Production of biochar.....	21
3.2.3 Preparation of BC-LDHs.....	22
3.2.4 Characterization of BC-LDHs.....	23
3.2.5 Phosphate adsorption experiments.....	23
3.3 Results and discussions.....	24
3.3.1 Characterization of BC-LDHs.....	24
3.3.2 Phosphate adsorption performance of BC-LDHs.....	30

3.4 Conclusions.....	32
Chapter 4 – Influence of various experimental parameters on phosphate adsorption	33
4.1 Introduction.....	33
4.2 Materials and methods	34
4.2.1 Materials	34
4.2.2 Effect of pH on phosphate adsorption	34
4.2.3 Effect of coexisting anions on phosphate adsorption	35
4.2.4 Adsorption kinetics and isotherms.....	35
4.3 Results and discussions.....	35
4.3.1 Effect of pH on phosphate adsorption	35
4.3.2 Effect of coexisting anions on phosphate adsorption	38
4.3.3 Adsorption kinetics	39
4.3.4 Adsorption isotherms	43
4.3.5 Adsorption mechanisms.....	46
4.4 Conclusions.....	51
Chapter 5 – Phosphate recovery from aqueous solution through adsorption-desorption cycles ..	52
5.1 Introduction.....	52
5.2 Materials and methods	53
5.2.1 Materials	53
5.2.2 Phosphate desorption and adsorbent regeneration.....	53
5.3 Results and discussions.....	54
5.3.1 Choice of desorbing solution	54
5.3.2 Regeneration of adsorbents.....	55
5.4 Conclusions.....	57
Chapter 6 – Potential use of biochar functionalized with layered double hydroxides after phosphate adsorption for seed germination.....	58
6.1 Introduction.....	58
6.2 Materials and methods	59
6.2.1 Materials	59
6.2.2 Characterization of fertilizers	59
6.2.3 Seed germination bioassay.....	60

6.2.4 Statistical analysis	61
6.3 Results and discussions.....	61
6.3.1 Characterization of fertilizers	61
6.3.2 Seed germination bioassay.....	64
6.4 Conclusions.....	74
Chapter 7 – Assessment of early plant growth performance for application of phosphate-loaded biochar functionalized with layered double hydroxides as fertilizer	75
7.1 Introduction.....	75
7.2 Materials and methods	75
7.2.1 Materials	75
7.2.2 Early plant growth experiments	76
7.2.3 Statistical analysis	76
7.3 Results and discussions.....	77
7.3.1 Effect of application rates of P-BC-LDHs 6 on early plant growth	77
7.3.2 Effect of application rates of P-LDHs on early plant growth	81
7.3.3 Comparison of plant growth performance derived from P-BC-LDH 6 and P-LDH treatments ..	85
7.4 Conclusions.....	86
Chapter 8 – Key summaries and recommendations.....	88
References.....	92
Appendices.....	106
Appendix A. Physicochemical characteristics of rice straw used in this study	106
Appendix B. Determination of optimal conditions for synthesis of BC-LDHs.....	107
Appendix C. List of equations used in the study	108

List of figures

Figure 1. Schematic overview of dissertation structure.....	4
Figure 2. Experimental outline of the present study.....	4
Figure 3. Simple process configuration of EBPR.....	8
Figure 4. Schematic illustration of metabolic processes of PAOs involved in EBPR.....	9
Figure 5. Schematic illustration of adsorption and desorption processes.....	12
Figure 6. Total cost for phosphate removal via different treatment methods.....	14
Figure 7. Schematic representation of LDH structure.....	16
Figure 8. Schematic diagram of pyrolysis system.....	22
Figure 9. XRD patterns of samples.....	24
Figure 10. SEM images and EDX elemental distribution mapping of samples.....	25
Figure 11. EDX spectrums of samples.....	26
Figure 12. Nitrogen adsorption-desorption isotherms of composites.....	29
Figure 13. Phosphate adsorption capacity of pure LDHs and BC-LDH composites.....	31
Figure 14. (a) Effect of initial pH on phosphate adsorption capacity of pure LDHs and BC-LDHs 6.....	36
(b) Effect of initial pH on final pH after adsorption process of pure LDHs and BC-LDHs 6.....	36
Figure 15. pH _{zpc} curve of pure LDHs and BC-LDHs 6.....	37
Figure 16. Effect of coexisting ions on phosphate adsorption by pure LDHs and BC-LDHs 6... ..	39
Figure 17. Adsorption kinetics for phosphate adsorption on samples.....	40
Figure 18. Intraparticle diffusion model for phosphate adsorption on pure LDHs and BC-LDHs 6.	43
Figure 19. Adsorption isotherms for phosphate adsorption on samples.....	44
Figure 20. XRD patterns of samples after adsorption.....	47
Figure 21. (a) TEM images of samples before adsorption (b) TEM images of samples after adsorption (c) SEM images of feedstock loaded with LDHs before and after pyrolysis process.....	48
Figure 22. EDX elemental distribution mapping of samples after adsorption.....	50
Figure 23. Schematic illustration of adsorption mechanisms on BC-LDHs 6.....	50
Figure 24. Effect of different concentrations of NaOH solution on phosphate desorption capacity of BC-LDHs 6 and pure LDHs.....	54
Figure 25. Phosphate adsorption and desorption profiles of BC-LDHs 6 and pure LDHs at different cycles of regeneration.....	56

Figure 26. Effect of P-BC-LDHs 6 applied at different rates on seed germination and growth parameters	65
Figure 27. Elemental composition of seedlings under different application rates of P-BC-LDHs 6.	66
Figure 28. Seeds germinated on day 5 under different concentrations of P-BC-LDHs 6	67
Figure 29. Effect of P-LDHs applied at different rates on seed germination and growth parameters	69
Figure 30. Negative effect of aluminum on seedling roots under P-LDH treatments	70
Figure 31. Elemental composition of seedlings under different application rates of P-LDHs	71
Figure 32. Seed responses under different concentrations of P-LDHs on the last day of germination.	72
Figure 33. Effect of P-BC-LDHs 6 at different dosages on growth parameters and elemental composition of lettuce from early plant growth experiments	79
Figure 34. Comparison of lettuce from the control and different treatments of P-BC-LDHs 6 ...	80
Figure 35. Effect of P-LDHs at different dosages on growth parameters and elemental composition of lettuce from early plant growth experiments	82
Figure 36. Comparison of lettuce plants among the control and different treatments of P-LDHs.	84

List of tables

Table 1. Textural properties of pure LDHs, pristine biochar, and BC-LDH composites	28
Table 2. Kinetic and isotherm parameters for phosphate adsorption.....	42
Table 3. Comparison of phosphate maximum adsorption capacity of various adsorbents.....	45
Table 4. Basic physical and chemical properties of P-BC-LDHs 6 and P-LDHs.....	62
Table 5. Comparison of plant growth performance from P-BC-LDH 6 and P-LDH treatments..	73
Table 6. Comparison of plant growth performance from P-BC-LDH 6 and P-LDH treatments..	85

Acknowledgements

I would like to express my deep and sincere gratitude to my advisor, Prof. Tsuyoshi Imai, for giving me the opportunity to undertake this research under his supervision and guidance. His immense knowledge and plentiful experience benefited me much in completion and success of this study. Additionally, his continuous support and encouragement have been invaluable through my academic journey.

I would also like to show my deepest gratitude to Prof. Tasuma Suzuki, who kindly assisted me with the specific surface area analysis in this dissertation. Moreover, with his profound knowledge of adsorption, he was always available for discussions on my research struggles. I am extremely thankful to him for sharing expertise and helpful guidance. My sincere gratitude also goes to Prof. Takaya Higuchi and Prof. Yoshihisa Sakata for kindly providing the necessary facilities used in this study.

My greatest appreciation extends to my committee members, including Prof. Masahiko Sekine, Prof. Takashi Saeki, Prof. Takaya Higuchi, and Prof. Tasuma Suzuki for generously offering their valuable time to serve on my committee. Their insightful comments and suggestions have made considerable contribution to completion of this research. I would also like to thank Prof. Koichi Yamamoto and Prof. Ariyo Kanno for their extensive discussions and useful comments in the English seminar course.

I would also like to acknowledge all of the staff and my colleagues from the Department of Environmental Engineering for helping me with the experimental work and creating a genuinely friendly atmosphere, which made working here more productive and enjoyable. Finally, I would also like to say a heartfelt thank you to my family for providing me with unfailing support and constant encouragement throughout my years of study in Japan. I am forever indebted to my dearest parents, my grandparents, and my sister for their unconditional love. Thank you all very much.

Abstract

The reduction of excessive discharge of phosphate into water bodies is a dominant theme to combat the critical eutrophication issue and requires the development of high-performance materials for effective phosphate treatment. In this study, rice straw was used as a raw material for the synthesis of biochar functionalized with layered double hydroxides (BC-LDHs) as efficacious phosphate adsorbents, and their successful synthesis was corroborated via characterization analysis. Experimental investigations, including pH, coexisting anion, reaction time, and initial phosphate concentration effects were systematically performed with selected BC-LDHs 6 and pure LDHs. An optimum pH of 3.0 was observed in both samples. Kinetic and isotherm studies indicated that phosphate adsorption on these samples was controlled by the pseudo-second-order model and the Freundlich model. Comparative kinetic tests also demonstrated that BC-LDHs 6 and pure LDHs reached the equilibrium within 24 h and 3 h, respectively. Nonetheless, the maximum adsorption capacity of the composite was 192 mg/g, which was higher than that of pure LDHs (166 mg/g). The coexistence of various anions negligibly affected the removal efficiency of the composite; however, fluoride was the most competitive anion for adsorption on pure LDHs. The adsorption mechanisms of the composite involved electrostatic interaction, inner-sphere complexation, pore diffusion, precipitation, and reconstruction. Furthermore, phosphate adsorbed on both materials could be easily recovered by 0.1 M NaOH solution owing to the displacement reaction between phosphate and hydroxyl ions. Additional evidence from reusability experiments exhibited that the composite could maintain its good adsorption performance even after three adsorption-desorption cycles. The transformation of BC-LDHs 6 after its usage in phosphate treatment (P-BC-LDHs 6) into a fertilizer was further explored by using seed germination and early growth assays of lettuce through a comparison with phosphate-loaded LDHs (P-LDHs). Lettuce seeds germinated in all P-BC-LDH 6 treatments showed undesirable growth characteristics compared with the controls, while total germination failure was observed under high concentrations of P-LDHs. In the latter experiments, the optimal application rates for plant growth were 2.5% for P-BC-LDHs 6 and 1.0% for P-LDHs. The considerably greater biomass development and length of lettuce were visible in samples delivered from P-BC-LDHs 6 compared to those from P-LDHs. The results obtained suggest that BC-LDHs 6 is a promising adsorbent for phosphate treatment and post-adsorption BC-LDHs 6 has the application potential to serve as a fertilizer for horticultural crop production.

Chapter 1 – Introduction

1.1 Background

Since a dramatic increase in global population growth imposes profound challenges of the fast-growing demand for agricultural products, there is a rising concern over the scarcity of non-renewable phosphate rock sources, which are the world's major supply for fertilizer production. At the same time, phosphate overloads in aquatic environments from industrial, agricultural, and domestic sources can cause undesirable eutrophication, which subsequently results in the serious decline of aquatic life and deterioration of water quality. Given these issues, the development of sustainable and affordable solutions for phosphate treatment and recovery requires urgent attention to ensure phosphate resource security and environmental protection.

Many phosphate remediation techniques are available, such as biological reduction, chemical precipitation, and adsorption. Among these available techniques, adsorption has been proven to be a successful approach with considerable advantages over other technologies owing to handling ease, cost efficiency, high performance, and reduced potential for harmful byproduct generation during operation [1,2]. In the adsorption process, it is particularly important to develop promising adsorbents with highly efficient, economical, and environmentally friendly characteristics for phosphate removal. To date, layered double hydroxides (LDHs), a class of synthetic anionic clays, have been the subject of considerable attention as a favorable candidate for phosphate adsorption. Considering the structure of LDHs, a stack of positively charged mixed metal hydroxide layers is intercalated by charge-balancing anions and water molecules [3]. The chemical formula of LDHs can be expressed as $[M^{2+}_{1-x}M^{3+}_x(OH)_2]^{x+}(A^{n-})_{x/n} \cdot mH_2O$, where M^{2+} and M^{3+} represent the divalent and trivalent cations, respectively; A^{n-} is the anion in the interlayer for charge compensation, and x is equal to the molar ratio of $M^{3+}/(M^{2+}+M^{3+})$ [4]. Although LDHs possess many remarkable properties, such as interlayer anion exchange and structural reconstruction, enabling enhanced accessibility to phosphate, one significant drawback leading to much inconvenience in practical applications is the difficulty of separating dispersed LDHs after remediation [5]. According to Yan et al. [6], to clearly separate LDHs from a phosphate solution, the suspension must be centrifuged at high speed and then filtered through a membrane, which requires significant time and energy.

As a possible solution, LDHs can be assembled on some carrier materials to further improve the density and dispersion of LDH particles. Biochar, a carbon-rich material produced from pyrolysis of biomass in an oxygen-limited environment, is suggested to be an interesting option, as it has multiple positive benefits. Biochar can be manufactured through affordable production with low energy requirements and a wide availability of raw materials, such as inexpensive agricultural residues and municipal solid waste materials [7]. The resultant biochar usually exhibits well developed porosity, a large surface area, and enriched surface functional groups due to the removal of moisture and volatile matter from the biomass [8]. Furthermore, the conversion of agricultural residues into biochar is a better approach for waste disposal compared to the traditional combustion or biomass burning, which can cause secondary pollution by releasing black carbon aerosols in the atmosphere and consequently harm human health [9]. Thus, biochar with a large surface area can be used as a support framework for LDHs, which can simultaneously reduce the aggregation of LDH particles and promote the pollutant accessibility into its porous structure. As stated above, biochar functionalized with layered double hydroxides (BC-LDHs) may be an attractive strategy for phosphate removal since it combines the outstanding properties of both LDHs and biochar, such as low cost, easy separation, excellent anion exchangeability, and non-toxicity. Moreover, the spent BC-LDHs can be recognized as a phosphate fertilizer providing environmentally safe disposal and nutrient recycling in agricultural fields.

Besides the fact that biochar becomes an important practice for phosphate remediation, the incredible textural characteristics as well as high concentrations of bioavailable nutrients contained in the biochar, such as carbon, nitrogen, hydrogen, and some trace elements, including potassium, calcium, sodium, and magnesium have been identified as the main reasons for the improvement in soil properties and crop productivity. Adekiya et al. [10] indicated that the reduced bulk density and increased porosity of biochar-treated soil was as a result of formation of macropores and rearrangement of soil particles induced by biochar addition. Moreover, the enhanced availability of nutrient supply in addition to the improved soil physical properties also aided the yield of vegetable crops in their study. Biochar as reported by Zhang et al. [11] had a significant effect on the bacterial community structure of acidic soil as the increased pH and organic matter, which were directly related to biochar application, were favored for bacterial growth. Likewise, there are a few studies reporting that LDHs have been used as an agrochemical or fertilizer because of their

potential in controlling herbicide and nutrient losses [12,13]. In this regard, BC-LDHs after phosphate reclamation were capable of being employed for the agricultural purposes, which will further support their possibility to boost food production. Indeed, both biochar and LDHs have been individually explored for their agricultural applications; however, the ability of BC-LDH composites to serve as fertilizers for plants has not been comprehensively studied. Hence, the present dissertation not only provides useful information for fabricating high-efficiency adsorbents for phosphate removal, but also gives new insights into the application potential of used BC-LDHs as a phosphate fertilizer.

1.2 Research objectives

The key goal of this study is to investigate the feasibility of BC-LDHs for effective phosphate removal and recovery from aqueous solutions. To do so, the assessment of several influencing parameters on phosphate adsorption characteristics, including solution pH, competing anions, reaction times, and initial concentrations of phosphate was accomplished. The maximum adsorption capacity and interaction mechanisms of the proposed composite with phosphate anions were evaluated in depth by considering the isotherm and kinetic models. The quantification of desorption amounts of phosphate for this composite was established consecutively. Moreover, in order to highlight the possibility of using the exhausted media at the end of life (after phosphate adsorption application) for further purposes, the phosphate-adsorbed composite was also examined for its performance in stimulating plant development with emphasis on plant responses to its various application rates.

1.3 Thesis structure

The present dissertation is divided into eight chapters as shown in Figure 1 and a brief description of contents of each chapter is as follows. Chapter 1 provides a general introduction of the present dissertation, including background, thesis objectives, and thesis structure. In Chapter 2, a detailed research background is provided. This chapter is devoted to severe problems of both phosphate resource shortage and eutrophication in aquatic systems. The current phosphate treatment technologies and applicability of BC-LDHs for phosphate removal are also discussed in this

chapter. Chapter 3 focuses on the development and characterization of BC-LDH composites. The influence of two alternative synthesis methods and different biochar contents on their adsorption performance was also assessed. In Chapter 4, various potential adsorption factors as well as adsorption kinetics and isotherms were performed for the selected adsorbents to describe their maximum adsorption capacity as well as relevant mechanisms in the phosphate adsorption process. Chapter 5 presents a detailed evaluation of regeneration and multiple application of adsorbents. Chapter 6 and 7 focus primarily on the reusability of adsorbents as agricultural fertilizers. The use of seed germination and early growth assays of lettuce was proposed in these two sections, where actual plant responses to the application of spent adsorbents and their optimal usage rates were revealed. Chapter 8 summarizes the major findings of this study, and recommendations for future research are also highlighted.

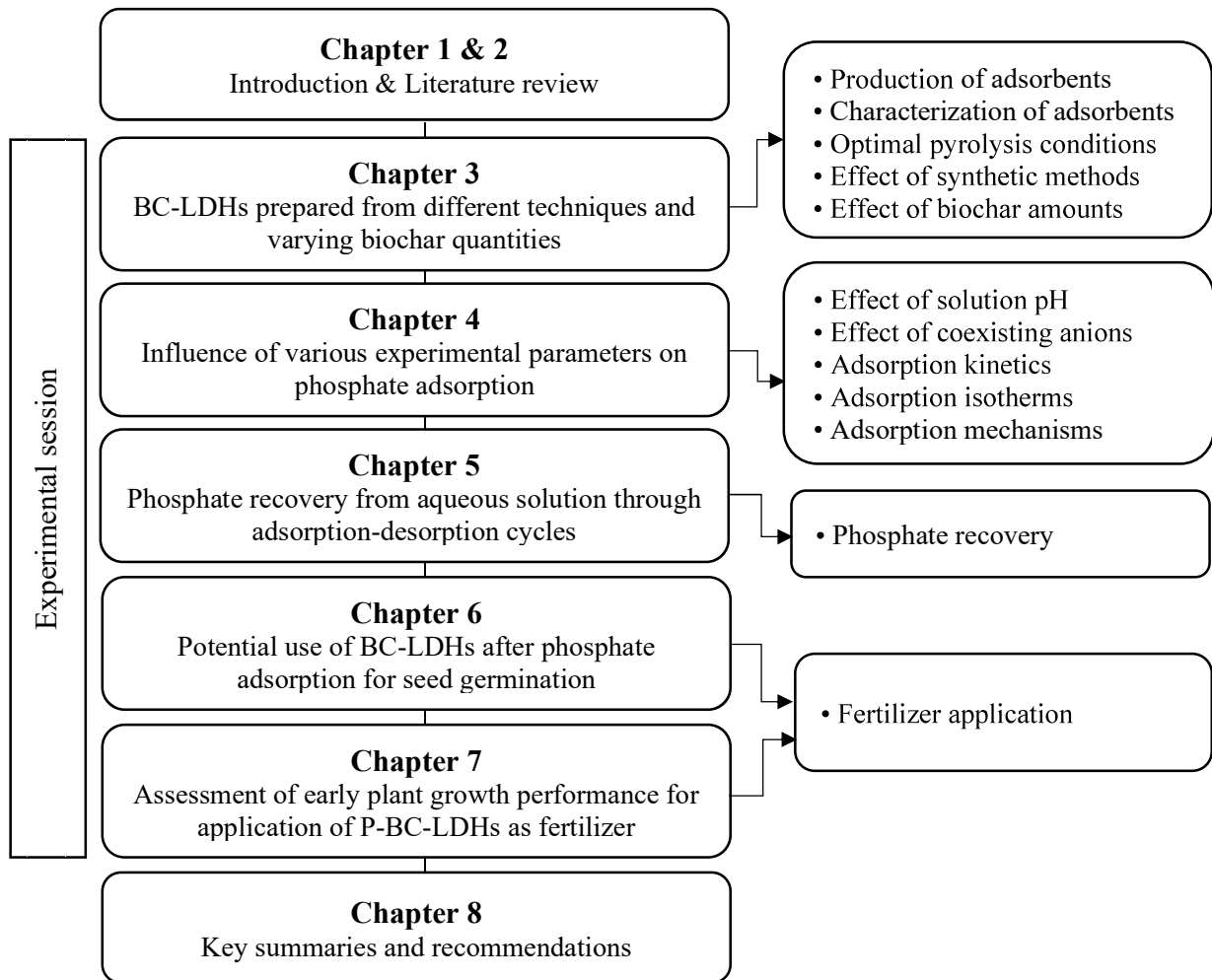


Figure 1. Schematic overview of dissertation structure

Chapter 2 – Literature review

2.1 The role and importance of phosphate

Phosphorus, in the form of phosphate, is a vital element required for the development of all living organisms, including in energy metabolism (ADP and ATP), membranes, structural support (teeth and bones), genetic components, and photosynthesis process for plants [14]. Phosphorus is also a primary constituent of agricultural fertilizers, which are usually derived from non-renewable natural phosphate rock. In a world, where the present population of 7.7 billion is expected to reach between 9.4 and 10.2 billion by 2050 [15], ensuring the future of food security is one of the fundamental priority, becoming a substantial challenge for humanity. At the same time, it has been estimated that the global phosphorus supply from this phosphate resource could peak as soon as 2033, after which the demand will inevitably outstrip the supply, causing the accessibility of phosphate reserves in the near future being limited [16]. Against this global background, there is no substitute for phosphate in food production, which means that even if all other conditions and nutrients are plentiful, only phosphate can make crops thrive [17]. Meanwhile, a substantial amount of phosphate has been discharged into aquatic environments that can promote the extreme production of photosynthetic aquatic microorganisms and eventually contributes to undesirable eutrophication.

Eutrophication is defined as the enrichment of water bodies with surplus nutrients, principally phosphate, leading to enhanced aquatic vegetation growth and algae blooms. Such excess nutrient accumulation has emerged as one of the most widespread environmental problems in the whole world since a rapid expansion of this problem has been accelerated by the anthropogenic practices, such as the intensive industrial and agricultural activities, inefficient or nonexistent wastewater treatment, and increase in aquaculture. There is no clear consensus on phosphorus concentration, which is accepted for the eutrophication prevention; however, most studies state that the phosphorus concentration as low as 0.1 mg/L is considered at a high risk of eutrophication, contributing to the nuisance algal blooms [18–21]. When freshwater bodies are richly supplied with phosphate nutrient, a subsequent well-established community of algae and aquatic plants has contributed to a thick layer of green scum on the water surface, which can shade out any aquatic

plants at the bottom of water layer. Once the algal organisms die, an excessive consumption of oxygen is required for bacterial degradation of their biomass, and thereby this condition of the absence of oxygen will eventually result in the deterioration of water quality and suffocation of aquatic creatures. Various common consequences of eutrophication include creation of dense algal blooms, tremendous organic and inorganic material accumulation, lower biodiversity, high turbidity, excessive sedimentation, and formation of hypoxic and mostly anoxic conditions, particularly in the deeper parts of water bodies [22].

Phosphate is regarded as the limiting nutrient in aquatic ecosystems, meaning that the available quantity of this nutrient controls the biological productivity of such systems. Phosphate is essential for maintaining natural biological communities and ecosystem functions in aquatic environments. Those aquatic plants and algae would not be able to grow without phosphate. The elevated concentration of phosphate exceeding its desirable limit, by contrast, can cause a tremendous increase in algal overdevelopment periodically [23]. Therefore, the legislation concerning about the control of phosphate discharge from wastewater treatment plants into surrounding environments has been exclusively applied. The average total phosphorus concentration in raw municipal wastewater is usually within the range between 7 and 10 mg/L; however, the United States Environmental Protection Agency (US EPA) introduces a strict regulation aiming to restrict the total phosphorus concentration of less than 0.01 mg/L in lakes and reservoirs [24]. Meanwhile, the World Health Organization (WHO) recommends a maximum discharge limit of phosphorus of 0.5 to 1.0 mg/L [25,26]. Consequently, diverse technological approaches for phosphate remediation from domestic and industrial wastewater have been continuously developed in response to the need to meet the stringent acceptable effluent standard and alleviate the adverse effects of phosphate. Considering the risk of running out of phosphate resources, some cases have also been implemented with the aim of recovering phosphate from waste streams.

2.2 Sources of phosphate in wastewater

Phosphate in municipal wastewater originates from many sources as follows: (a) fecal and waste materials, (b) synthetic detergents and household cleaning products, and (c) industrial and commercial uses. The contribution of phosphate pollution to municipal discharge significantly

derives from domestic sources, especially in densely populated countries. It was estimated that in the United States of America, phosphate loads from human excreta, laundry detergents, and other household cleaners were 0.6, 0.3, and 0.1 kg P/capita/year, respectively, while phosphate from the industrial and commercial sources was highly variable. Moreover, orthophosphate is the primary compound of phosphate in the wastewater dominating on other phosphate forms, namely, condensed phosphate and organic phosphate [27].

2.3 Phosphate treatment technologies

As phosphate present in wastewater is usually in the soluble form, the traditional phosphate elimination process in wastewater treatment facilities is based on the conversion of this dissolved phosphate into a solid phase, which can then be removed by solid-liquid separation techniques. The relevant basic phosphate treatment technologies are reviewed in more detail below.

2.3.1 Biological phosphate removal

The enhanced biological phosphate removal (EBPR) is a microbial process relying on polyphosphate accumulating organisms (PAOs) to accumulate phosphate in the form of polyphosphate in excess of their growth requirement for the phosphate removal enhancement. PAOs are able to store phosphate with proportions to the total dry biomass weight in the range of 4 to 15%, which is much higher than that of 2% of general microorganisms [28]. In EBPR, phosphate treatment can be attained through continuous recycling of the microbial biomass in anaerobic and aerobic zones to achieve a selection of microorganisms with high capacity to accumulate polyphosphate intracellularly in the aerobic period [29]. The simple process configuration of EBPR is represented in Figure 2.

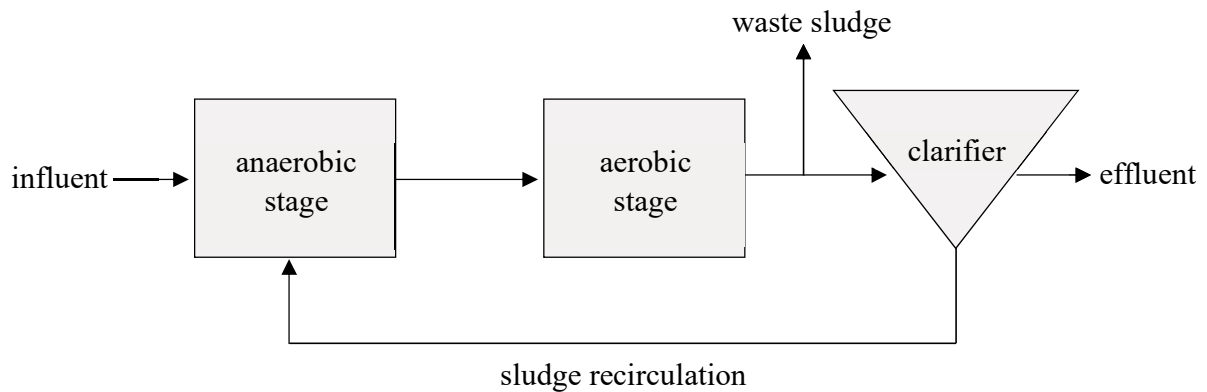


Figure 2. Simple process configuration of EBPR

Under the anaerobic condition, PAOs take up carbon sources, mainly in the form of volatile fatty acids (VFAs), from the influent and store them internally as poly- β -hydroxyalkanoates (PHAs) within their cells [30–32]. Such ability of PAOs to store organic carbon during this anaerobic phase allows them to gain a competitive advantage over other organisms. PAOs require energy and reducing power, which are generally generated by hydrolysis of intracellular polyphosphate and subsequent release of orthophosphate from their cells into wastewater, for the uptake of VFAs and formation of PHAs [31,32]. Furthermore, the combination of both glycolysis of stored glycogen and tricarboxylic acid (TCA) cycle has also been proposed as the major energy-yielding metabolic pathway in PAOs [33]. The phenomena during the anaerobic stage contribute to the reduction of BOD and the increase of phosphate in wastewater. In contrast, in the successive aerobic period, the released phosphate is taken back into PAO cells and stored in the form of polyphosphate, resulting in the decrease of phosphate concentration in wastewater [30–33]. The energy required for phosphate uptake can be obtained from the oxidation of organic reserve material (PHAs) using oxygen, and in some cases, nitrate or nitrite is used as an electron acceptor instead of oxygen [31]. PHAs are also assimilated as carbon and energy sources for glycogen replenishment and cell growth. The increased population of PAOs leads to the amounts of phosphate taken up from the aerobic period being far higher than phosphate excretion in the anaerobic phase. Also, the withdrawal of residue activated sludge containing high phosphate aids the phosphate removal from wastewater [29–32]. The schematic description of EBPR mechanism is illustrated in Figure 3.

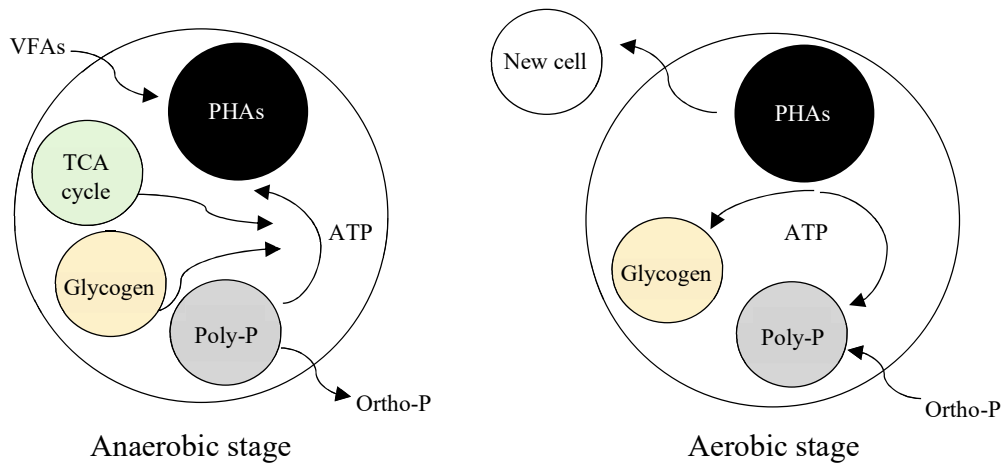


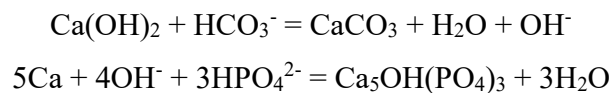
Figure 3. Schematic illustration of metabolic processes of PAOs involved in EBPR

Since the operation of EBPR is based on exploitation of metabolic activity of naturally occurring microorganisms for remediating phosphate, the integration of EBPR into the conventional wastewater treatment scheme is regarded as an environmentally-friendly and cost-effective means, allowing the elimination of chemical consumption for phosphate precipitation [34]. Further, the reduced chemical content of sludge would improve its quality for some purposes, such as land disposal and fertilizer value [35]. Unfortunately, the efficiency of EBPR is frequently hindered by its complicated system and operational constraints. The appearance of glycogen accumulating organisms (GAOs), for instance, has been reported to be the main reason to deteriorate the EBPR performance. GAOs utilize a similar metabolism to PAOs that they are also capable of storing VFAs as PHAs under the anaerobic condition. On the other hand, GAOs do not accumulate polyphosphate, but instead the intracellular glycogen will be used to provide energy and carbon sources for the VFA uptake [36]. Under the EBPR system, GAOs are therefore the undesirable microorganisms as they can compete with PAOs for available substrates in the anaerobic phase of EBPR that potentially leads to the unachievable phosphate removal.

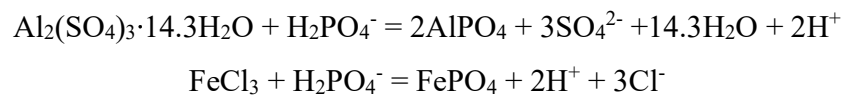
2.3.2 Chemical phosphate removal

Chemical phosphate removal in wastewater treatment typically involves the chemical addition, particularly divalent and trivalent metal salts, for precipitating phosphate in wastewater and the resultant solid residuals will be withdrawn from the system by either gravitational sedimentation or filtration. Those multivalent metal ions employed for phosphate precipitation are commonly calcium, aluminum, and iron.

Most phosphate precipitation from wastewater has been frequently conducted by the addition of lime (calcium hydroxide ($\text{Ca}(\text{OH})_2$)) as well as the pH adjustment of waste stream to at least 10.5 to obtain low dissolved phosphate residuals [37]. As phosphate precipitation process using calcium has been carried out at high pH value, the quantity of lime required for attaining the desired phosphate removal depends on the alkalinity and the amount of phosphate present in the wastewater. Lime can interact with natural alkalinity in wastewater in the form of bicarbonate ions and the insoluble calcium carbonate (CaCO_3) will be formed. With the pH continuing to increase, the interaction between abundant calcium ions and phosphate results in hydroxyapatite formation ($\text{Ca}_5\text{OH}(\text{PO}_4)_3$) that allows the precipitation of phosphate from the wastewater. The chemical equations for this reaction are shown below [38].



Other general chemicals used as coagulants are aluminum sulfate and ferric chloride. The mechanism for phosphate removal by these substances also obeys the interaction of dissolved cations and phosphate to form precipitates, which are subsequently removed as sludge. The following equations represent the phosphate reaction with either aluminum sulfate or ferric chloride [31].



The ratio of metal to phosphorus plays an important role for the phosphate removal efficiency by this salt addition technique. The higher the ratio of metal to phosphorus, the better is the improvement in phosphate elimination. However, the optimal chemical dosage is considered vital to ensure the environmental and economical sustainability. It has been reported previously that the excellent phosphate capture performance can be achieved with the Al/P ratio of 1.5, while the similar optimal ratio of Fe/P of 1.48 is observed for the precipitation using iron because of its same valence as aluminum [39]. Furthermore, the suitable pH range for high phosphate removal by these two coagulants is between 4 to 6. Even though the chemical precipitation has been shown to be an effectual treatment alternative, offering many advantages, such as flexible and convenient operating system with low maintenance, requiring only the replenishment of chemicals used, a major concern of this method is an extremely high volume of sludge production [40]. Such solid materials generated during the wastewater treatment process also contain significant quantities of unwanted chemical pollutants, which should be properly handled and disposed, otherwise these would create considerable health problems. The sludge treatment and disposal are seriously considered as the costliest operations in wastewater treatment plants [41].

2.3.3 Adsorption technique for phosphate removal

Apart from the biological and chemical processes mentioned above, adsorption has been proposed as an attractive technology allowing high-efficiency phosphate removal and, simultaneously, enabling phosphate recovery in a ready-to-use form. Adsorption includes, in general, the transfer of atoms, ions, or molecules from a fluid phase onto the surface of a solid phase. It differs from absorption, by which a fluid penetrates the entire volume of a material [42]. In the wastewater treatment system, pollutants are able to be removed from aqueous solution by solid materials, which provide surfaces for the adsorption reaction (Figure 4). The basic terms used to describe such materials as well as adsorbed species are adsorbents and adsorbates, respectively. In addition, the reverse process of adsorption, whereby the adsorbates are released from the surfaces of adsorbents is named desorption.

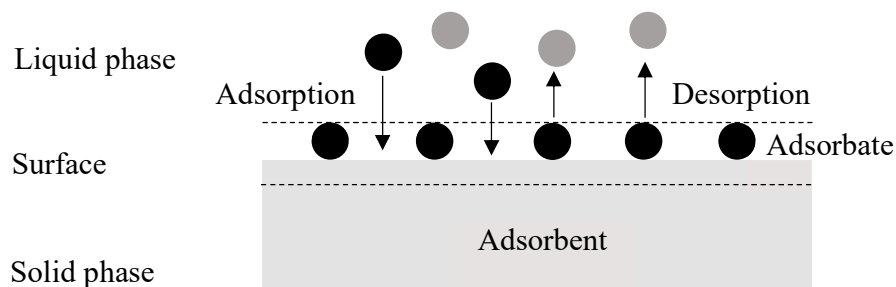


Figure 4. Schematic illustration of adsorption and desorption processes [42]

Since the adsorption process is directly related to the surfaces of adsorbents, a series of materials, which is frequently employed for the adsorption-based purification of phosphate, includes both porous materials (such as activated carbon and zeolite) and metal oxides (such as aluminum oxide and ferric oxide) [38,43]. An unrivaled combination of surface area and pore volume of porous products has been identified as the main reason for their favorable phosphate removal. For example, a very high surface area in excess of 1,000 m²/g of granular activated carbon is proportional to its high adsorption capacity and these materials have been sometimes used for coating with ferric oxide nanoparticles to enhance the phosphate adsorption [44]. Conversely, anion exchange taking place between phosphate and hydroxyl groups of solid surfaces is the predominant mechanism for the adsorption onto the latter materials [43]. Due to high cost of these widely used adsorbents, intensive attention has recently been directed toward naturally occurring and abundantly available resources for the manufacture of adsorbents. Biochar, for instance, has been recognized as one of the potential alternatives for phosphate removal application because there are various agricultural biomass residues and municipal solid wastes, which can be applied for its production. Moreover, the interesting features of biochar, such as large surface area, abundant pores, and rich functional groups have made it popular among researchers.

In comparison to other treatment techniques, adsorption has often been reported for achieving a very low phosphorus concentration of less than 0.1 mg/L or even lower than 0.01 mg/L [44–46]. Contrarily, the use of EBPR can decrease effluent levels of phosphorus to approximately 0.1 to 0.2 mg/L under ideal conditions; however, the optimal performance of microalgae in this EBPR

system relies significantly on varied environmental and operational parameters, such that the ideal conditions are rather narrow and this biological treatment scheme is known to be inconsistent in attaining the advanced phosphate removal [29,47]. On the other hand, effluents from chemical precipitation with metal salts usually possess phosphorus levels between 0.5 and 1 mg/L depending on the chemical dosage added, and reducing the residual phosphorus further by increasing chemicals consequently contributes to enormous sludge production [44,48]. Therefore, application of a combination method, where a lower phosphorus concentration of less than 0.015 mg/L is reached by both chemical precipitation and a series of sand filtration as well as ultra-filtration units, is required [45]. For this reason, adsorption technique outperforms other established phosphate removal technologies as it is proven to effectually remediate phosphate with minimum wastes produced and less reliance on the ideal conditions. In addition to direct interest in the phosphate purification, adsorption also facilitates the possibility to recover phosphate by regeneration of adsorbents, leading to a circular economy [44].

2.3.4 Cost comparison of phosphate treatment approaches

As stated earlier, the three technologies, namely EBPR, chemical precipitation, and adsorption, have the most widespread use among the established phosphate removal approaches. However, the data from the above section shows that adsorption is generally considered as a successful treatment scheme to reduce phosphate concentration levels to lower than either 0.1 mg P/L or 0.01 mg P/L with advantages of minimal waste generation and recovery option. With further focusing on cost effectiveness, comparison of phosphate reduction technologies in terms of the economic advantage is additionally discussed in this chapter.

In the study of Kumar et al. [44], total cost, which was evaluated based on a summation of the operational cost and capital cost, for phosphate purification through different treatment methods was compared as demonstrated in Figure 5. The other cost for handling sludge generation was not considered in this calculation. The specific four technologies established for such comparison were as follows:

- Microalgae: Estimated cost was based on biological phosphate uptake by microalgae to decrease phosphate concentration to up to 0.15 mg P/L.
- Actiflo: In this system, phosphate is first removed by chemical precipitation with iron salts. The resulting flocs are ballasted with microsand in the presence of polymer. After providing sufficient time in a mixing tank, water is passed onto a clarifier, which further removes the microsand along with those flocs. The effluent concentration of 0.17 mg P/L could be achieved.
- Phoslock: Phoslock is the commercial name for a lanthanum modified bentonite, which captures phosphate anions by forming lanthanum phosphate precipitates. Cost evaluation for this method was based on the price of Phoslock (2,750 €/ton) and its average removal capacity of 9 mg P/g to reduce phosphate concentration to less than 0.05 mg P/L.
- Adsorption using porous metal oxides: Cost estimation included phosphate reduction to the concentration levels ranging from 1 to 0.1 mg P/L (denoted as Ad-0.1) and 1 to 0.016 mg P/L (denoted as Ad-0.016).

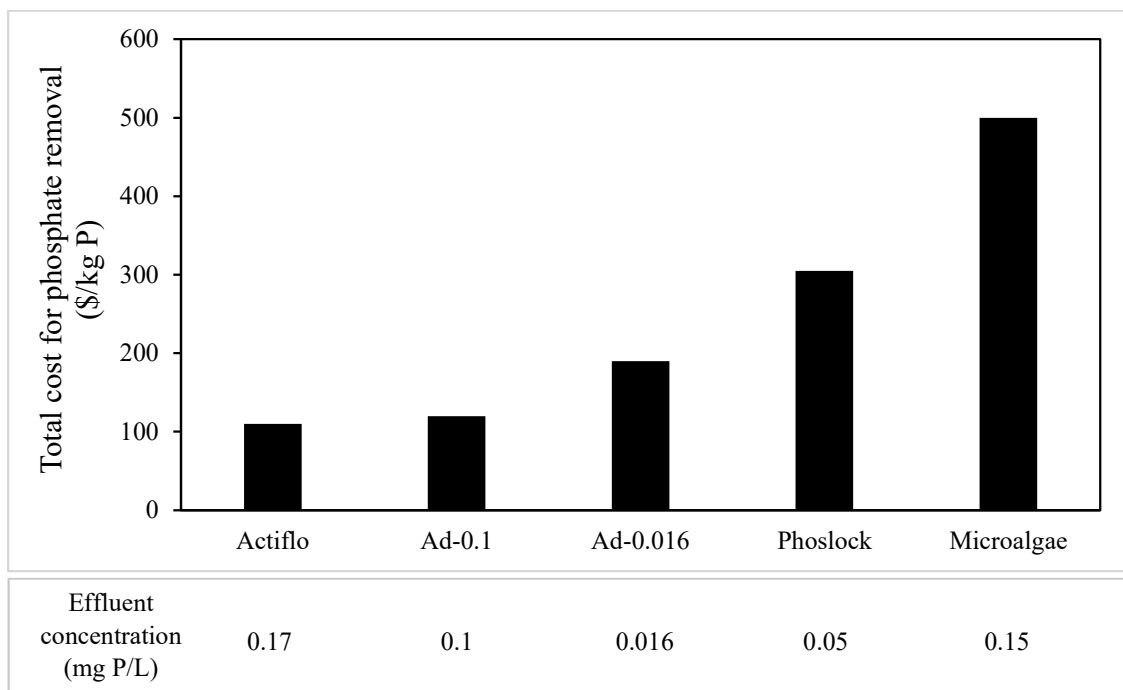


Figure 5. Total cost for phosphate removal via different treatment methods with the final effluent concentration values corresponding to each technique.

As can be seen from Figure 5, biological phosphate removal was the most expensive method among five different alternatives, which costed about 500 \$/kg P. On the other hand, chemical precipitation and adsorption offered by Actiflo and Ad-0.1, respectively were less expensive options for phosphate treatment, accounting for approximately 100 \$/kg P. However, Actiflo, which is a process combining the precipitation with metal salts and separation with sand, would produce a large sludge volume and require the proper sludge treatment and disposal. Moreover, extremely high amounts of these metal salts are certainly needed in order to eventually reach phosphate concentration of lower than 0.1 mg P/L. Compared to the adsorption process, overall cost for a further reduction to phosphate concentration of 0.016 mg P/L, which is about six times less than that of 0.1 mg P/L, was only approximately 190 \$/kg P. Therefore, the use of adsorption is more suitable than the chemical precipitation and the other methods for phosphate elimination, especially when a very low concentration of phosphate is required.

2.4 Biochar functionalized with layered double hydroxides for phosphate treatment

Removal of phosphate from aqueous solutions by adsorption technology is a prevailing remediation method, and extensive research in recent years has focused on developing efficient adsorbents with high adsorption capacity and economic viability. To date, biochar functionalized with layered double hydroxides (BC-LDHs) have been identified and proposed as a potent and low-cost alternative for phosphate treatment.

Biochar is a carbon-enriched material, which can be obtained from a variety of waste materials, such as forest and agricultural residues, industrial by-products, and municipal solid waste via pyrolysis under oxygen-limited conditions. Since biochar possesses a wide variation of interesting characteristics, such as high surface area, great porosity, and enriched surface functional groups, it exhibits tremendous potential for various applications, such as bioenergy production, carbon sequestration, soil amendment, and water purification [8,49]. Among different applications of biochar, remediation of water pollution has attracted considerable attention because of its obvious advantages of low energy requirements and the abundance of cheap feedstock materials for production that make it an ideal sustainable tool for wastewater treatment [7,49]. Biochar is

capable of removing a wide range of contaminants, including toxic metals, pharmaceuticals, personal care products, agrochemicals, organic compounds, and nutrients [50]. However, the net negative surface charge of biochar strictly limits its water purification application, especially for anionic pollutants, such as phosphate. For example, phosphate adsorption capacity of pristine biochar derived from agricultural wastes can be grouped in the range between 0.036 and 0.296 mg/g, and biochar modification is suggested to enhance its performance toward phosphate [51]. The formation of layered double hydroxides (LDHs) on the biochar surface has been extensively acknowledged as a possible solution that provides win-win benefits for manufacturing engineered biochar composites. Specifically, the resultant composites will exhibit significant improvement in phosphate removal owing to the excellent anionic adsorption capacity of LDHs [50]. At the same time, porous biochar can behave as an effective matrix, which provides a large surface area for LDH decoration and further prevents the aggregation of LDH particles [49].

In detail, LDHs are a class of synthetic anionic clays, whose structure is based on hydroxide sheets, in which some of the divalent cations are replaced by trivalent ions giving the positive charges, and these charges are balanced by intercalation of anions and water molecules in the hydrated interlayer regions [4]. The schematic representation of LDH structure is shown in Figure 6.

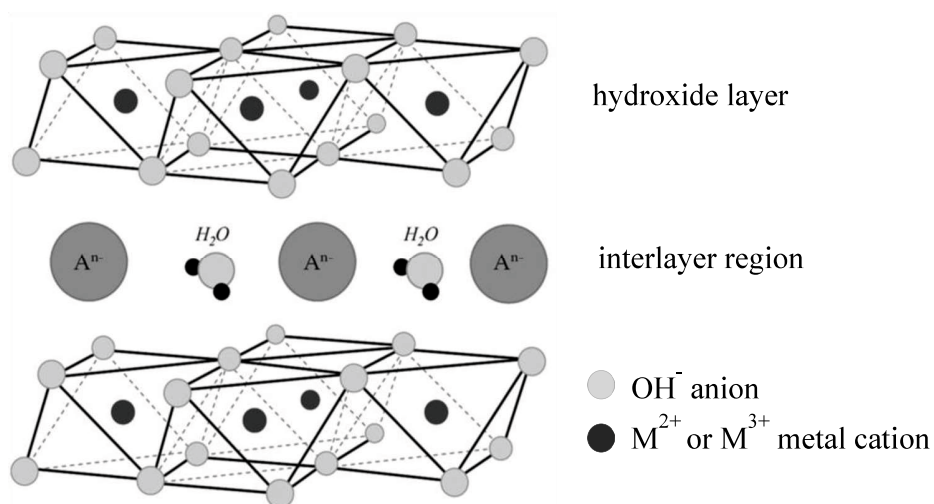


Figure 6. Schematic representation of LDH structure [155]

LDHs hold outstanding adsorption potential for anions due to their exchangeability of interlayer ions and other guest anions in solutions. Moreover, calcination of LDHs can be considered as a simple and efficacious method to improve the adsorption capability of these materials. Previous studies have demonstrated that calcined LDHs exhibit superior adsorption performance in comparison to non-calcined LDHs because the thermal treatment simultaneously causes the formation of reactive mixed metal oxides and the release of anions and water molecules in the interlayer space of LDHs, leading to the collapse of its original structure. However, during anion adsorption in aqueous systems, structural reconstruction of LDHs takes place by concomitant rehydration and intercalation of aqueous anions into LDHs that is termed the reconstruction process or memory effect [1,52,53]. Iftekhhar et al. [54] evaluated the effect of calcination on phosphate adsorption on Zn-Al based LDHs with a molar ratio of 3 and found that LDHs prepared with the thermal treatment reached their highest removal efficiency of close to 100%, whereas a capacity of approximately 70% was obtained for those without calcination. Although LDHs show great promise for enhanced phosphate treatment, LDHs pose the general problem of aggregation due to their relatively small particle sizes, which is recognized as a significant drawback of these products, consequently resulting in its inefficient separation and restricted practical application for phosphate removal [6,55,56]. Therefore, such a combination of LDHs and biochar is a highly preferable approach for the design of phosphate adsorbents, by which numerous advantages, including cost effectiveness, tremendous adsorption performance, and easy separation will emerge.

In spite of the fact that many previous researchers have conducted their studies of biochar and LDHs separately, BC-LDHs have been recently proposed to remediate toxic elements and inorganic anions, and phosphate is one of the most environmental contaminants that BC-LDH composites have been utilized for [49,50]. Zhang et al. [57] reported that from the adsorption kinetic study of phosphate with Mg-Al LDHs deposited on cotton wood biochar, phosphate adsorption behavior of the composite was as fast as calcined LDHs, and extremely high adsorption capacity of 410 mg/g was also achieved, suggesting that pore network of biochar might play an important role in dispersion of LDH flakes to efficiently increase their reaction with phosphate ions. Zhang et al. [58] exhibited the rapid phosphate adsorption on BC-LDHs prepared from the calcination of vegetable biomass coated with Mg-Al LDHs, which was reached within 5 minutes with the removal efficiency of more than 95%. The authors described that phosphate anions could

enter interlayers of LDHs quickly because of the memory effect and they were also attracted by protonated surface hydroxyl groups on the composites. He et al. [59] demonstrated that the adsorption performance of BC-LDHs was also associated with the initial pH of phosphate solutions. The better phosphate selectivity of the composites with the decline in solution pH was observed since the composite surface was entirely protonated at lower pH, leading to the strong electrostatic attraction with phosphate species. Apart from the purpose of favorably removing phosphate from contaminated water, Wan et al. [60] interestingly indicated that bamboo biochar functionalized with Mg-Al LDHs with a maximum phosphate adsorption capacity of 172 mg/g could be reused as slow-release fertilizers for boosting food production.

In order to further highlight the novelty of the present study, the author would like to point out that this work is innovative in following five aspects.

- In literature, the incorporation of LDHs into biochar has proven to be highly beneficial for the removal of phosphate from aqueous media. However, a remaining research gap is a lack of attention to the influence of modification techniques and biochar quantities on phosphate adsorption. Thus, in this study, physicochemical properties and phosphate adsorption capacity of various composites synthesized through two different available methods, which are precipitation of LDHs onto pristine biochar and pyrolysis of feedstock loaded with LDHs, were compared comprehensively. The present study contributes to a better understanding of these two approaches for the incorporation of LDHs into biochar and consequently fulfills a knowledge gap in this field.
- For each preparation route, the author also synthesized BC-LDHs by using varying amounts of biochar and compared adsorption performances among these composites in order to explore how the biochar content would affect phosphate adsorption. Such investigation is rarely available in the recent studies.
- The optimal conditions, including temperature and residence time for co-pyrolysis of feedstock preloaded with LDHs for BC-LDH production with efficient adsorption capability were reported for the first time in this study.

- Currently, BC-LDHs have been solely studied elsewhere for phosphate removal; however, comparative phosphate adsorption characteristics for both BC-LDHs and precursor LDHs were substantially and simultaneously investigated in this study.
- To the best of the author's knowledge, no previous research has assessed the subsequent application potential of BC-LDHs and precursor LDHs after their usage for phosphate remediation as fertilizers. In the present study, the impact of those materials at various application rates on seed germination and early plant growth was examined in order to address the questions of whether and how they could serve their application for agricultural purposes that also contributes to filling the knowledge gap in this area.

Chapter 3 – Biochar functionalized with layered double hydroxides composites prepared from different techniques and varying biochar quantities¹

3.1 Introduction

The two commonly used methods that have recently emerged to synthesize biochar functionalized with layered double hydroxides (BC-LDHs) are the following: (a) precipitation of LDHs onto pristine biochar, which is first produced by pyrolysis of biomass, and (b) pyrolysis of feedstock loaded with LDHs. Zhang et al. [57] were the first research group to successfully introduce the self-assembly of LDHs on biochar matrices as adsorbents for phosphate removal. Meili et al. [61] further clarified that biochar could serve as an effective support framework for LDHs to be deposited, resulting in an increase of surface area and the improvement of methylene blue adsorption. Li et al. [62] evaluated the adsorption performance of europium on the different mass ratios of LDHs and biochar. Interestingly, the composites with high biochar ratios had greater sorption affinity than those with high LDH ratios because of the larger porosity of the former. Thereafter, Tan et al. [63] developed BC-LDHs through direct impregnation of ramie stem (*Boehmeria nivea* (L.) Gaud.) powder into LDH solution and a subsequent pyrolysis process. Their results indicated that by this technique, the metal oxide formed on the biochar surface was capable of being restored to its original layered structure when rehydrated, which may contribute to the high adsorption capacity for crystal violet treatment. Similarly, synthesis of bagasse-derived biochar supported LDHs for the adsorption of antibiotic tetracycline was achieved using the same technique, which could lower the production cost and time for the preparation of high-performance materials for antibiotic contaminated effluent treatment [8].

While extensive studies of BC-LDHs for the remediation of various aqueous contaminants have been conducted, comparative information about the effectiveness of phosphate removal with different amounts of biochar added in composites and different synthesis techniques remains

¹ This chapter is a slightly modified version of an article published as Buates J, Imai T. Biochar functionalization with layered double hydroxides composites: Preparation, characterization, and application for effective phosphate removal. *J. Water Process Eng.* 2020; 37: 101508 [64].

limited. To the best of the author's knowledge, no previous research has addressed the optimal conditions (temperature and residence time) for the co-pyrolysis of feedstock preloaded with LDHs for creating BC-LDHs and achieving efficient adsorption capacities, which is an issue that represents an important knowledge gap in this field. The specific objectives of this chapter were as follows: (1) prepare BC-LDH composites with varying amounts of biochar through two distinct methods and characterize their physicochemical properties, (2) evaluate the performances of BC-LDHs in terms of phosphate adsorption through comparisons, and (3) determine the optimal co-pyrolysis conditions.

3.2 Materials and methods

3.2.1 Materials

Analytical grade aluminum chloride hexahydrate ($\text{AlCl}_3 \cdot 6\text{H}_2\text{O}$), magnesium chloride hexahydrate ($\text{MgCl}_2 \cdot 6\text{H}_2\text{O}$), sodium hydroxide (NaOH), hydrochloric acid (HCl), potassium dihydrogen phosphate (KH_2PO_4), and other reagents used for adsorbent synthesis and analysis were purchased from Wako Pure Chemical Industries, Ltd., Osaka, Japan. Deionized water (18.2 M Ω , Eyela Still Ace SA-2100E, Tokyo Rikakikai Co., Ltd., Tokyo, Japan) was used in all the experiments. Rice straw for biochar production was collected from a local agricultural field in Yamaguchi, Japan. Prior to use, the rice straw was washed with deionized water followed by oven drying at 100 °C for 24 h. The dried rice straw was then ground, passed through a 0.2 mm sieve, and kept in a sealed container. Physicochemical characteristics of the rice straw used in this study are detailed in Appendix A.

3.2.2 Production of biochar

Biochar was produced in a horizontal electric tube furnace (New Separation Muffle AMF-N with Ceramic Electric Tubular Furnace ARF-30K, Asahi-Rika Co., Ltd., Aichi, Japan). Before beginning the experiments, an oxygen-limited atmosphere was created inside a reactor by supplying highly purified nitrogen gas for 30 min at a flow rate of 200 mL/min, and a sample vessel containing rice straw was subsequently heated at a temperature of 600 °C with a retention

time of 1 h. These conditions are adequate for producing biochar for anionic pollutant removal [65,66]. The flow rate of nitrogen gas was maintained until the biochar had cooled to room temperature. A schematic diagram of pyrolysis system is presented in Figure 7.

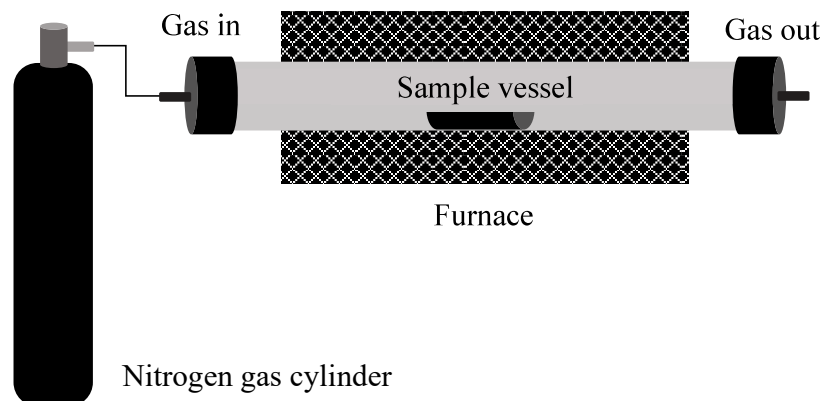


Figure 7. Schematic diagram of pyrolysis system

3.2.3 Preparation of BC-LDHs

BC-LDH composites were then prepared using two different techniques based on methods modified from previous studies [8,57,60]. To synthesize LDHs deposited on biochar materials by the first technique, three different amounts of resulting biochar (1 g, 5 g, and 10 g) were separately impregnated with 100 mL of solution containing $\text{AlCl}_3 \cdot 6\text{H}_2\text{O}$ (0.01 mol, 2.4 g) and $\text{MgCl}_2 \cdot 6\text{H}_2\text{O}$ (0.03 mol, 6.1 g). Percentages by weight corresponding to 1 g, 5 g, and 10 g of biochar used for the adsorbent production are approximately 11%, 37%, and 54%, respectively. After pH value being adjusted to 10 using 1.0 M NaOH solution, the mixture was incubated at 80 °C for 3 days, and the final precipitate was washed with deionized water and dried at 105 °C for 24 h. The media obtained from 1 g, 5 g, and 10 g by this technique were denoted as BC-LDHs 1, BC-LDHs 2, and BC-LDHs 3, respectively.

Using the second technique, rice straw batches of 1 g, 5 g, and 10 g were precoated with LDHs and were prepared following the same procedure outlined above. The amounts of rice straw of 1 g, 5 g, and 10 g are also expressed as weight percentages of approximately 11%, 37%, and 54%,

respectively. The dried feedstock was loaded with precipitate and was then allowed to be pyrolyzed at 475 °C for 2 h, which was the suitable conditions for converting biomass into biochar and calcining LDHs simultaneously. Detailed information is described in Appendix B (see in Figure B1 and Figure B2). The pyrolysis procedure was the same as that employed for biochar production. The composites were named BC-LDHs 4, BC-LDHs 5, and BC-LDHs 6, corresponding to feedstock quantities of 1 g, 5 g, and 10 g used for this production, respectively.

3.2.4 Characterization of BC-LDHs

X-ray diffraction (XRD) was conducted using an Ultima IV X-Ray Diffractometer (Rigaku Co., Ltd., Tokyo, Japan). Surface morphology was examined by scanning electron microscopy (SEM) using a JSM-7600F Scanning Microscope (JEOL, Ltd., Tokyo, Japan). Energy dispersive X-ray spectroscopy (EDX, JED-2300, JEOL, Ltd., Tokyo, Japan) was used to determine the distribution of chemical elements. Textural properties were measured with a BELSORP-mini II-S (BEL Japan, Inc., Osaka, Japan) based on nitrogen gas sorption and Brunauer-Emmett-Teller (BET) theory.

3.2.5 Phosphate adsorption experiments

Since a preliminary study of phosphate adsorption onto pristine biochar (without LDHs) demonstrated a small adsorption capacity, ongoing experiments focused on six BC-LDHs samples and original LDHs. Triplicate measurements were taken, and average values were calculated for all experiments. To evaluate phosphate adsorption behavior among those adsorbents, batch adsorption experiments were conducted at room temperature (23 ± 0.5 °C) in Erlenmeyer flasks containing 0.1 g of each adsorbent and 50 mL of phosphate solution (50 mg P/L) without adjusting the initial pH. After continuously mixing at 100 rpm for 24 h, the mixtures were immediately filtered through 1.0 μm PTFE membrane filters, and residual phosphate concentrations were analyzed using a U-1800 UV/VIS Spectrophotometer (Hitachi High-Technologies Corp., Tokyo, Japan) based on an ascorbic acid method outlined in the standard methods of examination of water and wastewater [67]. Equations for calculating the adsorption capacity (q_e) and other equations used in the study are included in Appendix C.

3.3 Results and discussions

3.3.1 Characterization of BC-LDHs

Typical XRD patterns of prepared BC-LDHs in the range of 5-70° are represented in Figure 8. Pristine biochar and pure LDHs were also investigated for comparison. The diffractogram feature of the pristine biochar indicates a cellulose identifier, which is clearly marked by a broad diffraction peak at 2θ around 23°. For BC-LDHs derived from the first method, the results match characteristic XRD peaks of pure LDHs. The high intensity of the main reflection peaks corresponds to crystal planes (003), (006), and (012). This clearly implies the successful deposition of LDHs on biochar matrices without ruining the crystalline structures of their composites. Contrarily, the common basal reflections (003) and (006), which indicate the layered structure attributed to LDHs, were not detected from the diffractograms of the other three BC-LDH samples. The poor characteristics of those composites suggest the disordering in stacked layers of LDHs during the pyrolysis process.

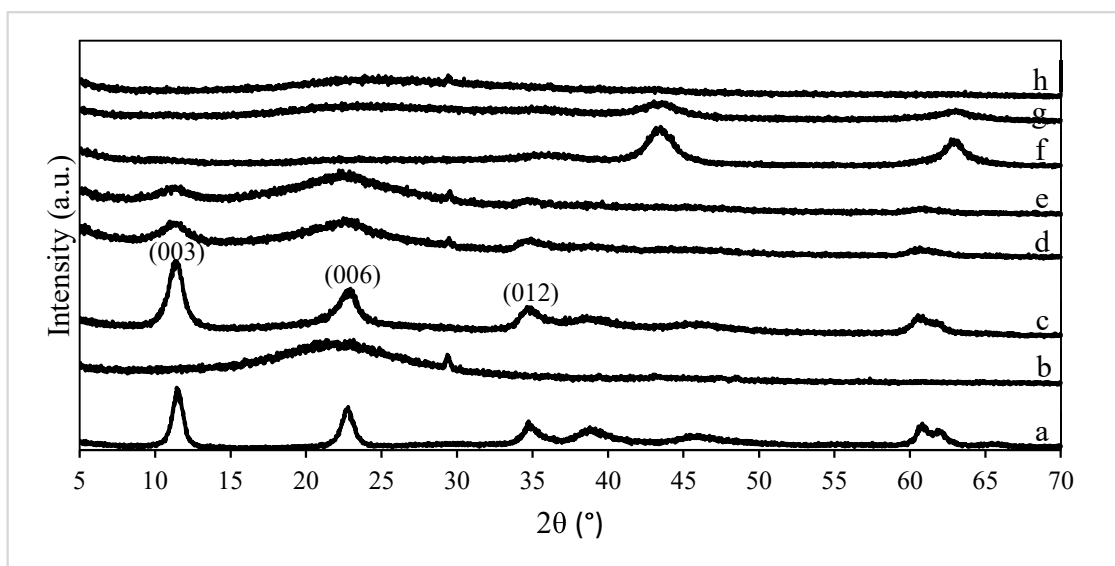


Figure 8. XRD patterns of samples: (a) pure LDHs (b) pristine biochar (c) BC-LDHs 1 (d) BC-LDHs 2 (e) BC-LDHs 3 (f) BC-LDHs 4 (g) BC-LDHs 5 (h) BC-LDHs 6

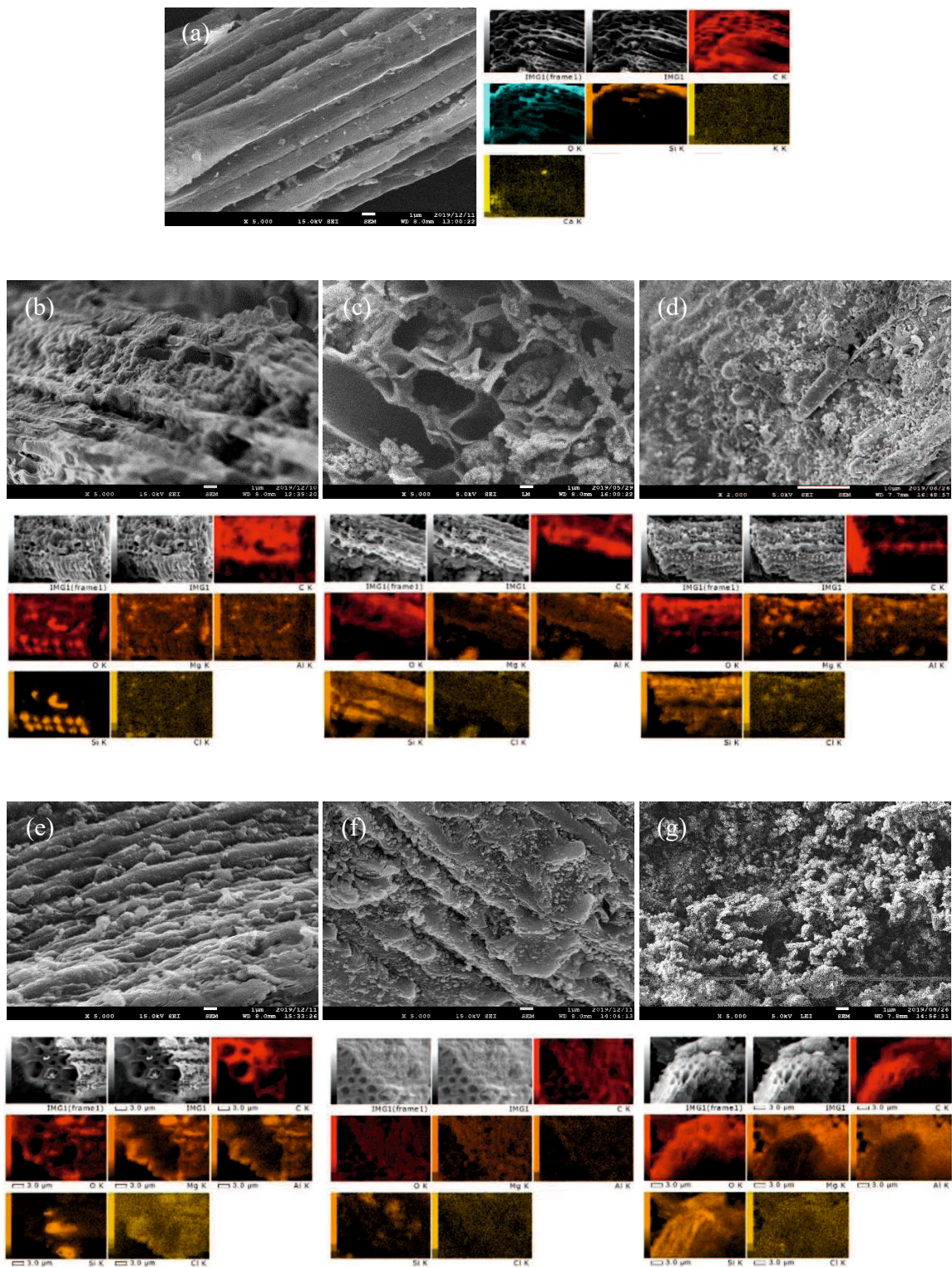


Figure 9. SEM images and EDX elemental distribution mapping of samples: (a) pristine biochar (b) BC-LDHs 1 (c) BC-LDHs 2 (d) BC-LDHs 3 (e) BC-LDHs 4 (f) BC-LDHs 5 (g) BC-LDHs 6

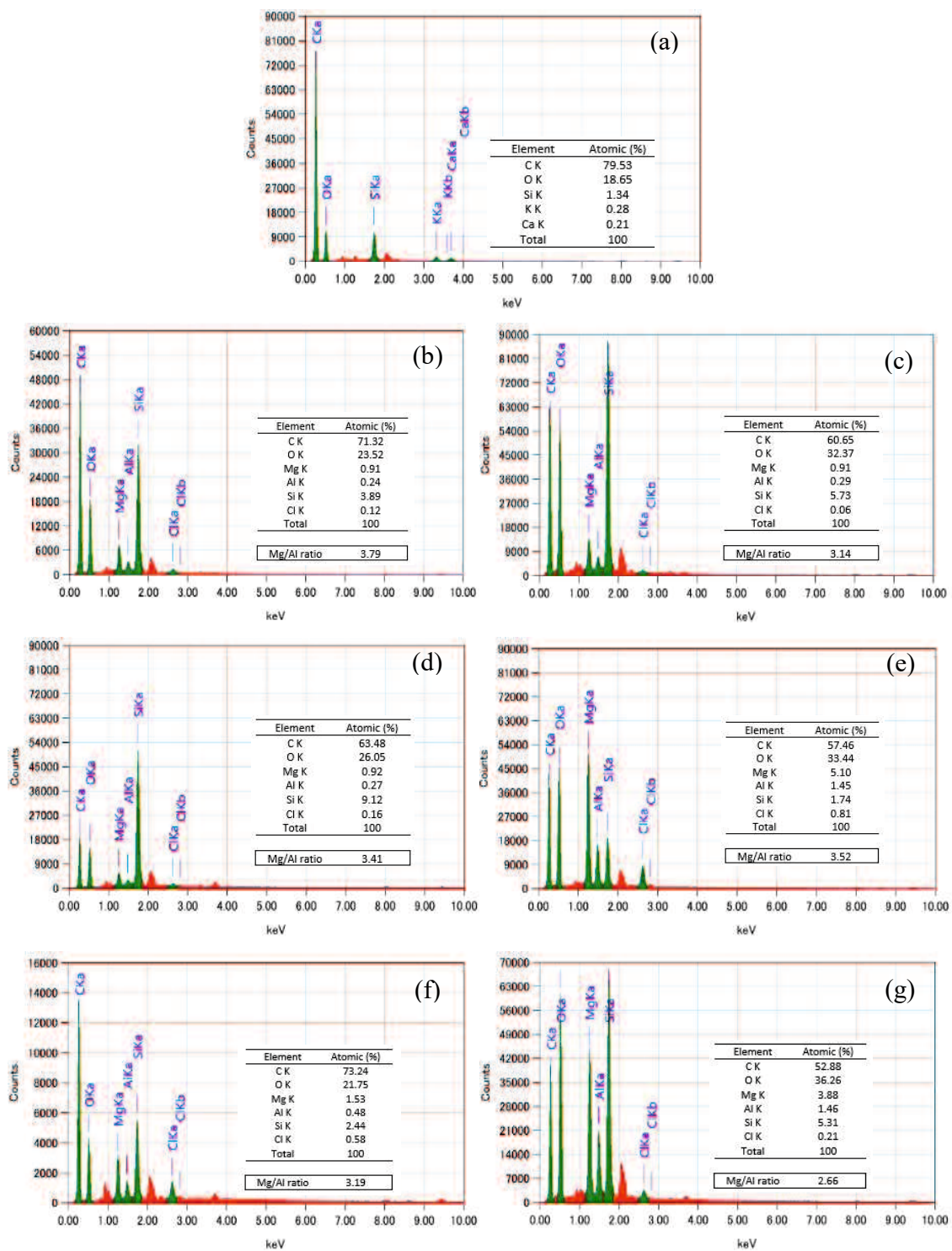


Figure 10. EDX spectrums of samples: (a) pristine biochar (b) BC-LDHs 1 (c) BC-LDHs 2 (d) BC-LDHs 3 (e) BC-LDHs 4 (f) BC-LDHs 5 (g) BC-LDHs 6

SEM micrographs in Figure 9 depict an extremely complex network of pores and channels appearing in raw biochar, together with a smooth surface and tubular structure. As demonstrated, surfaces of all BC-LDHs tested were entirely different from that of pristine biochar. The composites possessed homogeneous deposition of LDH particles on biochar carriers. In addition, the morphology indicates that the LDH particles were distributed not only on the biochar surfaces but also in pore channels. Elemental distribution mapping and EDX spectrums (Figure 9 and Figure 10) further confirm the successful modification of composites. The typical elements (Mg, Al, and Cl) of LDHs were clearly observed and were heavily concentrated all over the biochar structure. The corresponding EDX spectrums evidently reveal that pristine biochar had prominent peaks for C and O, which are the major constituents of rice straw and much lower-level peaks for minor mineral elements, including Si, K, and Ca, while additional peaks for Mg, Al, and Cl were detected for every BC-LDH. Considering the atomic percentages of elemental compositions, there were no other impurities appearing in the samples and the actual Mg/Al loading ratios of prepared materials ranged from 2.66 to 3.79, exhibiting the efficient introduction of mixed metal salts within the biochar matrices during synthesis.

Textural properties obtained from BET analysis are presented in Table 1. Pure LDHs had a low surface area and small pore volume, whereas the extremely high surface areas and porosity could be achieved in pristine biochar and BC-LDH composites. Moreover, most samples from the first technique showed a greater surface area (345-380 m²/g) compared with those from the second technique (165-200 m²/g). Figure 11 shows nitrogen adsorption-desorption isotherms of composites obtained from both techniques. The volume of adsorbed gas increased substantially with increasing relative pressure, and the highest adsorbed nitrogen volume was detected for BC-LDHs 3. Since adsorption and desorption curves were not overlapping, resulting in hysteresis loops, all isotherms could be classified as type IV, according to the classification of IUPAC [68]. This isotherm type is characteristic for monolayer-multilayer gas adsorption, together with capillary condensation occurring in the pores. Furthermore, a mesoporous structure could be regarded as the major component within the composites. This is in accordance with average pore diameter results in Table 1 that report pore sizes ranging from 3.46 to 5.82 nm, which are considered as the mesopore type. These isotherms also correlated to multiple hysteresis loops,

whose shapes were closely relevant to type H2, H3, and H4, suggesting the existence of ink-bottle-shaped, slit-type, and narrow slit-like pores, respectively.

Table 1. Textural properties of pure LDHs, pristine biochar, and BC-LDH composites

Samples	BET surface area (m²/g)	Total pore volume (cm³/g)	Average pore diameter (nm)
Pure LDHs	20.11	0.042	8.30
Pristine biochar	242.40	0.134	2.21
BC-LDHs 1	154.33	0.134	3.46
BC-LDHs 2	344.61	0.326	4.39
BC-LDHs 3	380.32	0.377	3.97
BC-LDHs 4	199.51	0.286	5.73
BC-LDHs 5	189.85	0.221	4.66
BC-LDHs 6	165.10	0.139	5.82

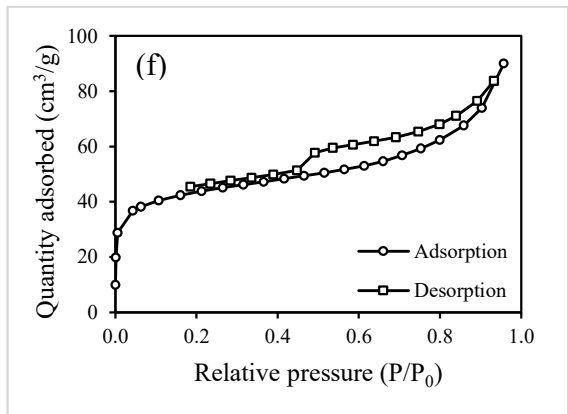
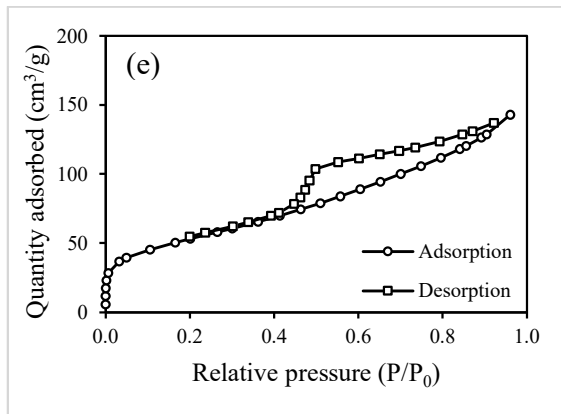
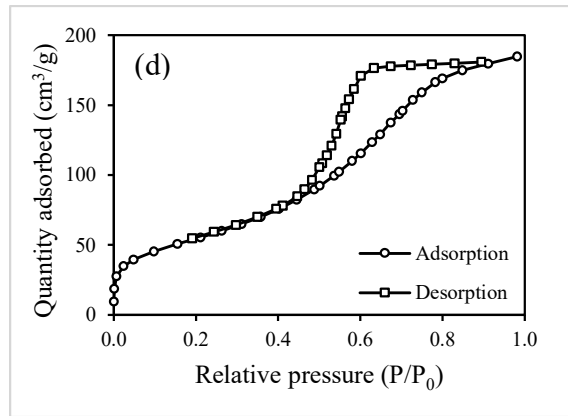
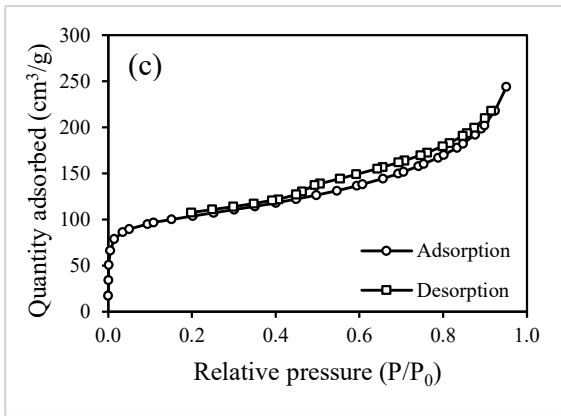
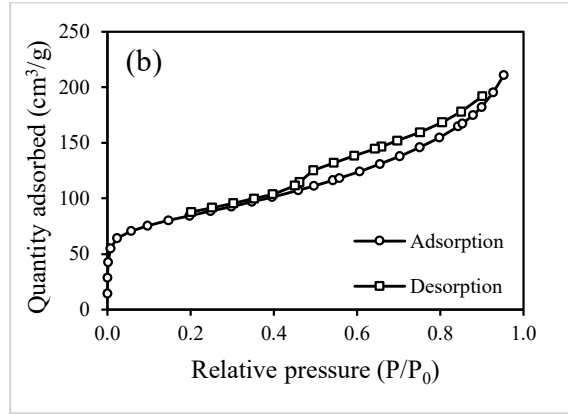
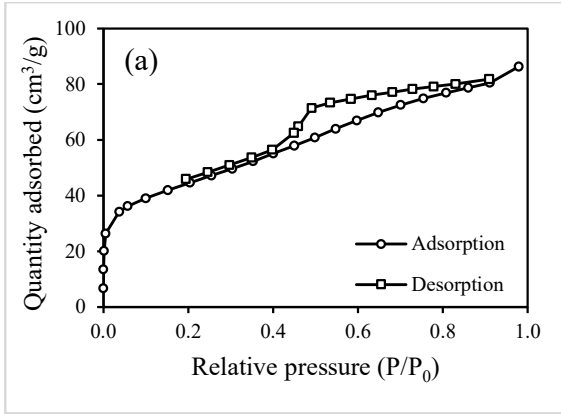


Figure 11. Nitrogen adsorption-desorption isotherms of composites: (a) BC-LDHs 1 (b) BC-LDHs 2 (c) BC-LDHs 3 (d) BC-LDHs 4 (e) BC-LDHs 5 (f) BC-LDHs 6

3.3.2 Phosphate adsorption performance of BC-LDHs

A comparison of phosphate adsorption capacity between pure LDHs and BC-LDHs has allowed conclusions to be drawn regarding the significance of synthetic routes as well as biochar contents. As shown in Figure 12(a), superior phosphate adsorption, which reached a capacity of approximately 21-25 mg/g, was achieved with adsorbents derived from the second method; in this method, the pyrolysis procedure was employed at the end of the production process. Conversely, a reduction of at least 30% in the quantity of adsorbed phosphate was attained for the other group of adsorbents. Among samples studied, BC-LDHs 4 possessed an excellent phosphate capture performance, which was found to be slightly higher than pure LDHs. Moreover, the amounts of phosphate ions adsorbed from solution decreased with increasing biochar dosing quantity. Specifically, phosphate was more strongly adsorbed onto the composites containing high LDHs. Fortunately, when the adsorption ability per unit mass of contained LDHs was applied (Figure 12(b)), the progressive enhancement in adsorption amounts coincided with a rise in biochar contents, particularly in BC-LDHs 6, where far more biochar was loaded on. Although raw biochar had a net negative surface charge, which restricted the favorable electrostatic interaction, its abundant mesoporous structure could serve as a transport pathway for LDHs to interact with phosphate anions, contributing to good adsorption capacity.

It is noteworthy that the method with the pyrolysis step designed at the end of process provided the better performance of BC-LDHs to uptake phosphate than the alternative, in which pyrolysis was included at the beginning. This phenomenon is related to the structural evolution of LDHs by thermal treatment. Upon pyrolysis process, anions and water molecules located in the interlayer regions were gradually eliminated, leading to the collapse of the layered structure. With the adsorption continuing, rehydration as well as phosphate incorporation allowed the destroyed LDHs to be reformed into its original structure. This structural conversion has been described as the reconstruction process or memory effect. The improvement in adsorption by heat-treated LDHs has also been reported previously by several authors [69,70]. In this regard, the composites based on thermal treatment of LDHs (BC-LDHs 4, BC-LDHs 5, and BC-LDHs 6) were successful. However, as rice straw is one of the least expensive and most abundant agricultural by-products

[71], BC-LDHs 6 is attractive because of its cost effectiveness and superb adsorption capacity; hence, it was employed for subsequent experiments.

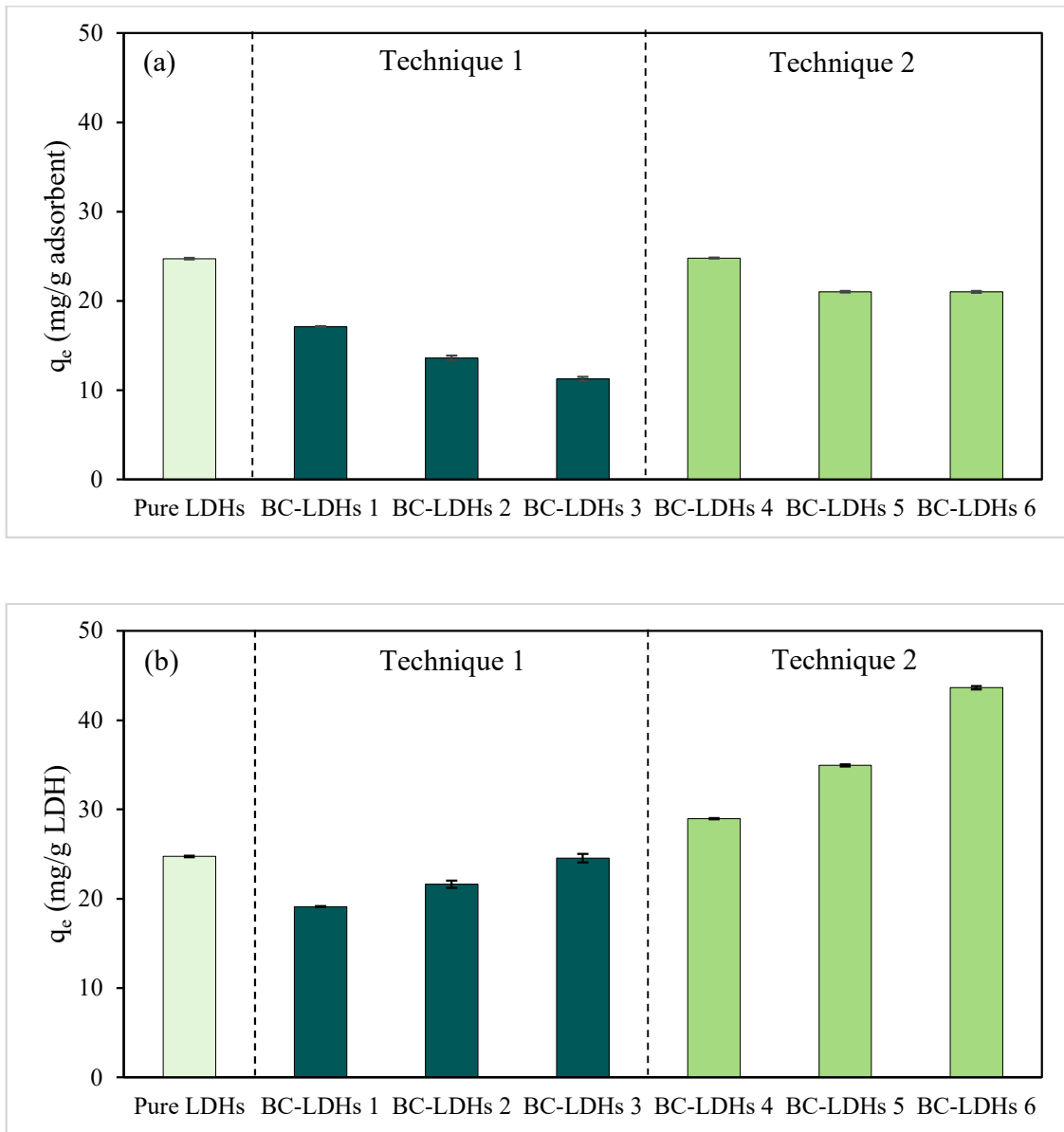


Figure 12. Phosphate adsorption capacity of pure LDHs and BC-LDH composites: (a) per unit mass of adsorbent (b) per unit mass of LDHs

Except for the above-explained considerations, the second method had some interesting features as it could reduce the production costs and duration; simultaneously, it offered a simple and effective single step treatment option during the preparation process to produce composites with an enhanced adsorption performance. Compared to the first technique, there should be an additional pyrolysis process after the coprecipitation step in order to provide heat treatment of the materials so that their adsorption capacity can be improved. From this point of view, the as-prepared BC-LDHs 6 is an inexpensive material with an outstanding potential for applications involving phosphate removal.

3.4 Conclusions

Biochar functionalized with LDHs was assessed as a means for remediating phosphate in aqueous solutions. Each composite type was developed by using two fabrication techniques and successful synthesis of composites was confirmed by characterization analyses. A temperature of 475 °C and residence time of 2 h were suitable conditions for the co-pyrolysis of feedstock and LDHs. The synthetic materials from pyrolysis of biomass loaded with LDHs exhibited superior capacities for phosphate removal (21-25 mg/g) compared to those from the other method (11-17 mg/g), in which LDHs were deposited on pristine biochar. The greater adsorbed amounts of phosphate were attained by composites from the former since this technique allowed calcined LDHs to be rehydrated and reconstructed into their original layered structures that is termed as the memory effect. The results of phosphate adsorption capacity per unit mass of LDHs also reveal that the composites with more biochar showed the better performances in comparison to ones with less biochar. This implies that biochar could serve as an effective matrix to support LDHs, leading to the composites with increased active sites for phosphate adsorption.

Chapter 4 – Influence of various experimental parameters on phosphate adsorption²

4.1 Introduction

Although adsorption has been recognized as a promising alternative for effective phosphate removal, the successful operation of this technique is also dependent upon the adsorption conditions, such as pH, initial phosphate concentrations, and coexisting ions. Alagha et al. [72] stated that the effect of pH on the adsorption of phosphate onto biochar-based LDH composites was significant due to the fact that the pH value was closely related to the factors of surface characteristics of adsorbents and the distribution of phosphate species. In general, effective adsorption of target anions can be restricted by coexisting anions in aqueous solutions because of the competition for available active sites. However, it was reported in literature [1,73] that the presence of monovalent and divalent anions, including NO_3^- , Cl^- , HCO_3^- , and SO_4^{2-} exhibited minor interference in phosphate removal on BC-LDH composites due to the strong and stable interactions between LDHs and phosphate, resulting from both electrostatic attraction and anion exchange reaction. Moreover, the effectiveness of these materials in phosphate treatment relative to an increase in adsorbent dosages and initial adsorbate concentrations was also documented in previously published studies [60,72,74].

In the previous chapter, highlights of different preparation techniques and amounts of biochar in composites, which affected the phosphate adsorption performances, were provided. The results indicated that BC-LDHs 6, which is an adsorbent derived from the second fabrication method with more biochar, outperformed other adsorbents in decreasing phosphate concentrations in aqueous solutions and its economical feature made it an appealing choice to be used in wastewater treatment. However, further efforts are required to systematically estimate the important role of operating conditions in controlling phosphate adsorption on this selected composite. Hence, successive experimental investigations, including those for pH effects, coexisting anion effects,

² Parts of this section were previously published by Buates J, Imai T. Biochar functionalization with layered double hydroxides composites: Preparation, characterization, and application for effective phosphate removal. *J. Water Process Eng.* 2020; 37: 101508 [64].

reaction times, and initial phosphate concentrations were performed with BC-LDHs 6. Likewise, pure LDHs were also examined under the same conditions for the comparison. In addition, phosphate adsorption mechanisms on these two adsorbents were also elucidated in this section. Specifically, the main objectives of this chapter were as follows: (1) investigate the influencing factors on phosphate adsorption behavior on BC-LDHs 6 and pure LDHs, (2) examine the adsorption kinetics and isotherms of both adsorbents, and (3) investigate their possible mechanisms for phosphate removal. Such data provides new insights into the application potential of rice straw-derived biochar as a high value-added adsorbent material for phosphate removal.

4.2 Materials and methods

4.2.1 Materials

All chemical reagents used in this work were of analytical grade and purchased from Wako Pure Chemical Industries, Ltd., Osaka, Japan. Deionized water (18.2 M Ω) obtained from Eyela Still Ace SA-2100E (Tokyo Rikakikai Co., Ltd., Tokyo, Japan) was used in all the experimental procedures.

4.2.2 Effect of pH on phosphate adsorption

Solution pH is an essential parameter that controls the phosphate adsorption process, so the initial pH of phosphate solution was adjusted by 0.1 M HCl and 0.1 M NaOH to prepare a series of solutions with pH ranging from 3.0 to 11. Next, 0.1 g of each sample was added in 50 mL of phosphate solution (50 mg P/L) and then applied by agitating at 100 rpm for 24 h. The zero-point charge (pH_{zpc}) of both samples was additionally measured by following the salt addition technique outlined by those of Mahmood et al. and Bakatula et al. [75,76]. 0.2 g of each sample was added in 40 mL of 0.1 M NaNO₃ solution. The pH of suspension was then adjusted by using 0.1 M HNO₃ and 0.1 M NaOH to obtain the initial pH values in the range of 2-11. After sample vessels being shaken vigorously at 200 rpm for 24 h, the final pH of each mixture was measured, and the differences between the final and initial pH (Δ pH) were then plotted against the initial pH values. The initial pH, at which Δ pH is zero, was taken as pH_{zpc}.

4.2.3 Effect of coexisting anions on phosphate adsorption

To understand the competitive interaction between the phosphate and various anion species, which are usually present in contaminated water bodies, the effect of coexisting anions on adsorbent characteristics was evaluated. The experiments were completed by 1-day agitation of 0.1 g of each adsorbent with 50 mL of phosphate solution (50 mg P/L, pH 3.0) containing an equal concentration of coexisting anions, including Cl^- , F^- , NO_2^- , NO_3^- , HCO_3^- , and SO_4^{2-} .

4.2.4 Adsorption kinetics and isotherms

In order to determine the preferable contact time required to reach equilibrium and describe the adsorption rate, the phosphate adsorption behavior of samples was observed by using the same ratio of adsorbent to phosphate solution as described previously and the pH value of solution, which was adjusted to 3.0. The final concentrations of phosphate in filtrates collected at different time intervals were then analyzed.

Phosphate adsorption isotherms for adsorbents were produced by introducing 0.1 g of each material in phosphate solution (50 mL) of varying concentrations (25-500 mg P/L), which were adjusted to the desired pH. The experiments were terminated after 24 h of agitating, which is known to be sufficient time to reach the adsorption equilibrium. Thereafter, the samples were withdrawn and filtered to determine the remaining phosphate concentration. Various adsorption isotherm and kinetic models were formulated to describe the experimental adsorption data as shown in Table C1 (Appendix C).

4.3 Results and discussions

4.3.1 Effect of pH on phosphate adsorption

Concerns about the significant effect of pH on the surface charge of adsorbents have stimulated the study of phosphate adsorption on pure LDHs and BC-LDHs 6 at different pH values. Figure

13(a) reveals that the process of phosphate adsorption for both adsorbents was less dependent on solution pH; however, the steady decrease in adsorption capacity was noticed with increasing pH. Pure LDHs and BC-LDHs 6 showed the best performance for phosphate uptake at pH of 3.0, accounting for 24.4 and 19.8 mg/g, respectively.

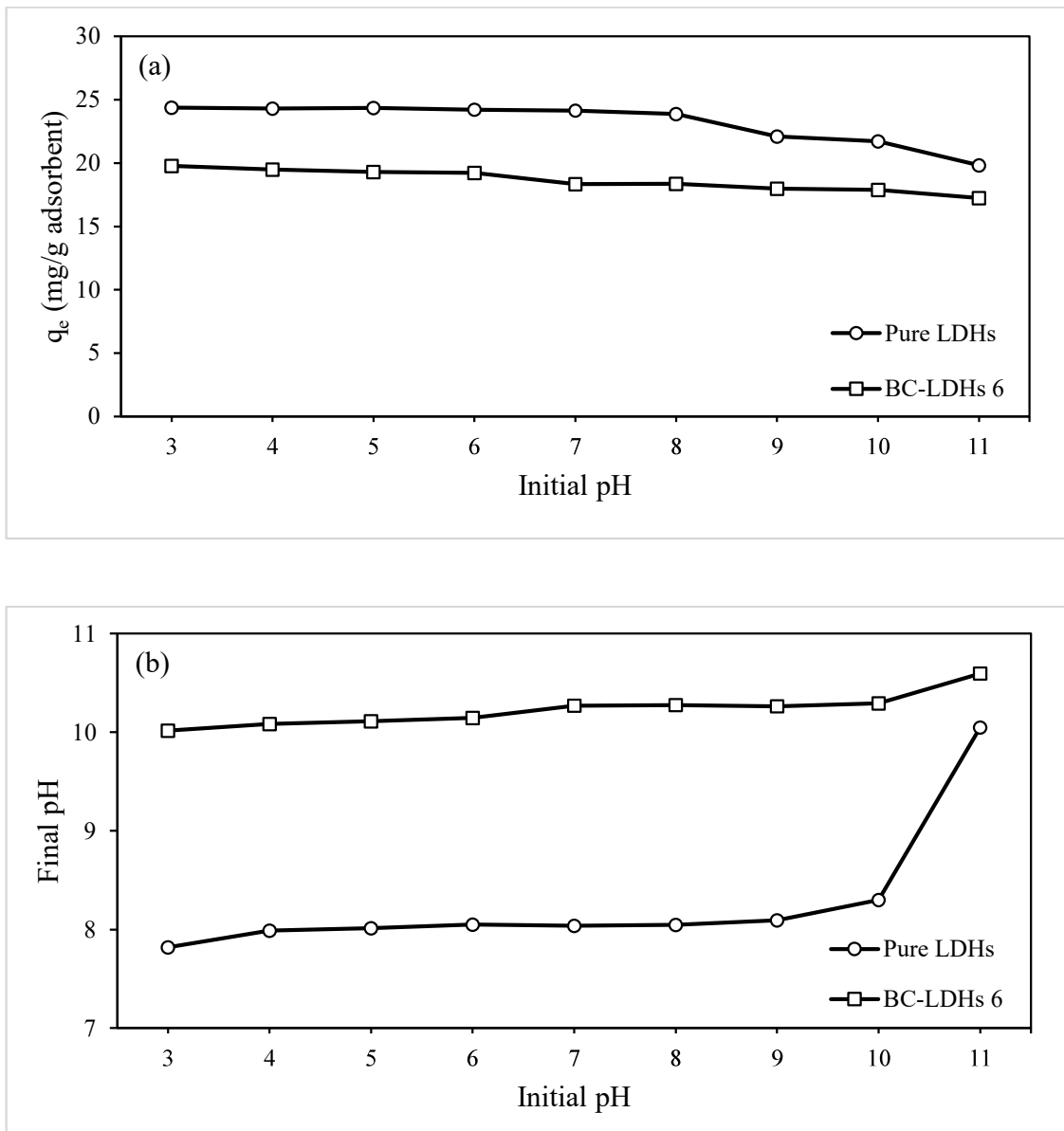


Figure 13. (a) Effect of initial pH on phosphate adsorption capacity of pure LDHs and BC-LDHs 6
 (b) Effect of initial pH on final pH after adsorption process of pure LDHs and BC-LDHs 6

To obtain a deeper understanding of pH-dependent surface charging behavior, the point of zero charge measurement was introduced. The point of zero charge defines the conditions of solution, in particular, the solution pH, for which the surface density of positive charges of particles equals that of negative charges. It is often regarded as a characteristic parameter for a given surface in a given aqueous solution [77]. The surface charge distribution in Figure 14 shows that at zero-point charge (pHzpc), pH for both pure LDHs and BC-LDHs 6 was about 10. Generally, in solution with pH less than pHzpc, the adsorbent surface became more positively charged. The adsorbent, by contrast, had a net negative charge on the surface when pH greater than pHzpc [78]. Consequently, the high pHzpc of pure LDHs and BC-LDHs 6 led to phosphate being well adsorbed over a wide pH range and their protonated surfaces were desirable to H_2PO_4^- and HPO_4^{2-} , which were the dominant phosphate species at the studied pH, causing the maximum adsorption at pH of 3.0. Even though the sensitive pH range for high phosphate removal was within a broad range, a pH of 3.0 was selected for further measurements of the other influential parameters because it corresponded to the results showing the highest adsorption efficiency.

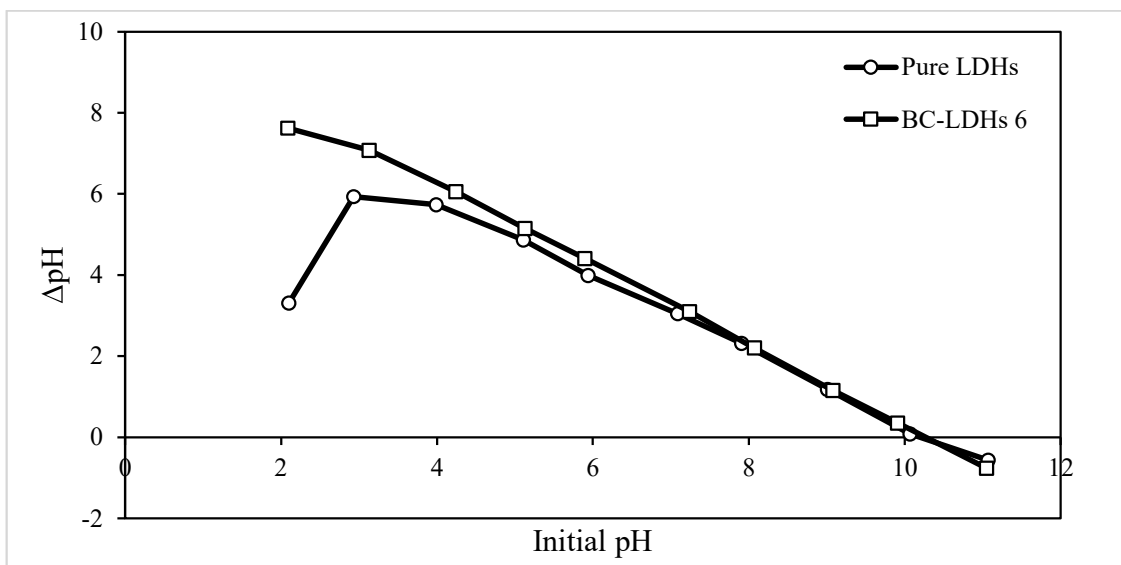


Figure 14. pHzpc curve of pure LDHs and BC-LDHs 6

As shown in Figure 13(b), the higher final pH than the actual pH was found in both adsorbents that could be attributed to the release of hydroxyl groups on adsorbent surfaces into the solution. However, there was a sharp shift in the final pH evidenced in pure LDHs. The solution with the

initial pH of 11 for instance, had a final pH of 10, which was higher than the average value of pH of 8.0. Again, this result could be explained as the surface of pure LDHs carried more negative charge at solution pH of 11, which was higher than its pHzpc; thus, the surface hydroxyl ions were readily released into the solution [79]. In contrast, such phenomenon was not observed with the other adsorbent, BC-LDHs 6, because of its stronger buffering capacity for phosphate adsorption against the pH change [80].

4.3.2 Effect of coexisting anions on phosphate adsorption

Since contaminated water in the environment typically contains other anions, which may interfere with phosphate removal, the adsorption performance of studied materials in the absence and presence of coexisting anions was compared and verified. The results are illustrated in Figure 15. Six competitive anions had negligible impact on phosphate removal by BC-LDHs 6, revealing the ability to effectively resist disturbances caused by foreign species, which is a critical quality for practical applicability. The phosphate adsorption was not adversely affected with common anions because of the large electroselectivity of divalent ions compared to the monovalent ones [81]. Thus, the binding of HPO_4^{2-} was preferred over that of Cl^- , F^- , NO_2^- , NO_3^- , and HCO_3^- . Therefore, the SO_4^{2-} divalent ion was expected to strongly interfere with the adsorption; however, the adsorption ability remained almost unchanged. The relatively higher pK_b value of SO_4^{2-} (12.08) than that of HPO_4^{2-} (6.79) was proposed to be the reason for this finding. Therefore, the smaller the pK_b value of anions, the higher is the basicity of anions [82]. Hence, the protonated composite preferred HPO_4^{2-} to SO_4^{2-} .

Among these anions, fluoride significantly depleted the removal efficiency of pure LDHs. The inhibition caused by the fluoride addition could be interpreted as competing for adsorbed phosphate for similar active sites on pure LDHs [83]. Under such a competitive system, fluoride ions were easily able to interact with the adsorbent and to compete for the common sites because pure LDHs had greater affinity for F^- compared with H_2PO_4^- ; therefore, it was more difficult to displace the occupied active sites when F^- was captured first on the sample [53]. The adsorption of phosphate was, as a consequence, prevented on pure LDHs.

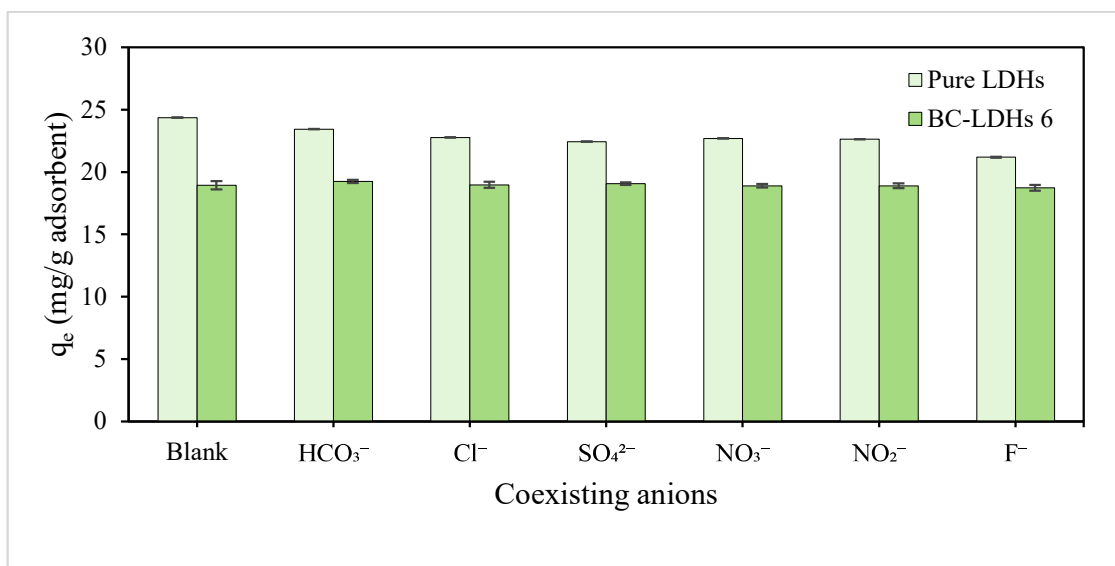


Figure 15. Effect of coexisting ions on phosphate adsorption by pure LDHs and BC-LDHs 6

Besides the textural properties, including a high surface area, large pore volume, and pore sizes that many functional materials have been fabricated with over the last two decades, the sensitivity and selectivity are also important aspects to consider for practical operations [84]. Hence, BC-LDHs 6 was always desirable based on its efficient phosphate capturing under various environmental conditions, including the changes in the pH and the presence of coexisting ions, and its excellent textural properties.

4.3.3 Adsorption kinetics

The two most popular kinetic models, pseudo-first-order and pseudo-second-order models, were required to gain deeper insight into adsorption mechanisms. The kinetic profiles of phosphate adsorption by pure LDHs and BC-LDHs 6 are displayed in Figure 16. The rate of phosphate removal was found to reach equilibrium within 3 h for pure LDHs and 24 h for BC-LDHs 6. Although more time was required for attaining the adsorption equilibrium of BC-LDHs 6 than that of pure LDHs, the adsorption on BC-LDHs 6 was comparatively faster to achieve equilibrium than other previously reported fabricated biochar (about 90 h) [85].

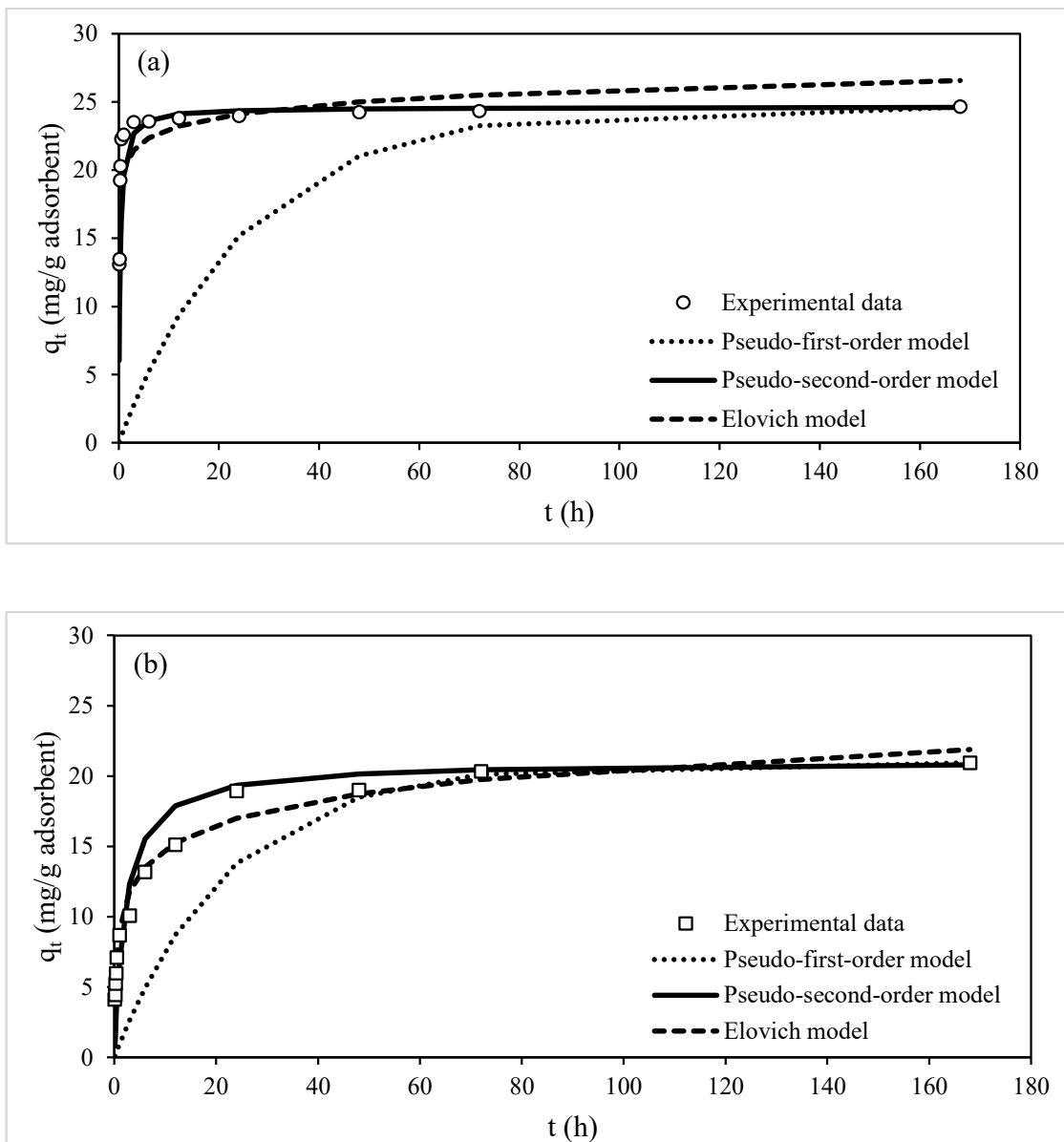


Figure 16. Adsorption kinetics for phosphate adsorption on samples: (a) pure LDHs (b) BC-LDHs 6

The derived rate constants, together with the correlation coefficient (R^2) for these models are summarized in Table 2. The comparison of kinetic models revealed that the pseudo-second-order model was the most suitable for describing the adsorption kinetics of phosphate on pure LDHs and BC-LDHs 6 with R^2 values relatively close to 1.0, which were indicative of good curve fitting between the experimental data and predicted curves obtained by modeling the phosphate uptake

values. The theoretical values of $q_{e,cal}$ predicted by the model were also much closer to the experimental ones ($q_{e,exp}$). Pure LDHs showed $q_{e,cal}$ of 24.6 mg/g, which was comparable to BC-LDHs 6 (21.1 mg/g). An evaluation of the experimental data also confirms a good correlation with the pseudo-second-order model (Figure 16), suggesting that the phosphate adsorption was greatly contributed to by chemisorption involving electron sharing or transfer between adsorbents and adsorbates [86]. Moreover, the Elovich model was also adopted to describe the kinetic data because such a model is often valid for systems, in which the adsorbing surface is heterogeneous [87]. The findings reveal that the Elovich model was also capable of defining phosphate uptake in the BC-LDHs 6 (Figure 16, Table 2). Consequently, it can be concluded that the adsorption process of this composite was governed by chemical adsorption on its heterogeneous surface.

Except for external surface adsorption, phosphate removal is able to proceed through pore diffusion, particularly when the adsorbent is a porous material. Hence, the intraparticle diffusion model was also applied to investigate the occurrence of adsorption mechanisms. According to this model, if the plot of q_t against $t^{1/2}$ gives a straight line and passes through the origin, the adsorption process occurs via intra-particle diffusion only [88]. The multilinear profiles of pure LDHs and BC-LDHs 6 with no linear portions intersecting the origin (Figure 17) were indicative of not only the pore diffusion but also a combination of several mechanisms impacting the adsorption process. The results of rate constants (k_i) determined from the slopes of linear plots illustrate that the diffusion rates for both adsorbents decreased with higher contact time and were at their lowest immediately after they reached equilibrium. The trilinearity also reveals that the diffusion process of materials could be distinguished into three stages: a fast initial stage; a subsequent slower stage; and a stable stage. The steepest curve at the initial stage represents the external mass transfer of phosphate molecules across liquid films around the particles (boundary layer diffusion). The second linear plateau corresponds to the ongoing transportation of phosphate from the outer surface of adsorbent to the internal pore structure (intraparticle diffusion) [89]. In the last step, the reaction has slowed and reached equilibrium due to the extremely low concentration of adsorbate remaining in solution and a relative decrease in unoccupied active sites available for the reaction [73].

Table 2. Kinetic and isotherm parameters for phosphate adsorption on pure LDHs and BC-LDHs 6

Kinetic parameters			
Models	Parameters	Samples	
		Pure LDHs	BC-LDHs 6
Pseudo-first-order	$q_{e,exp}$ (mg/g)	23.5	18.9
	$q_{e,cal}$ (mg/g)	3.16	13.0
	k_1 (1/h)	0.040	0.045
	R^2	0.578	0.919
Pseudo-second-order	$q_{e,exp}$ (mg/g)	23.5	18.9
	$q_{e,cal}$ (mg/g)	24.6	21.1
	k_2 (g/mg/h)	0.16	0.022
	R^2	1.000	0.999
Elovich	α (mg/g/h)	9377281	91
	β (g/mg)	0.79	0.40
	R^2	0.659	0.980
Isotherm parameters			
Models	Parameters	Samples	
		Pure LDHs	BC-LDHs 6
Langmuir	Q_m (mg/g)	166	192
	K_L (L/mg)	0.027	0.038
	R^2	0.852	0.910
Freundlich	K_F ((mg/g)(L/mg) ^{1/n})	17.9	23.3
	n	2.7	2.5
	R^2	0.941	0.995

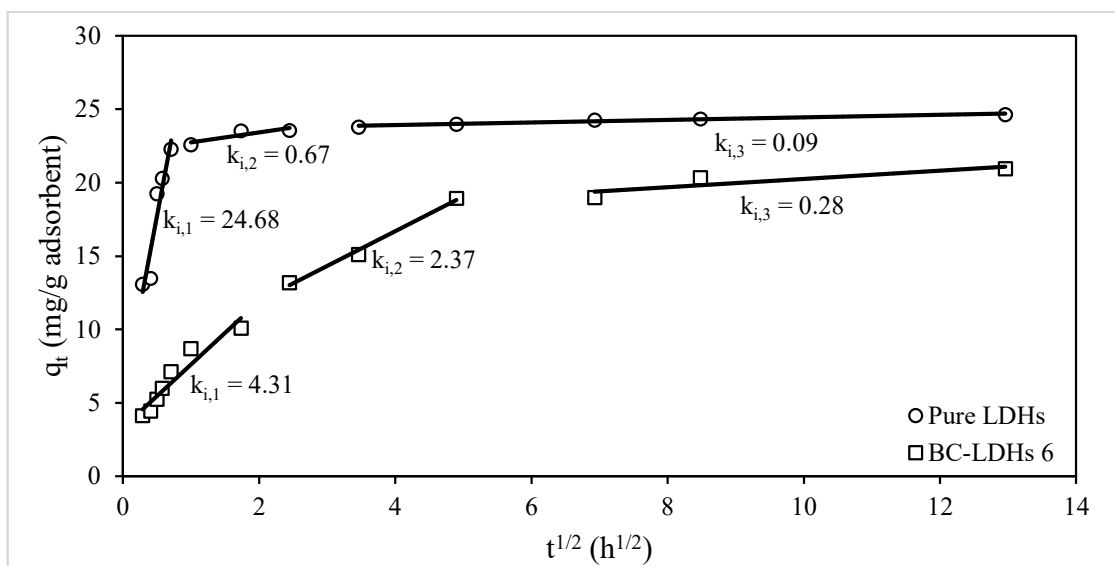


Figure 17. Intraparticle diffusion model for phosphate adsorption on pure LDHs and BC-LDHs 6

4.3.4 Adsorption isotherms

To further describe the phosphate adsorption behavior and quantitatively evaluate the adsorption capacity, the adsorption isotherms were examined under optimized conditions (pH of 3.0, contact time of 24 h), and the experimental data was fitted with Langmuir and Freundlich isotherm models. Figure 18 presents the adsorption isotherms of phosphate on pure LDHs and BC-LDHs 6. The amounts of adsorbed phosphate were observed to increase in relation to the initial phosphate concentration. Interestingly, despite the fact that BC-LDHs 6 was unable to achieve the adsorption equilibrium rapidly, its adsorption ability enabling a high phosphate concentration was greater than that of pure LDHs. This is due to the distribution of the pore network in its structure, which aids the dispersion of LDHs particles to efficiently increase their reaction with phosphate [57].

The characteristic values calculated for the two models indicated that the phosphate adsorption on all synthesized materials showed higher R^2 for the Freundlich model (Table 2), thus suggesting multilayer adsorption on adsorbents. The Freundlich linearity constant (n), which corresponds to the intensity of adsorption, attained within the range of 1-10, confirmed that phosphate anions were

favorably adsorbed by these samples under the conditions studied. The maximum Langmuir capacity (Q_m) for the adsorption of BC-LDHs 6 (192 mg/g) was observed to be larger by a factor of approximately 1.2 than pure LDHs (166 mg/g). Meanwhile, the actual maximum adsorption amounts for the former and latter materials were 180 mg/g and 159 mg/g, respectively.

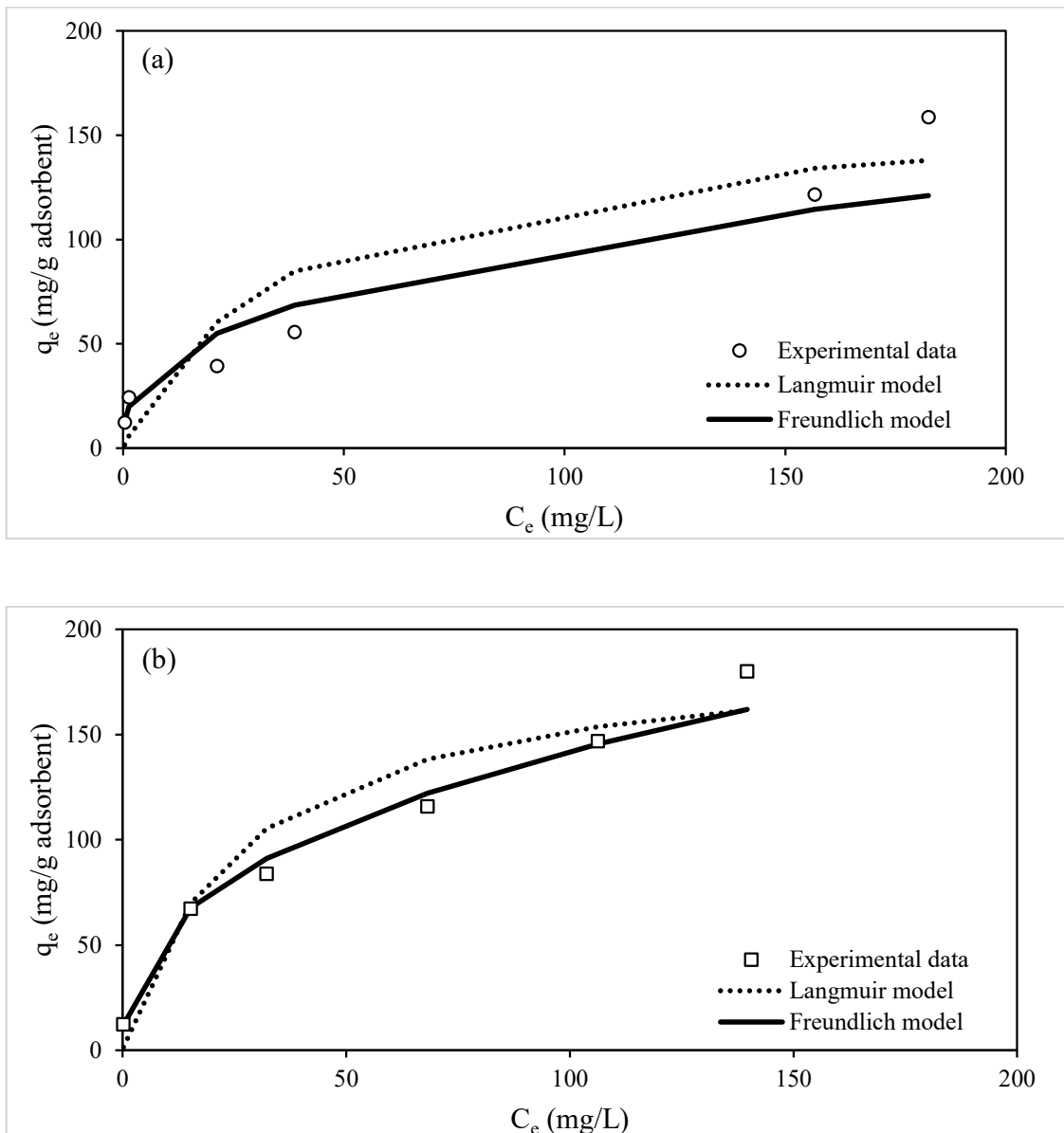


Figure 18. Adsorption isotherms for phosphate adsorption on samples: (a) pure LDHs (b) BC-LDHs 6

Table 3. Comparison of phosphate maximum adsorption capacity of various adsorbents

Adsorbents	Experimental conditions			Q _m (mg/g)	References
	Temperature (°C)	pH	Dosage (g/L)		
Cattail biochar loaded with lanthanum	25	7.0	2.0	36.1	[90]
ZnAl-LDHs loaded with magnetic Fe ₃ O ₄	25	3.0	2.0	36.9	[6]
Sugarcane leave biochar loaded with MgAl-LDHs	23	3.0	2.5	81.8	[80]
Calcined MgAl-LDHs	25	6.5	2.0	101	[91]
Pure LDHs	23	3.0	2.0	166	This study
Date palm biochar loaded with MgAl-LDHs	45	6.0	0.125	181	[72]
BC-LDHs 6	23	3.0	2.0	192	This study
Magnetic <i>C. korshinskii</i> biochar loaded with MgAl-LDHs	25	3.0	1.0	253	[73]
Cotton wood biochar loaded with MgAl-LDHs	22	-	2.0	410	[57]

The comparison of the maximum adsorption capacity of pure LDHs and BC-LDHs 6 with other available adsorbents is presented in Table 3. In most cases, calcination facilitated the inorganic pollutant adsorption of raw LDHs through a structural reconstruction mechanism. Pure LDHs in this study performed extremely well in removing phosphate even without heat treatment compared

with other modified LDHs [6] and calcined LDHs [91]. Indeed, BC-LDHs 6 was found to be more efficient than those LDHs materials and most of the biochar-based adsorbents reported in literature [72,80,90]. The excellent adsorption behavior of BC-LDHs 6 confirms that biochar, when combined with LDHs, exhibits a synergistic benefit during the removal of phosphate beyond that of other materials. Besides its satisfactory adsorption ability, BC-LDHs 6 appears more promising than other candidates in dealing with phosphate selectivity as common foreign anions had distinctly negative influences on phosphate adsorption by several of the adsorbents tested [73,80,90]. The high selectivity of BC-LDHs 6 for phosphate in the presence of diverse competitive anions is suggestive of its promise for practical employment in wastewater treatment applications and also for the recovery of phosphate with high purity.

4.3.5 Adsorption mechanisms

Experimental observations and comprehensive, theoretical interpretation of the adsorption characteristics have led to conclusions that electrostatic attraction, inner-sphere surface complexation via ligand exchange, pore diffusion, and precipitation were the most prevalent mechanisms for both pure LDHs and BC-LDHs 6. Memory effect has also been recognized to accompany the phosphate adsorption on the latter adsorbent. As previously discussed, the amounts of phosphate adsorbed on both materials smoothly increased with the decline in solution pH, where a significant positive charge was developed on the surfaces of the adsorbents, thereby aiding in the strong electrostatic interaction with negatively charged phosphate species. It is worth remembering that before modification, pristine biochar had poor natural adsorption properties. Nevertheless, the elevated phosphate adsorption performance for newly engineered BC-LDHs 6 could be observed to be considerable. This demonstrates that the successful surface optimization could be achieved in pristine biochar, which acquires the substantial negative charge.

Another important mechanism featuring the adsorption is the ligand exchange reaction. The presence of hydroxyl groups on adsorbents offered the possibility of phosphate–OH ion exchange. Such behavior could occur via monodentate and bidentate inner-sphere surface complexations, where phosphate ions created covalent chemical bonds with metal oxide surfaces (Mg–O and Al–O) or functional groups of biochar (O–C=O), leading to the liberation of other anions

[1,92,93]. The accompanying rise in the equilibrium pH can be seen as the evidence of the ligand substitution reaction of hydroxyl groups loaded onto phosphate adsorbents. Meanwhile, findings from the kinetic research further demonstrated the important role of pore diffusion in controlling phosphate adsorption on BC-LDHs 6. During the initial reaction process, phosphate molecules were captured by the exterior surface of BC-LDHs 6. Later, phosphate molecules passed into the pores of this media and were subsequently captured by the interior surface, such that the adsorption onto BC-LDHs 6 was controlled by the intraparticle diffusion. The higher rate constant for this step ($k_{i,2}$) of BC-LDHs 6 than for pure LDHs was consistent with its higher surface area and greater volume of mesopores for phosphate molecules, allowing these molecules greater accessibility into the interior structure. Since metal ions, Mg^{2+} and Al^{3+} , were used in the synthesis of LDHs and have been widely acknowledged for their precipitation with phosphates, XRD spectra were recorded for the two post-adsorption samples. The analysis data (Figure 19) provides evidence for the formation of phosphate compounds with the magnesium element ($Mg(H_2PO_4)_2$) on both adsorbents, indicating that the effective phosphate removal using these materials can be partially attributed to the precipitation reaction. The fact that all the final solution pH ranges increased to values between 7.82-10.60 after phosphate adsorption was consistent with precipitation being one of the mechanisms [94].

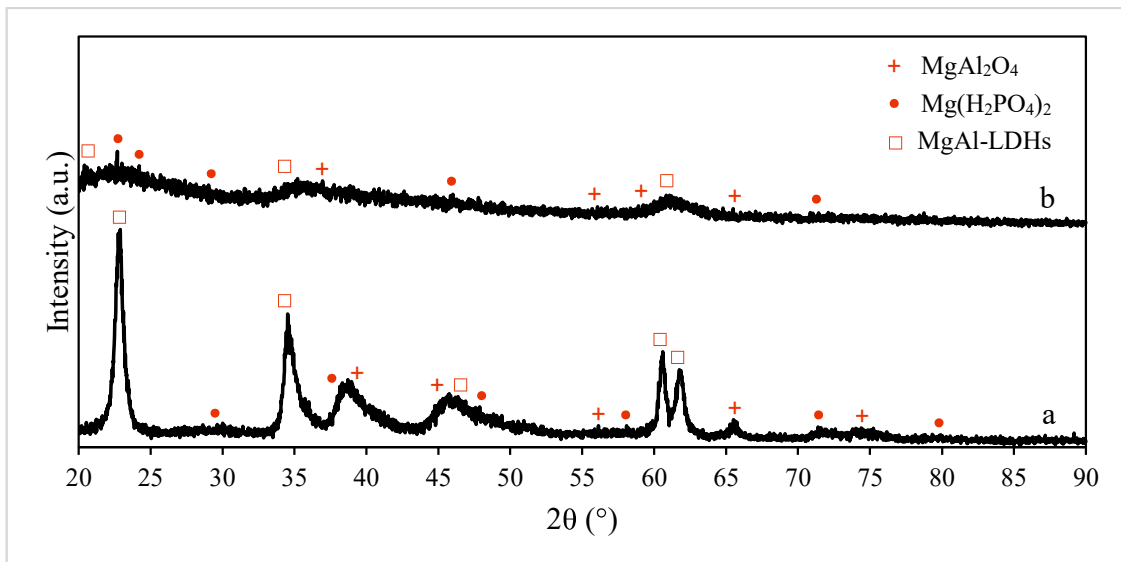


Figure 19. XRD patterns of samples after adsorption: (a) pure LDHs (b) BC-LDHs 6

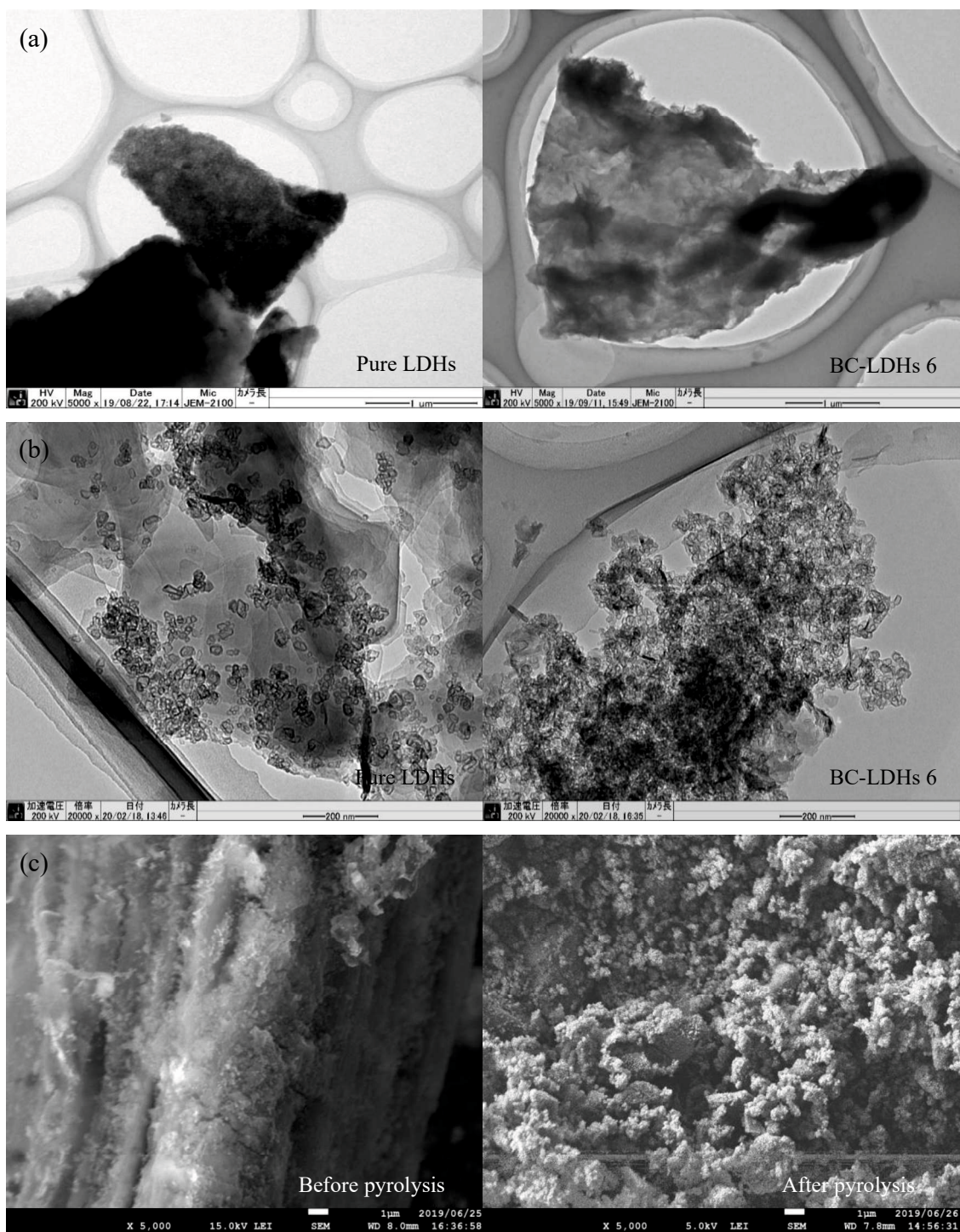


Figure 20. (a) TEM images of samples before adsorption (b) TEM images of samples after adsorption (c) SEM images of feedstock loaded with LDHs before and after pyrolysis process

The potential associated mechanism of BC-LDHs 6 is also established and described via a complex procedure of dehydration, rehydration, and reconstruction of lamellar material. As such, the structural transformation of BC-LDHs 6 was accurately explored through two kinds of electron microscopic technologies: TEM and SEM. TEM images reveal that BC-LDHs 6 after synthesis had discrete features from that of pure LDHs. BC-LDHs 6 could be assigned to the needle-like structure, whereas precursor LDHs were observed displaying distinctive crystalline platelet clusters (Figure 20(a)). These findings imply that preparation routes of materials contributed to the structural differences of LDHs within both samples. Without doubt, the pyrolysis procedure after LDHs being loaded on raw feedstock induced the disappearance of well-defined platelet structures for LDHs particles in BC-LDHs 6. When the LDHs on this media were submitted to the thermal treatment, their original morphology was lost because of the removal of hydroxyl groups in metal hydroxide layers [95], and further developed into the needle-like structure, which markedly differed from the precursor material without heat treatment. These outcomes are in agreement with those of Tan et al. and Zhang et al. [8,96].

With the repeated observation by SEM, Figure 20(c) reveals a surface alteration of this media after the thermal treatment process, possibly because of additional dehydration of water both from the surface of the material and the interlayer galleries. Following this, a substantial change in the BC-LDHs 6 characteristic took place again after phosphate adsorption. The needle-like structures that had formed returned to form new groups of spherical lamellar crystallites, which were the same structures as the precursor LDHs (Figure 20(b)). This structural transformation also verified the rebuilding of the original layered structure by incorporating anions into the collapsed structure [4]. When BC-LDHs 6 was exposed to phosphate-containing water, the thermally treated LDHs in the composite rapidly rehydrated in the solution and phosphate could be simultaneously adsorbed during the reconstruction process. More importantly, EDX elemental mapping evidently provides the indication of phosphate adsorption on pure LDHs and BC-LDHs 6 (Figure 21). The high density of yellow dots verifies the abundance of captured phosphate distributed on surfaces of post-adsorption samples. The schematic description of mechanisms for phosphate adsorption in BC-LDHs 6 is also illustrated in Figure 22.

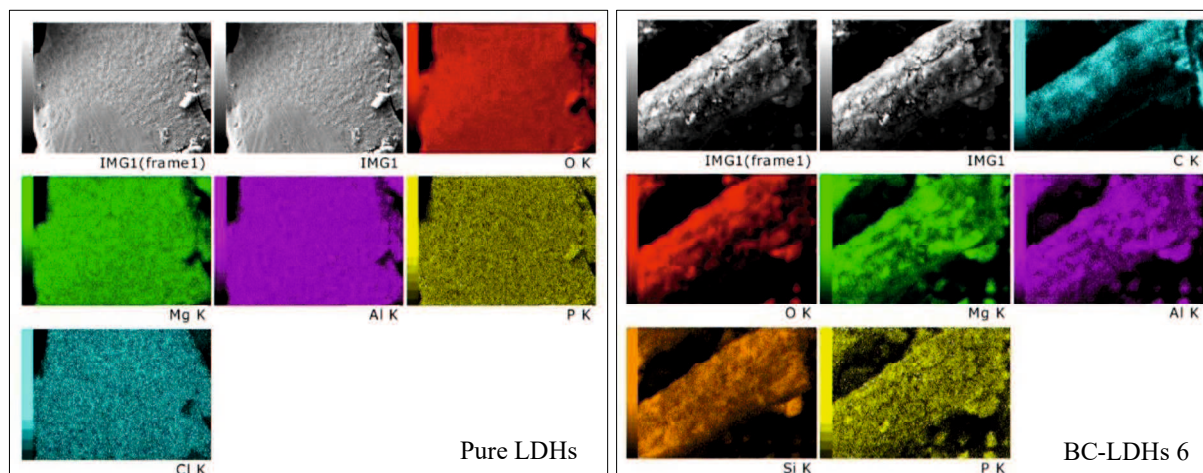


Figure 21. EDX elemental distribution mapping of samples after adsorption

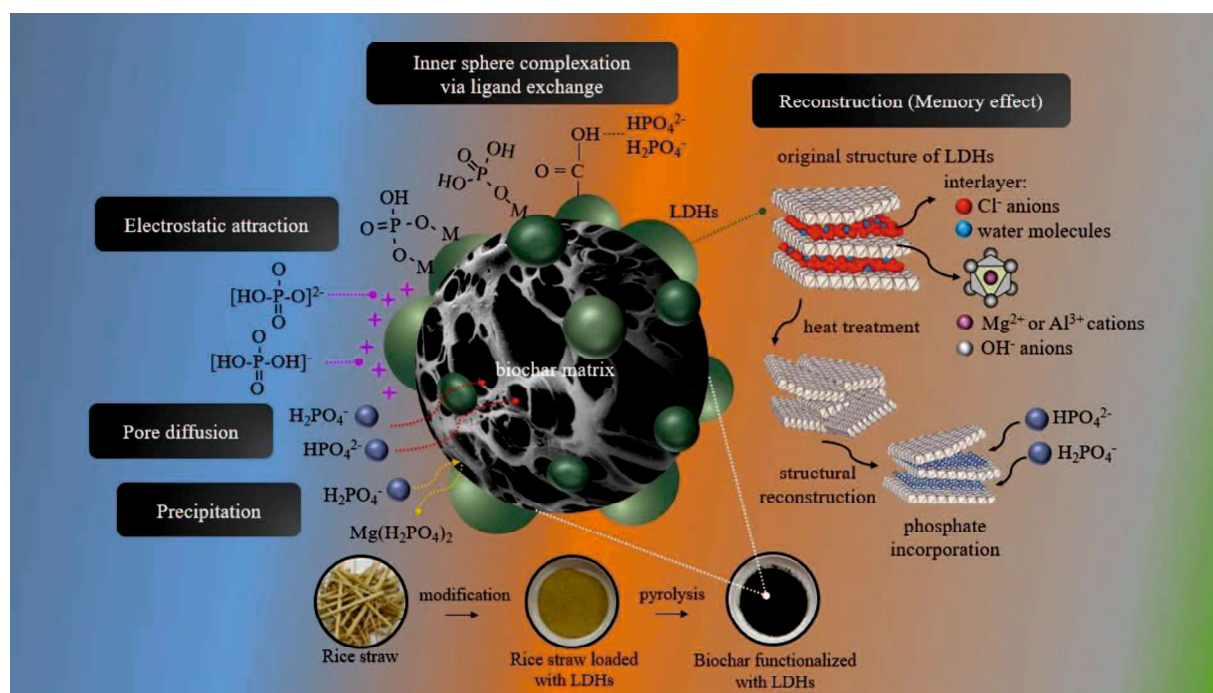


Figure 22. Schematic illustration of adsorption mechanisms on BC-LDHs 6

4.4 Conclusions

The influence of aqueous pH and coexisting anions, along with adsorption kinetics and isotherms were studied for the selected BC-LDH 6 composite and pure LDHs. Based on data collected from experiments, the utilization of biochar as a raw material for composite preparation provided for a positive correlation with LDHs and satisfactory adsorption performance. The composite was highly stable over a broad pH range or even in the presence of various foreign anions, indicating its benefits for practical application in contaminated environmental wastewater treatment. Conversely, the presence of fluoride resulted in a visible decrease in the removal efficiency for the precursor adsorbent, where LDHs were left isolated. The maximum adsorption capacity of the composite (192 mg/g) was improved by approximately 16 % compared with that of pure LDHs (166 mg/g). Additionally, the composite was found to adsorb a greater amount of phosphate than the values reported for other engineered adsorbents. The equilibrium data was adequately described by the Freundlich isotherm model, which exhibited a higher R^2 value (0.995) compared to the Langmuir model. The adsorption mechanisms of the composite obeyed electrostatic interaction, ligand exchange, pore diffusion, and precipitation reactions. Reconstruction also might have influenced the adsorption process of BC-LDHs 6. In addition to direct interest in the adsorption capacity, multiple advantages of using biochar have been discussed, such as its abundance, availability in low-cost feedstocks, simplicity, inexpensive production, and attractive physicochemical properties. Biochar functionalized with LDHs is a promising and valuable adsorbent for sustainable and affordable phosphate treatments.

Chapter 5 – Phosphate recovery from aqueous solution through adsorption-desorption cycles

5.1 Introduction

As mentioned previously, in addition to the eutrophication issue induced by anthropogenic discharge of phosphate into the environment, the demand for phosphate rock, which is a non-renewable resource, is expected to undergo a rapid growth, and future depletion of phosphate supply is a considerable concern. In this context, phosphate has to be used more sustainably, and technologies that allow for both removal and subsequent recovery of phosphate from polluted streams are imperative [97]. As a method for phosphate recovery with adsorbents, an adsorption-desorption cycle, where phosphate in the liquid phase is adsorbed first on the surface of the material, and adsorbed phosphate is then transferred to the desorption solution, has been proposed [98]. This technique provides adsorbent recycling, material life cycle extension, and cost reduction for phosphate treatment [99].

In the earlier section, evidence revealed that the noteworthy properties of the proposed composite included its economical feature, unique physicochemical characteristics, and excellent adsorption capacity for phosphate over a wide range of pH and foreign anion conditions, enabling desirable practical implementation in contaminated wastewater treatment. As a secondary goal of the study, the possibility of simultaneous phosphate recovery for this product was also addressed in order to ensure its applicability. Since an experimental investigation of the effect of pH demonstrated that phosphate adsorption on BC-LDHs 6 steadily decreased with increasing solution pH, adsorbed phosphate ions would be easily detached from particles in alkaline solvents. Hence, in this chapter, desorption and regeneration characteristics of phosphate adsorbed onto BC-LDHs 6 were consecutively investigated with sodium hydroxide (NaOH) solution, which was used as a desorbing agent based on its low cost and effective ability to elute adsorbed phosphate [100]. The obtained results were also compared with the desorption performance and reusability of pure LDHs.

5.2 Materials and methods

5.2.1 Materials

All analytical grade chemicals used in the desorption and regeneration tests were purchased from Wako Pure Chemical Industries, Ltd., Osaka, Japan. Deionized water obtained from Eyela Still Ace SA-2100E (Tokyo Rikakikai Co., Ltd., Tokyo, Japan) was used throughout the study.

5.2.2 Phosphate desorption and adsorbent regeneration

Selected BC-LDHs 6 was studied for phosphate adsorption-desorption-regeneration cycles. In the first cycle, phosphate adsorption was conducted at room temperature (23 ± 0.5 °C) by mixing 0.1 g of this adsorbent material in 50 mL of phosphate solution (50 mg P/L) without adjusting the initial pH. The suspension was stirred vigorously at 100 rpm for 24 h. Phosphate-saturated sample was then separated through filtration using 1.0 μm PTFE membrane filters followed by rinsing with deionized water and oven drying at 105 °C for 24 h.

Thereafter, phosphate desorption from phosphate-loaded BC-LDHs 6 was performed in 50 mL of NaOH solution at three different concentrations (0.01, 0.1, and 1.0 M). Each suspension was shaken at 100 rpm for 24 h and filtered as previously described in adsorption trials. The phosphate concentrations were measured using a U-1800 UV/VIS Spectrophotometer (Hitachi High-Technologies Corp., Tokyo, Japan). Four adsorption and desorption cycles were further conducted in order to investigate the potential reusability of regenerated particles with the adsorption performance measured in each cycle. For these consecutive regeneration cycles, 0.1 M NaOH solution was selected for phosphate recovery because it corresponded to the results exhibiting its good desorption efficiency. Prior to re-adsorption trials, the particles were oven-dried at 105 °C for 24 h and then reused for subsequent phosphate adsorption and desorption processes. The same experiment procedure as described above was also employed for pure LDHs. Equations for calculating the removal and desorption efficiency are presented in Appendix C.

5.3 Results and discussions

5.3.1 Choice of desorbing solution

A number of previous studies demonstrated that phosphate desorption with NaOH solution was the most effective and frequently used method, in which NaOH concentrations ranging from 0.01 M to 1.0 M were often employed [44,98,101,102]. To select the suitable concentration for desired adsorbent replenishment, the effect of three concentrations of this basic solvent (0.01, 0.1, and 1.0 M) on desorption ability were evaluated.

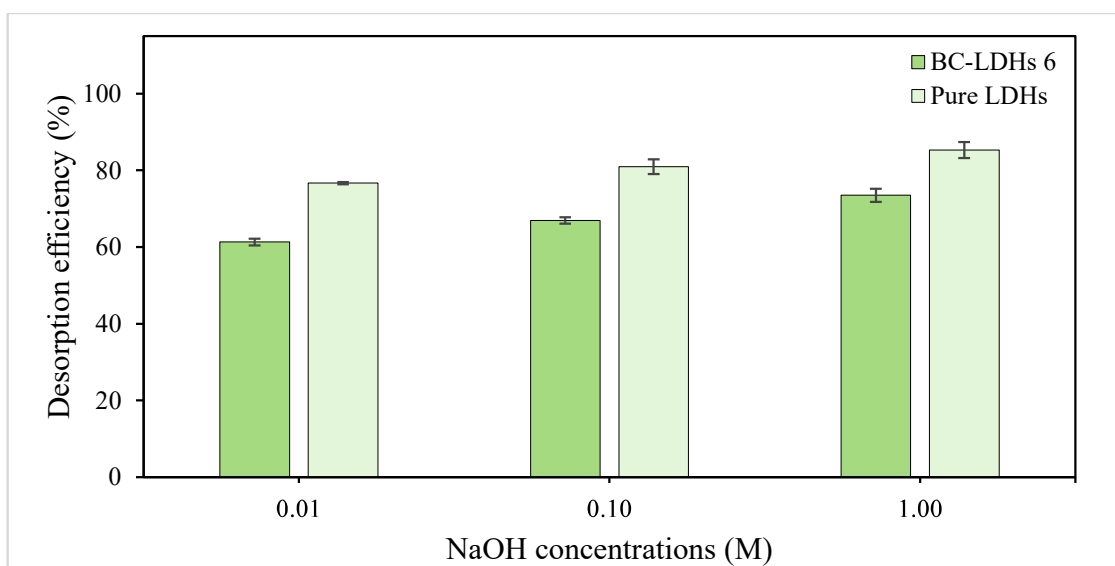


Figure 23. Effect of different concentrations of NaOH solution on phosphate desorption capacity of BC-LDHs 6 and pure LDHs.

It is clear from Figure 23 that the amounts of phosphate released from both products increased with increasing alkalinity. This phenomenon can be explained by the fact that excess hydroxyl ions from NaOH solution could replace phosphate adsorbed on adsorbent surfaces through the anion exchange process [100,103]. Phosphate desorption efficiency of approximately 61% and 77% was obtained when BC-LDHs 6 and pure LDHs, respectively, were treated with 0.01 M NaOH solution. Meanwhile, a further increase in NaOH concentration of up to 1.0 M resulted in

the maximum desorption amounts for the former and latter materials, reaching their capacity of about 73% and 85%, respectively. However, 0.1 M NaOH solution was chosen as a potential elution agent for the successive regeneration study since there was no statistically significant change in desorption performance between samples treated with 0.1 M and 1.0 M NaOH.

5.3.2 Regeneration of adsorbents

Adsorbent regeneration, where both BC-LDHs 6 and pure LDHs were subjected to sequential adsorption-desorption cycles, was done for two reasons as follows: (a) recover phosphate molecules bound on adsorbent media, and (b) replenish active sites on adsorbents for their reusability purpose. When the regeneration assessment was established, the newly available capacity of regenerated adsorbents and the amounts of desorbed phosphate were calculated, and the data is presented in Figure 24.

The results indicated that phosphate adsorption-desorption cycles over both adsorbents could be repeated several times. Moreover, the adsorption performance of BC-LDHs 6 was still high throughout three cycles of regeneration, accounting for approximately 20-24 mg/g, and then markedly dropped to approximately 16 mg/g in the last operation cycle. When it comes to pure LDHs, a considerable capacity degradation with additional cycle numbers was noticed. Also, their adsorption capacity was significantly lower than that of BC-LDHs 6 after treatment with NaOH solution, disclosing amounts of adsorbed phosphate ranging from 7 to 23 mg/g (Figure 24(a)). The progressive decrease in adsorption ability of both samples could be attributed to the depletion of active binding sites from the previous adsorption by strongly attached phosphate [104]. Also, the structure of LDHs within both adsorbents would become amorphous after the first stage, leading to the difficult accessibility of phosphate molecules into its structure. With further consideration on the adsorption mechanisms on the composite, memory effect and other proposed mechanisms could occur during the first adsorption stage. However, for three successive adsorption-desorption cycles, it was expected that the memory effect was not responsible for phosphate removal because unlike the fresh adsorbent, the regenerated sample was reused without further heat treatment to facilitate the structural reconstruction mechanism. As presented thereafter in Figure 24(b), the desorption capacity of pure LDHs in the first regeneration stage was 17.9 mg/g, which was slightly

higher than that of BC-LDHs 6 (16.0 mg/g). Nevertheless, desorbed phosphate in the last three regeneration sequences for BC-LDHs 6 exceeded that of pure LDHs. At the end of operation cycle, desorption quantities of those tested materials were found to be 7.8 mg/g for BC-LDHs 6 and 2.4 mg/g for pure LDHs. These results demonstrated that BC-LDHs 6 could be successfully replenished in alkaline solution for at least three cycles without greatly suppressing the removal ability, implying its good reusability and stability for practical applications.

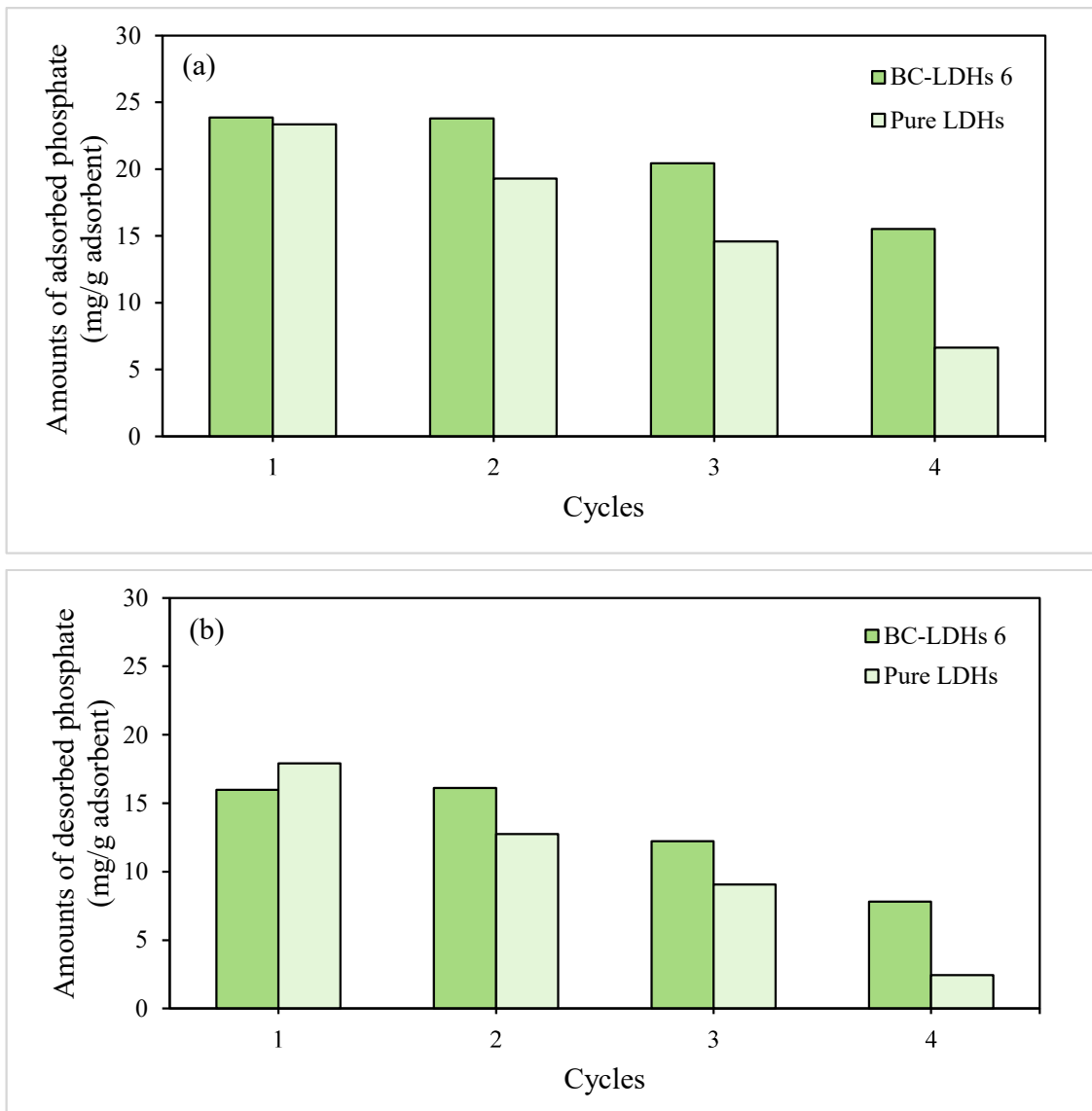


Figure 24. Phosphate adsorption and desorption profiles of BC-LDHs 6 and pure LDHs at different cycles of regeneration: (a) adsorption capacity (b) desorption capacity

5.4 Conclusions

Regeneration study was undertaken to find the reusability of BC-LDHs 6 and pure LDHs for phosphate removal and recovery by performing multiple adsorption-desorption cycles. The findings indicated that alkaline conditions facilitated retrieval of exhausted adsorbents, and the achieved desorption efficiency of samples regenerated with 1.0 M NaOH solution was greater than those with 0.01 M and 0.1 M NaOH. However, no significant improvement in desorption ability was observed for samples dispersed in 0.1 M and 1.0 M NaOH solution. Further results from successive regeneration experiments with 0.1 M NaOH also revealed that superb adsorption capacity of BC-LDHs 6 of over 20 mg/g was still maintained after three consecutive cycles, and then dropped to 16 mg/g in the last cycle. On the other hand, the phosphate adsorption amounts on pure LDHs progressively decreased from about 23 mg/g to 7 mg/g during the entire regeneration operation. Furthermore, BC-LDHs 6 still continued its outperformance of desorption ability against the alternative. It is evident from these regeneration tests that the proposed composite could be easily reused several times by applying NaOH solution, and thus provided an economically favorable option for phosphate treatment.

Chapter 6 – Potential use of biochar functionalized with layered double hydroxides after phosphate adsorption for seed germination³

6.1 Introduction

Phosphate is a vital nutrient and a non-substitutable constituent of agricultural fertilizers. However, a non-renewable phosphate rock resource, which is the world's major supply for fertilizer production, is getting depleted and expected to be exhausted in the near future. Meanwhile, phosphate-rich waste streams are currently considered as a main cause of eutrophication problem in aquatic ecosystems. Therefore, phosphate recovery from secondary sources, particularly in wastewater, is a desirable alternative to not only achieve sustainable phosphate supplies but also simultaneously reduce detrimental environmental impacts.

In addition to being capable of preferentially recovering phosphate from wastewater, a few studies have reported that biochar functionalized with layered double hydroxides (BC-LDHs) can be used for agricultural purposes. Wan et al. [60] demonstrated that from phosphate adsorption with the bamboo biochar composite containing 40% of LDHs, 172 mg/g of phosphate could be reclaimed from contaminated solution and recycled as a phosphate slow-release fertilizer to improve soil productivity and reduce soluble phosphate losses. Interestingly, Azimzadeh et al. [105] evaluated the effect of phosphate-adsorbed BC-LDHs on soil properties and found that soil fertility was improved after treatment with this product due to essential nutrients available in the biochar structure, such as phosphorus, nitrogen, and potassium. Moreover, Yan et al. [106] developed calcined Mg-Al LDHs for phosphate removal, and post-adsorption materials were desorbed by ammonia solution. The nutrient leaching experiments showed that ammonia-treated LDHs released only 31% of the phosphorus present in aqueous solution, and thus provided great promise as a slow-release fertilizer.

³ This chapter is adapted from Buates J, Imai T. Assessment of plant growth performance and nutrient release for application of phosphorus-loaded layered double hydroxides as fertilizer. *Environmental Technology & Innovation*. 2021; 22: 101505 [153] and Buates J, Imai T. Application of biochar functionalized with layered double hydroxides: Improved plant growth performance after use as phosphate adsorbent. *Applied Sciences*. 2021; 11: 6489 [154].

As extensive studies have only targeted the application of BC-LDHs for the remediation of aqueous contaminants, limited knowledge is available on the potential of recycling BC-LDHs containing phosphate as a fertilizer, which is worth the effort to overcome the challenges of nutrient recovery. Indeed, the direct observation of the interaction between BC-LDHs and plants has not been comprehensively studied, and the feasibility of using this composite as a fertilizer would also need to be confirmed. Therefore, the present study assessed plant responses to the application of BC-LDHs by using a seed germination assay to address the questions of whether and how BC-LDHs could serve their application for agricultural purposes that contribute to filling the knowledge gap in this area. In this section, BC-LDHs 6, which previously served a purpose for phosphate removal, was investigated to confirm their subsequent application as a fertilizer through actual plant response observations, in which the impact of phosphate-loaded BC-LDHs 6 (P-BC-LDHs 6) at various application rates on seed germination was examined. The results were also compared with that of phosphate-containing pure LDHs (P-LDHs).

6.2 Materials and methods

6.2.1 Materials

The reagents used for all analyses were of analytical grade and purchased from Wako Pure Chemical Industries, Ltd., Osaka, Japan. Deionized water used for all the experimental procedures was obtained from Eyela Still Ace SA-2100E, Tokyo Rikakikai Co., Ltd. (Tokyo, Japan). Lettuce seeds (*Lactuca sativa* L.) were purchased from a local market in Yamaguchi, Japan.

6.2.2 Characterization of fertilizers

The pH and electrical conductivity (EC) were measured in a suspension of each fertilizer with deionized water at a 1:2.5 (w/v) ratio using a pH meter (D-51, Horiba, Ltd., Kyoto, Japan) and an EC meter (ES-14, Horiba, Ltd., Kyoto, Japan), respectively. The moisture content was determined by the mass loss after drying the samples overnight at 105 °C. Water-holding capacity was expressed as the amount of deionized water held by the dry samples. The cation exchange capacity (CEC) measurement was carried out by saturation with sodium acetate solution with a pH value

of 8.2. All analyses were performed according to the methods outlined by the Food and Agricultural Organization of the United Nations [107]. The elemental composition of the fertilizer products was determined using inductively coupled plasma atomic emission spectroscopy (ICP-AES, SPS3500, SII Nano Technology Inc., Tokyo, Japan) after acid digestion.

6.2.3 Seed germination bioassay

In order to predict the plant responses on the addition of P-BC-LDHs 6 and evaluate its effective dosage for stimulation of seedling growth, seed germination was conducted as a bioassay for the quality assessment of P-BC-LDHs 6. This method has been the subject of considerable attention, recently owing to its time-saving processability, reliability, and low cost [108]. Lettuce (*Lactuca sativa* L.) was selected as a testing plant because of its short growth cycle and its common consumption worldwide.

Lettuce seeds were initially soaked in 0.1% sodium hypochlorite solution for 5 min for sterilization, followed by washing with deionized water. Fifty seeds were then germinated in Petri dishes, where 0.5, 1.0, 2.5, and 5.0 g of P-BC-LDHs 6 were separately placed on a filter paper (Whatman No. 1), which was moistened with 10 mL of deionized water. The sample application rates were applied as recommended by Morrison and Morris [109]. The covered Petri dishes were kept in a chamber at 25 ± 0.5 °C for 5 d under darkness. Deionized water was used as a control. All plant germination experiments were carried out in four replicates with a randomized block design. After incubation, the seeds were evaluated for the percentage of germination and early seedling growth by measuring seedling length, which is the sum of leaf, stem, and root lengths [110], using the Image J 1.41 software (National Institute of Mental Health, Bethesda, Maryland, USA). A seed was considered to have germinated if the length of the radicle was at least 1 mm [111,112]. Moreover, the fresh and dry weights together with the elemental contents of the biomass were recorded. Treatments were named T1, T2, T3, and T4, corresponding to P-BC-LDHs 6 quantities of 0.5, 1.0, 2.5, and 5.0 g used for the germination test, respectively. P-LDHs were also carried by following the same procedure as that employed for P-BC-LDHs 6. Treatments containing 0.5, 1.0, 2.5, and 5.0 g of P-LDHs were denoted as t1, t2, t3, and t4, respectively.

6.2.4 Statistical analysis

The mean and standard deviation were obtained for all data. Differences among treatment groups and controls were calculated and compared by one-way analysis of variance (ANOVA) with a Tukey-Kramer post-hoc test using Microsoft Excel (Microsoft Japan Co., Ltd., Tokyo, Japan). The level of statistical significance was set at $p < 0.05$.

6.3 Results and discussions

6.3.1 Characterization of fertilizers

The physicochemical properties of the as-prepared P-BC-LDHs 6 and P-LDHs from this study are detailed in Table 4. As both samples were synthesized under alkaline conditions, the resultant P-LDHs and P-BC-LDHs 6 exhibited a high pH value of 8.25 and 9.02, respectively. It is worth mentioning that the pH of fertilizer is one of the crucial factors in controlling plant nutrient availability in soil because the deficiency of major nutrients, including phosphorus, potassium, calcium, and magnesium, is directly affected by acidic soil, particularly phosphorus, which is able to react with aluminum and iron, leading to the formation of highly insoluble compounds, and thereby becoming unavailable to plants [113]. In this context, the use of these materials to soil would exert a positive liming effect, which can remediate soil acidity, thus leading to soil fertility improvement. The EC of P-BC-LDHs 6, which is expressed as the level of nutrient concentration in the sample, is relatively high (1.36 dS/m) compared to that of P-LDHs (0.00365 dS/m). The moisture content of P-BC-LDHs 6 and P-LDHs were 2.20 and 4.99, respectively. It was expected that high surface area and porosity of biochar in P-BC-LDHs 6 were responsible for its great water retention (65%), which was far higher than that of P-LDHs (40%). The high water-holding capacity of the composite, which refers to the amount of water held within the samples, will develop the ability of soil to retain water and enhance the efficiency of water use in agricultural production in terms of water supply for plants. It was also observed that P-BC-LDHs 6 had high nutrient retention capacity with CEC of 23.1 cmol/kg because of a combined effect of specific surface area, porosity, and chemical functional groups of biochar [114]. On the other hand, the CEC of P-LDHs was found to be 7.50 cmol/kg.

Table 4. Basic physical and chemical properties of P-BC-LDHs 6 and P-LDHs

Parameters	P-BC-LDHs 6	P-LDHs	
pH	9.02 (0.02)	8.25 (0.01)	
Electrical conductivity (EC) (dS/m)	1.36 (0.02)	0.00365 (0.11)	
Moisture content (%)	2.20 (0.29)	4.99 (0.09)	
Water holding capacity (%)	65 (0.00)	40 (0.00)	
Cation exchange capacity (CEC) (cmol/kg)	23.1 (1.27)	7.50 (0.02)	
Phosphorus (mg/g)	4.67 (0.06)	4.41 (0.14)	
Magnesium (mg/g)	138 (2.81)	200 (1.45)	
Aluminum (mg/g)	64.7 (2.22)	88.3 (1.08)	
Pollutants	P-BC-LDHs 6	P-LDHs	Maximum acceptable levels
Cobalt (mg/g)	ND	ND	0.15
Nickle (mg/g)	ND	ND	0.18
Copper (mg/g)	0.0325 (0.01)	ND	-
Zinc (mg/g)	0.0519 (0.00)	ND	1.85
Cadmium (mg/g)	ND	ND	0.02
Molybdenum (mg/g)	ND	ND	0.02
Lead (mg/g)	ND	ND	0.50

Values represented in the table are the average data of triplicate measurements with standard deviations in parentheses. ND: not determined.

Moreover, elemental analysis demonstrated that approximately 5 mg/g of phosphorus, 138 mg/g of magnesium, and 65 mg/g of aluminum were accommodated in P-BC-LDHs 6. On the contrary, the determination of elemental composition in P-LDHs represents approximately 4 mg/g of phosphorus, 200 mg/g of magnesium, and 88 mg/g of aluminum. Undoubtedly, heavy metals are influential contributors to pollution in agricultural fields, and heavy metal accumulation in crops grown in metal-polluted soil or growing media can have deleterious effects on human health through the food chain [115]. The assessment of heavy metal contamination shows that there were no hazard elements, including cobalt, nickel, cadmium, molybdenum, and lead, contained in P-BC-LDHs 6. Nonetheless, copper and zinc were detected probably due to the fact that biochar has inherent heavy metals within the structure derived from its source materials, which may be concentrated in ash fractions during pyrolysis [116]. However, the concentrations of these two elements were extremely low (less than 0.1 mg/g) and below the Canadian standard adopted for heavy metals in fertilizer products [117], indicating that P-BC-LDHs 6 application is not considered to cause detrimental impacts with regards to heavy metal pollution. Similarly, there was no heavy metal contamination in the P-LDHs, that they exhibited high purity, and that the introduction of mixed metal salts during synthesis was efficient.

These results suggest that the essential nutrients available in P-BC-LDHs 6, phosphorus and magnesium, would become a valuable resource for crop production when they are applied to soil or growing substrates. In addition, their interesting properties, such as high pH and water-holding capacity, would potentially improve soil properties in terms of increasing pH in acidic soil and enhancing soil water retention, which in turn promotes water availability to plants. Indeed, considering the need for producing fertilizers without harmful substances, both for humans and the environment, the transformation of P-BC-LDHs 6 to a fertilizer could be recognized as a safe and sustainable practice that does not create further pollution and offer an interesting option for waste disposal of used adsorbents.

6.3.2 Seed germination bioassay

6.3.2.1 Effect of application rates of P-BC-LDHs 6 on seed germination

Seed germination is one of the most crucial phases in the plant life cycle and can be expected as a determinant for crop productivity. Hence, the successful seed germination and early seedling growth characteristics can be an early indicator to evaluate the usability of P-BC-LDHs 6 in agronomic systems. As a first step to understand whether and how P-BC-LDHs 6 can modulate the production of plants, the effects of P-BC-LDHs 6 on yield and quality of lettuce seeds cultivated in the different dosages of these products were compared as demonstrated in Figure 25.

On the first day of experiments, it is likely that the simulation of seedling emergence was observed in response to an increase in concentrations of P-BC-LDHs 6 (Figure 25(a)). Seed germination percentages for T1, T2, T3, and T4 were 93%, 94%, 96%, and 96%, respectively, whereas that of untreated seeds was 94%. Meanwhile, the final percentages of seedling establishment on the last day of germination for all treatment groups were still high with the maximum germinability of 99%. However, statistical analysis exhibits that there were no significant differences among lettuce seeds planted with and without P-BC-LDHs 6 ($p > 0.05$). Figure 25(b and c) thereafter presents growth characteristics of seedlings harvested after the experiments. Seedling lengths were substantially different between the control and treatment groups ($p < 0.05$). The greatest seedling length (36.43 mm) was found in the control plants, whereas that of treated plants ranged from 18.41 mm to 24.52 mm. Similarly, fresh biomass was also significantly affected by the application rates of P-BC-LDHs 6. The total mass of seedling for all cases of P-BC-LDH 6 addition decreased by approximately 20% to 54% compared to that of the non-treatment. On the contrary, the promotion of dry matter accumulation was observed, showing seedlings with the better condition (0.044-0.051 g) derived from P-BC-LDH 6 treatments, which was comparable to the controls (0.039 g). The overall findings from this seed germination bioassay identified that across all treatments, T3 showed the best potential for efficient seedling establishment as well as development of seedling lengths and biomass yields; however, the cultivation of seeds under non-treatment condition allowed healthier growth of germinated seeds.

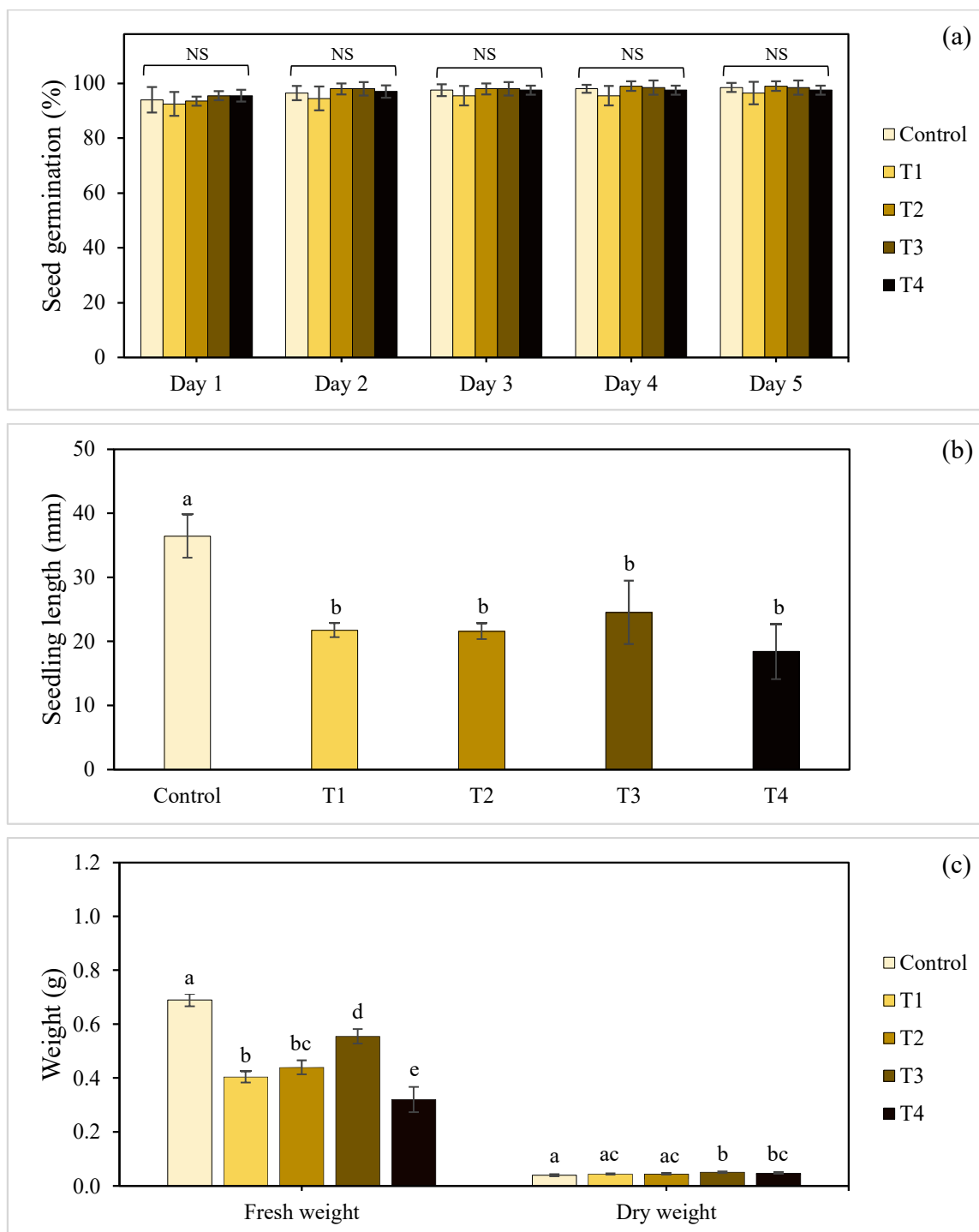


Figure 25. Effect of P-BC-LDHs 6 applied at different rates on seed germination and growth parameters: (a) germination percentage (b) seedling length (c) fresh and dry weight. Different letters indicate statistically significant differences. NS indicates no significance.

Considering that the presence of soluble forms of aluminum in soil has been long recognized as the main deterrent restricting the growth of several agricultural crops, it is possible that the phytotoxic effect of aluminum would occur among seedlings exposed to P-BC-LDHs 6 since this element was used for the synthesis of composite. Apparently, aluminum did not interfere in a clear way with seed germination, but it impaired their morphological features, including seedling height and fresh biomass. Such inhibition on plant growth has been broadly indicated as the primary responses to aluminum toxicity, which is also in accordance with other studies detecting a significant reduction in biomass as well as root and shoot length of many plants treated with varying levels of aluminum [118–120]. This negative feedback in plants was a consequence of aluminum penetration into plant tissues, which then promoted the rigidification of cell wall and resulted in the prevention of root development. Further, the suppression of root growth could ultimately cause blockade of nutrient and water transport, leading to the decrease in biomass content and seedling length [121].

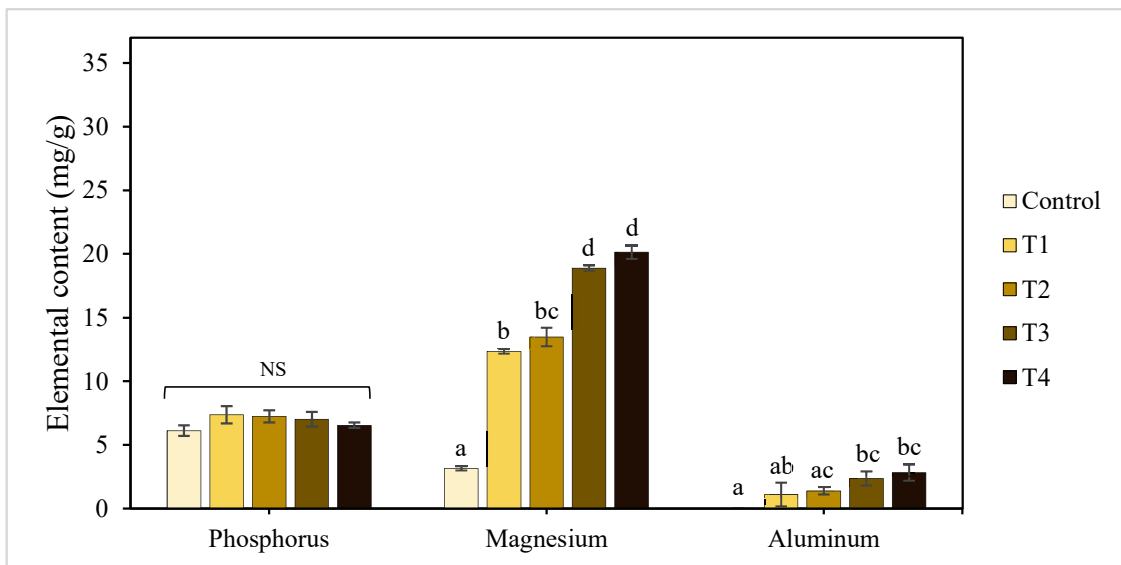


Figure 26. Elemental composition of seedlings under different application rates of P-BC-LDHs 6. Same letters indicate that there are no statistically significant differences among groups. NS indicates no significance.

Data recorded from the elemental composition analysis also confirms the aluminum accumulation in dried seedlings with fertilization (Figure 26). There was a clear correlation between a rise of aluminum levels with the addition of P-BC-LDHs 6. Lettuce seeds imbued in T1, T2, T3, and T4 had the average accumulation of aluminum values, accounting for 1.10, 1.39, 2.36, and 2.81 mg/g, respectively. By contrast, the control lettuce contained almost absence of this metal. Additionally, the results similarly reveal a dosage-dependent content of magnesium in seedlings, but the slight drop in phosphorus was verified as enhanced concentrations of P-BC-LDHs 6. It has been established that phosphorus deficiency is generally correlated to aluminum because of the formation of insoluble aluminum phosphate compounds, by which the absorption of such nutrient becomes ineffective [122]. In these experiments, the author proposes that such undissolved complexes could be formed and progressively accumulate in root tissues of lettuce seedlings with increasing aluminum coincided with P-BC-LDH 6 supply, inducing decreased translocation of phosphorus to their stem and leaves. A photograph of seed germination in response to different intakes of P-BC-LDHs 6 on day 5 was also displayed in Figure 27.



Figure 27. Seeds germinated on day 5 under different concentrations of P-BC-LDHs 6

6.3.2.2 Effect of application rates of P-LDHs on seed germination

The germination percentage and the growth of seedlings at various application rates of P-LDHs were successively investigated and compared. As shown in Figure 28(a), significant differences ($p < 0.05$) in the germination percentage compared with the control were observed in treated seeds with the addition of P-LDHs from 1.0 to 5.0 g. It was found that higher dosages of P-LDHs suppressed seed germination. The total percentages of seedling emergence on the last day of germination for the control, t1, and t2 were 95%, 94%, and 84%, respectively, whereas lettuce seeds completely failed to germinate when they were imbued in t3 and t4. The detailed effects of P-LDHs on lettuce seedlings were also demonstrated. Nevertheless, the growth parameters of plants from t3 and t4 were not displayed because it corresponded to the results showing the complete failure of germination. As shown in Figure 28(b), all P-LDH treatments significantly arrested seedling length as compared to untreated plants, with a reduction of at least 77%. Similarly, the yields of biomass grown in P-LDHs were considerably lower than those of the control ($p < 0.05$) (Figure 28(c)). The highest fresh weight, 1.055 g, was achieved with seedlings derived from non-treatment groups, while the biomass under t1 and t2 were 0.223 and 0.145 g, respectively. However, there was no significant change in the dry weight among the control and P-LDH treatments ($p > 0.05$).

In the experiment, the author also visually observed that the presence of P-LDHs induced many roots to be shorter and more swollen, having a stubby appearance in comparison with that of the control. Moreover, their root tips were characteristically brown and thick (Figure 29). These morphological features are normally associated with the phytotoxic effect of aluminum, and such modification of the root system has consequently resulted in inefficient water uptake and nutrient supply by plants [123,124]. It was also established that these negative responses were due to the aluminum interference with cell division of radical apices, promoting rigidification of cell wall, and inevitably resulting in the prohibition of root elongation as well as poor or no root-hair development [125]. The effect of aluminum toxicity on plants, for example, the restraint of seed germination, prevention of lateral root and root hair formation, biomass reduction, and disruption of cell wall has been broadly reported previously by several authors [126–128].

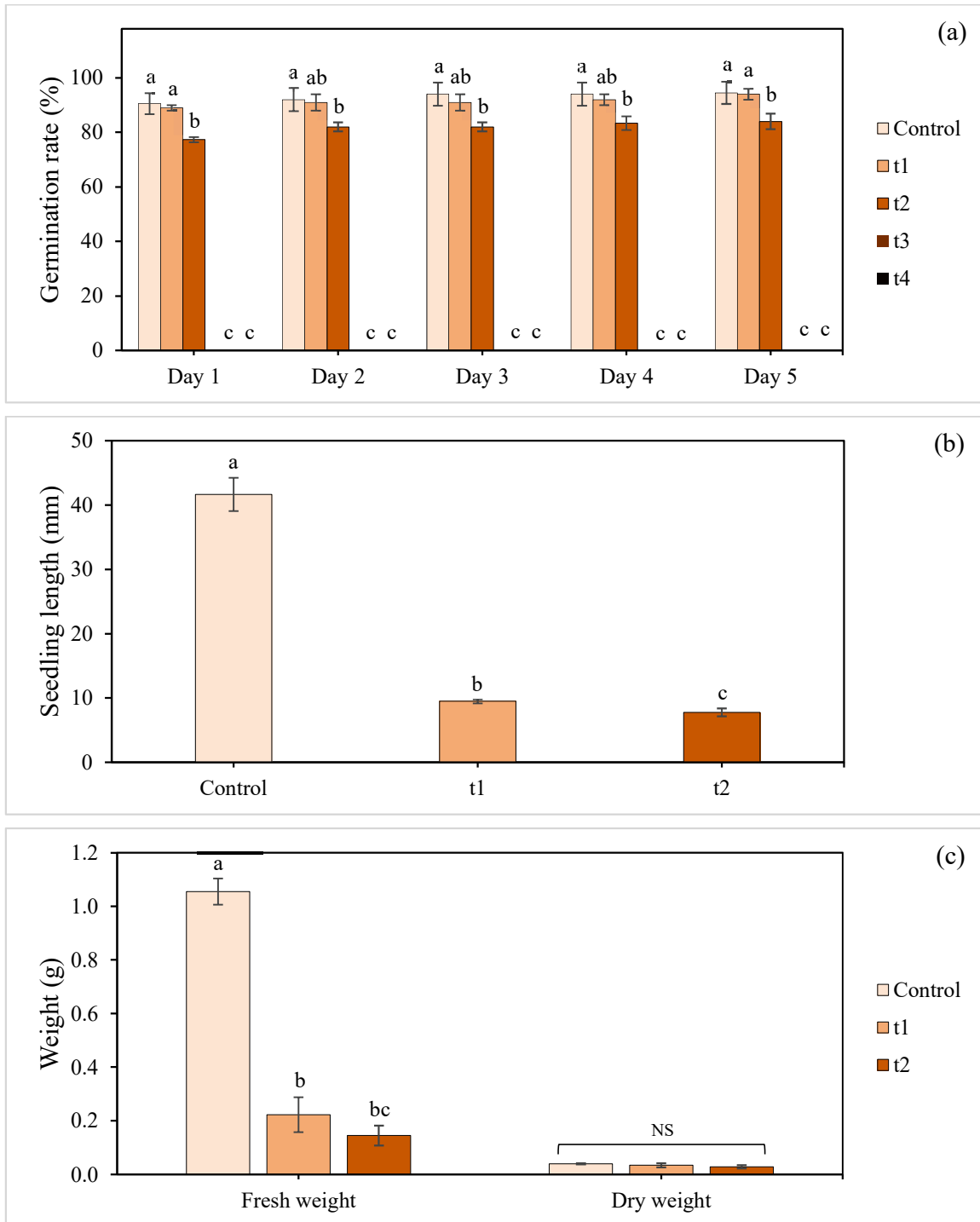


Figure 28. Effect of P-LDHs applied at different rates on seed germination and growth parameters: (a) germination percentage (b) seedling length (c) fresh and dry weight. Same letters describe that there are no statistically significant differences among groups. NS indicates no significance.



Figure 29. Negative effect of aluminum on seedling roots under P-LDH treatments. Position of symptoms caused by aluminum toxicity is indicated by arrows. The inset shows untreated roots, which were longer and appeared white in color, including the presence of root hairs.

Furthermore, Eisenmenger [129] and Neenu and Karthika [130] also highlighted that lettuce can be grouped under the category of aluminum-sensitive plant species along with beet and barley, especially with respect to young seedlings, which are more susceptible to aluminum stress than the older plants. When the amount of aluminum for each treatment was calculated in terms of aluminum weight per unit volume of solution in Petri dishes, the aluminum concentration attained was within a range of 4,415 to 44,150 mg/L, which was far greater than that of sufficient levels (3.50-5.00 mg/L), which can lead to severe restrictions on the growth of several agricultural crops

[131]. These findings clearly imply that aluminum toxicity, which correlated with an increase in P-LDH levels, could be explained as the main factor contributing to plant growth inhibition in the treatment groups. The excessive accumulation of aluminum was further confirmed by the elemental contents of lettuce seedlings in Figure 30. The total quantity of aluminum notably increased with increasing concentration of P-LDHs, and this increase was negligible in the control plants. In contrast, only minor differences, in comparison to the control, were observed for phosphorus, suggesting that the existence of large amounts of aluminum might be related to decreased phosphorus availability by the production of insoluble aluminum phosphate compounds, thereby plants found it difficult to absorb the phosphorus [122]. This result also turned out to be in agreement with those of Macedo and Jan [132] and Wenzl et al. [133], proposing that the formation of aluminum-phosphorus complexes inside plant roots can render the part of unavailable phosphorus, and the translocation of this nutrient within the plants, as a consequence, would become inefficacious. For these reasons, the disruption of the phosphorus absorption process was undoubtedly susceptible to aluminum stress. In the case of magnesium, there was no detrimental effect influenced by excess aluminum. Photographs of seed germination responses under different concentrations of P-LDHs on day 5 are also illustrated in Figure 31.

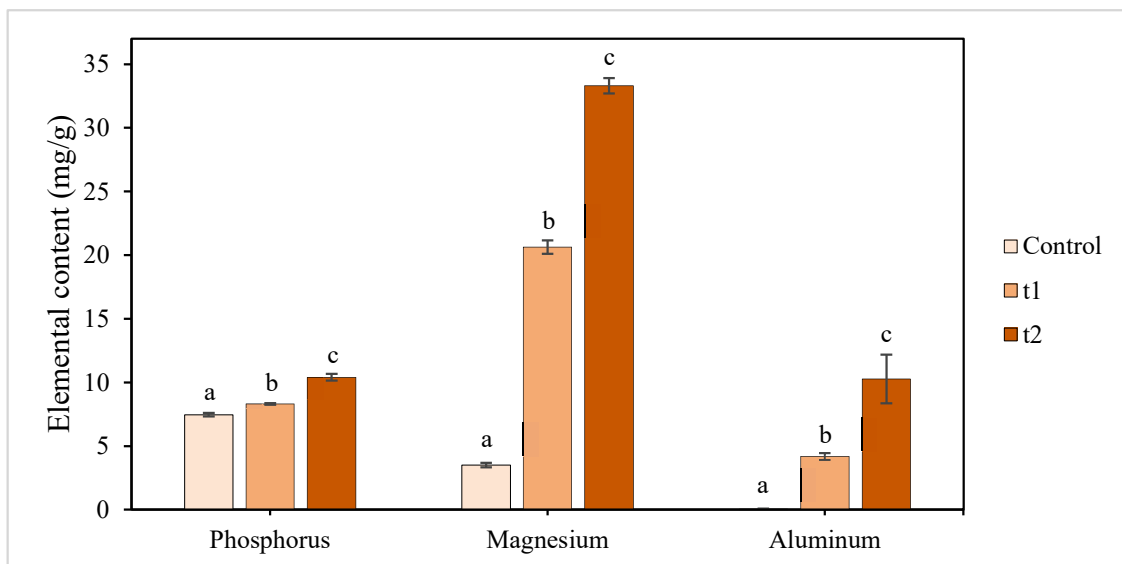


Figure 30. Elemental composition of seedlings under different application rates of P-LDHs. Different letters indicate statistically significant differences.

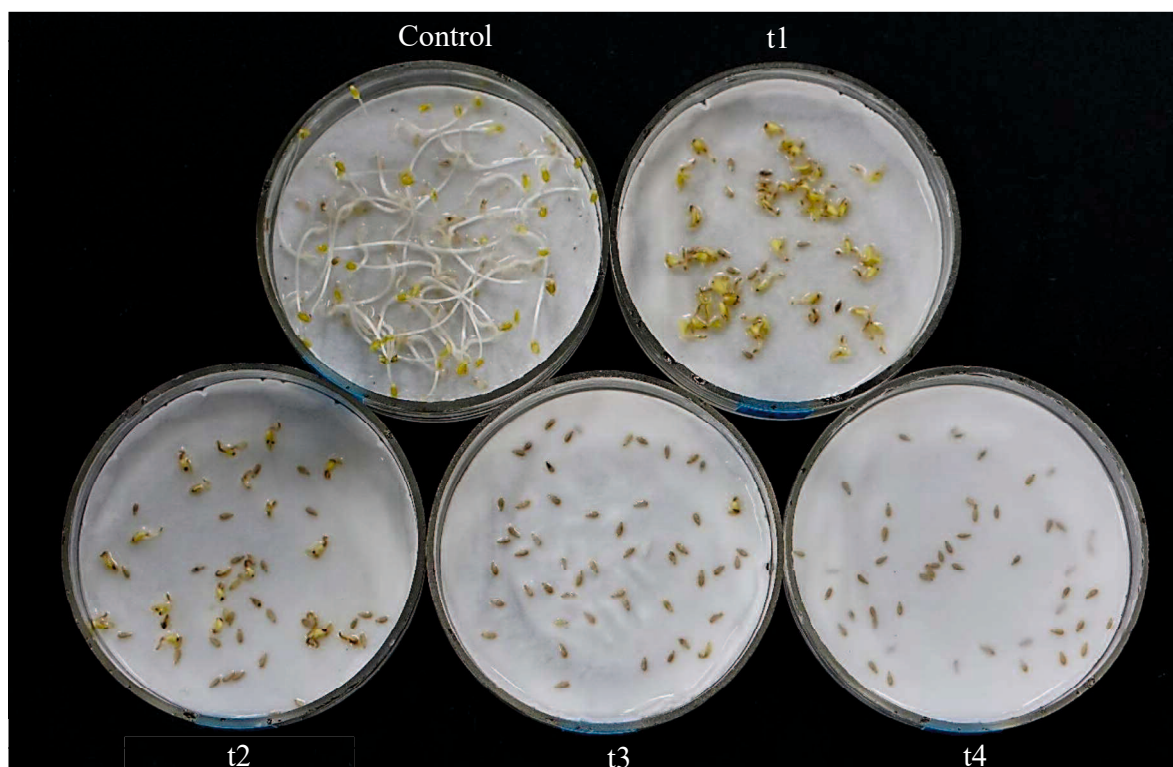


Figure 31. Seed responses under different concentrations of P-LDHs on the last day of germination.

6.3.2.3 Comparison of plant growth performance derived from P-BC-LDH 6 and P-LDH treatments

The data from the above observations, which had conducted the effectiveness of P-BC-LDHs 6 and P-LDHs as fertilizers for the optimized germination and initial development of lettuce seedlings, has overall supported that aluminum was expected to adversely interfere with seedling establishment, not only through delayed germination but also diminishing seedling development, mainly by reducing the length of seedlings as well as their fresh biomass. It is noteworthy that seed germination is regarded as the most sensitive stage in the life cycle of plants [134]. Therefore, the exposure of lettuce seeds in direct contact with those fertilizers was not recommended for this study because of the aluminum toxicity, which was more perilous for the seedling period of plants,

resulting in unhealthy growth. However, in order to discriminate between P-BC-LDH 6 and P-LDH performance, the comparison of plant growth indices of lettuce seedlings cultured in both products is drawn and presented in Table 5. Since previous findings suggested that the most adequate rates for P-BC-LDH 6 and P-LDH application for seed germination were 2.5 g (T3) and 0.5 g (t1), respectively, this section is focused solely on the interaction between these two treatments and lettuce plants.

Table 5. Comparison of plant growth performance from P-BC-LDH 6 and P-LDH treatments

Growth parameters	Treatments	
	P-BC-LDHs 6 (T3)	P-LDHs (t1)
Seed germination (%)	99 ^a (2.60)	94 ^a (2.00)
Seedling length (mm)	24.52 ^a (4.94)	9.50 ^b (0.32)
Fresh weight (g)	0.555 ^a (0.03)	0.223 ^b (0.07)
Dry weight (g)	0.051 ^a (0.00)	0.034 ^b (0.01)

Values represented in the table are the average data with standard deviations in parentheses and different letters indicate statistically significant differences between different groups.

It is noticeable from the table that T3 showed higher values in all the parameters. In detail, T3 induced higher seed germination (99%) than t1 (94%), although the differences were not statistically significant ($p > 0.05$). Also, lettuce seeds treated with T3 had the capability to significantly produce more longer seedling length (24.52 mm) compared to ones treated with t1 (9.50 mm) ($p < 0.05$). Moreover, fresh and dry weight of plants markedly decreased by approximately 60% and 33%, respectively, when they were grown in P-LDHs ($p < 0.05$). In conclusion, lettuce germinated in T3 appeared to be more vigorous than those from t1 that could be attributed to the presence of lower aluminum content in the P-BC-LDH 6 composite.

6.4 Conclusions

P-BC-LDHs 6 with several application rates were investigated to confirm their subsequent application as a fertilizer through actual plant response observations by using the seed germination assay of lettuce crops. The obtained results were indicative of inhibitory effect of P-BC-LDHs 6 induced by aluminum toxicity on seedling development, revealing unfavorable plant appearances from all treatment groups, including significantly low seedling growth and fresh biomass, with a reduction of at least 20% in comparison to the non-treated control. However, P-BC-LDH 6 application still provided much more seed germination ability and favorable seedling traits in comparison to P-LDHs. Lettuce cultivated under the suitable dosage of P-BC-LDHs 6 (T3) possessed superb seed germination percentage (99%) over those from P-LDHs (94%) (t1). In addition, the length of lettuce seedlings from such treatment as well as their biomass yields were increased by at least 50% compared to P-LDH-treated samples. In summary, this study pointed out that post-adsorption BC-LDHs 6 did not have the ability to boost seed germination and improve seedling quality in comparison with the control plants.

Chapter 7 – Assessment of early plant growth performance for application of phosphate-loaded biochar functionalized with layered double hydroxides as fertilizer⁴

7.1 Introduction

In addition to direct interest in the evaluation of varied dosage performances of P-BC-LDHs 6 on seed germination, fertilizer administration is also critical during the initial period of plant development in order to maintain adequate nutrient levels for crop nutrition. In addition, since nutrient requirements vary depending on the crop growth stage, such relationship would be synergistic at a certain concentration range of P-BC-LDHs 6 but it may become antagonistic when the concentration of P-BC-LDHs 6 is too high. In these contexts, the successive early-stage growth responses of lettuce in relation to the application of P-BC-LDHs 6 were more evaluated. Moreover, a comparative investigation was also conducted on P-LDHs in order to competitively estimate their performance on the initial growth and development of those crops. Specifically, the purposes of this chapter were as follows: (1) investigate the early growth responses of leafy vegetables to a comprehensive range of P-BC-LDH 6 and P-LDH concentrations in realistic growing systems, (2) determine the optimal application rates of each fertilizer to induce plant growth, and (3) evaluate the application potential of these two adsorbents for agricultural purposes through a comparison of multiple vegetative growth indices.

7.2 Materials and methods

7.2.1 Materials

The chemicals used in this study were of analytical grade, which were purchased from Wako Pure Chemical Industries, Ltd., Osaka, Japan. All the experiments were performed using deionized

⁴ Parts of this chapter were previously published by Buates J, Imai T. Assessment of plant growth performance and nutrient release for application of phosphorus-loaded layered double hydroxides as fertilizer. *Environmental Technology & Innovation*. 2021; 22: 101505 [153] and Buates J, Imai T. Application of biochar functionalized with layered double hydroxides: Improved plant growth performance after use as phosphate adsorbent. *Applied Sciences*. 2021; 11: 6489 [154].

water obtained from Eyela Still Ace SA-2100E, Tokyo Rikakikai Co., Ltd. (Tokyo, Japan). Lettuce seeds (*Lactuca sativa* L.) were purchased from a local market in Yamaguchi, Japan.

7.2.2 Early plant growth experiments

To further explore the responses of plant growth to P-BC-LDH 6 application during the initial period of plant development, ongoing experiments involving four treatments, 0.5%, 1.0%, 2.5%, and 5.0% (w/w), which were denoted as T5, T6, T7, and T8, respectively, were carried out. These application rates were applied based on common use rates provided in earlier published reports of biochar fertilization [135,136].

In these experiments, 20 g of commercially supplied peat-based growing media was thoroughly blended with each treatment in plastic containers. A control treatment, without P-BC-LDH 6 addition, was also included. Each lettuce seedling germinated after 5 d with a similar size was planted individually in those containers, after which all seedlings were cultured in a growth chamber at a temperature of 23 ± 0.5 °C and a daily photoperiod of 18 h under LED light (two 7.5-watt tubes, Nikki Trading Corp., Osaka, Japan). Early plant growth tests were also performed in four replicates. Multiple vegetative growth indices as well as their elemental composition were evaluated after 21 d of transplanting. Shoot length is expressed as the base of lettuce to the tip of the tallest leaf, and root length refers to the base of lettuce to the longest root tip [137]. These variables were also measured using the Image J 1.41 software. Additionally, early plant growth experiments were similarly performed with P-LDHs at ratios of 0.5%, 1.0%, 2.5%, and 5.0% (w/w), which were named t5, t6, t7, and t8, respectively.

7.2.3 Statistical analysis

Mean values of obtained data among treatment groups and controls were compared by one-way analysis of variance (ANOVA) with a Tukey-Kramer post-hoc test using Microsoft Excel (Microsoft Japan Co., Ltd., Tokyo, Japan) at the statistical significance level of $p < 0.05$.

7.3 Results and discussions

7.3.1 Effect of application rates of P-BC-LDHs 6 on early plant growth

The early plant growth investigations were then adopted to further examine whether the proposed P-BC-LDHs 6 have similar consequences on plants when they are grown in a realistic growing system. Fortunately, the addition of P-BC-LDHs 6 at all application rates in combination with the substrate cultures did not pose a serious problem threatening the productivity of lettuce, which was inconsistent with the outcomes from seed germination tests. It is likely that the effect of this composite on plants relied on the dosing quantity.

The results indicating shoot and root length of 21-day-old lettuce plants are reported in Figure 32(a). The treatments of P-BC-LDHs 6 positively impacted these growth attributes, enabling the gradual increment values of total plant height over the untreated controls. Specifically, those lettuce grown under the mixtures with more P-BC-LDHs 6 disclosed the superior performance of shoot growth, which was larger by a factor of approximately 1.1 in comparison to ones with less P-BC-LDHs 6, while shoot height was lowest for plants grown without amendment. Following a similar trend, the presence of P-BC-LDHs 6 was also beneficial for root elongation. Under the normal condition (substrate alone), the poorest root improvement was observed in samples with 69.45 mm in length. Contrarily, when growing media was amended with P-BC-LDHs 6, they emphatically possessed longer roots, especially those from T7 and T8, of which the significant enhancement of up to 45% was attained ($p < 0.05$). When it comes to lettuce yield responses, all treatments, particularly T7 and T8, still acquired the promotion ability of their fresh biomass as exhibited in Figure 32(b). With fertilization, the observed biomass production averaged from 2.035 g to 2.229 g, which was higher than that of vegetables from pure cultures (1.946 g). Nevertheless, there were no significant differences among the control and treatments ($p > 0.05$). Moreover, a reduction of at least 10% in dry weight values was appeared when the composite was not used; however, the application of this material insignificantly affected both fresh weight and dry matter accumulation ($p > 0.05$). Even though it seems that these favorable outcomes were in progress corresponded to a rise in P-BC-LDH 6 dosages and the outstanding growth quality was more pronounced in plants from the last two highest composite intakes, there were no meaningful

differences among samples from T7 and T8. Also, some growth indices of lettuce crops from T8 were observed to be slightly lower than that from T7. In this regard, 2.5% (w/w) of P-BC-LDH 6 supply was sufficient for advancement of lettuce traits from this study.

Elemental analysis in Figure 32(c) further highlights the effect of dosing quantity of P-BC-LDHs 6 on nutrient uptake by plants. The assimilation of P-BC-LDHs 6 in substrates resulted in the excellent phosphorus concentration within plant tissues. Especially, more profound influence on phosphorus uptake was indeed noticeable in the treatments with higher dosages (T7 and T8), which increased by up to 21% and 27% in comparison to the rest treatments and controls, respectively. Simultaneously, a larger amount of magnesium by a factor of about 1.1 was also detected for every treated lettuce. These findings clearly imply that the resultant fertilizer could provide such agricultural growing media with more available nutrients for plants, and therefore contributing to satisfactory progress in vegetable growth beyond ones grown without P-BC-LDHs 6. Surprisingly, the changes of aluminum, which is a potentially toxic constituent for crop production and a concerned issue in this study, were extremely modest as evidenced by a statistically insignificant relationship among individual treated and control plants ($p > 0.05$).

In general, aluminum is typically found as minerals in soil. Nevertheless, in strongly acid soil, especially at pH lower than 4.3, it will turn up to severely impede physiological and biochemical processes of plants and consequently their productivity due to its excessive solubilization and enhanced presence of trivalent aluminum (Al^{3+}), which is known to be the most toxic form [138,139]. Thanks to the alkalinity of P-BC-LDHs 6 as indicated in Table 4, P-BC-LDH 6 application could compensate for acidity of growing media used that greatly assisted the amelioration of aluminum phytotoxicity. To support this explanation, pH measurement of each substrate was performed after 21 d of experiments. The results disclosed effectiveness of this composite in pH improvement of all growing media with values ranging from 4.7 to 5.2, which was comparable to those without amendment (4.4). In addition, the fact that young seedlings are more prone to aluminum stress than older plants was proposed to be the reason [130], for which lettuce from this observation did not present any signals of toxicity even at high concentrations of P-BC-LDHs 6 applied, which was inconsistent with their interaction from seed germination.

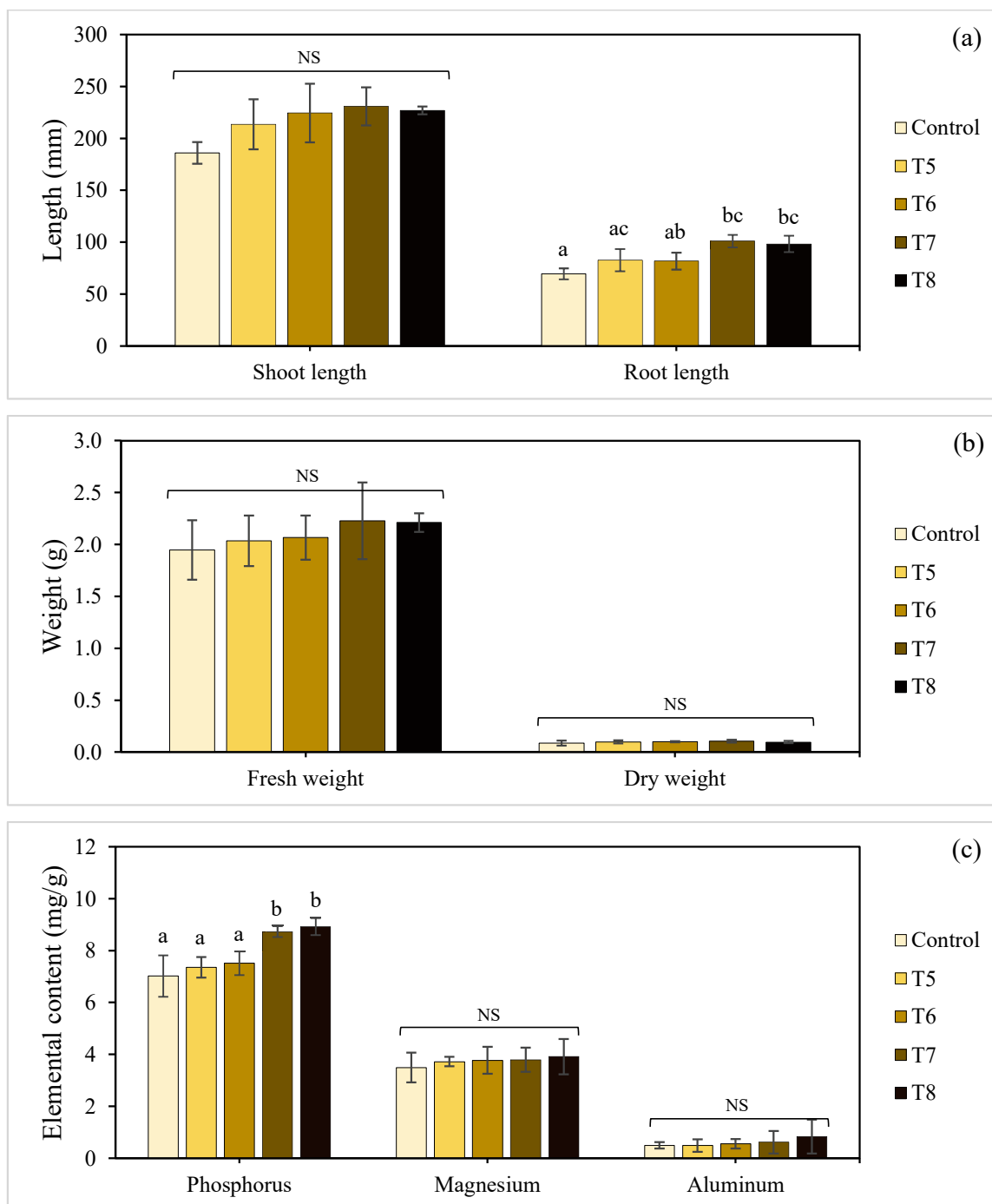


Figure 32. Effect of P-BC-LDHs 6 at different dosages on growth parameters and elemental composition of lettuce from early plant growth experiments: (a) shoot and root length (b) fresh and dry weight (c) elemental analysis. Different letters indicate statistically significant differences. NS indicates no significance.



Figure 33. Comparison of lettuce from the control and different treatments of P-BC-LDHs 6.

It is noteworthy that apart from serving as a good source of nutrients, its excellent characteristics, including high pH, water retention, and CEC could partly account for growth stimulation in lettuce. There were correlated consequences on increasing pH in P-BC-LDHs 6-treated growing media, where microorganism activity and nutrient availability would be consecutively promoted in addition to aluminum tolerance and thus being beneficial to plant growth [140]. At the same time, since biochar used in this study exhibited well-developed porosity and large surface area, there were many advantages behind the addition of P-BC-LDHs 6 in terms of alteration of physical properties of substrates, such as water storage capacity, penetration resistance, and bulk density. This in turn encouraged water and nutrient retention as well as minimized nutrient leaching, which indirectly complemented lettuce development [141,142]. Also, it has been previously stated that high CEC of biochar could be another reason for improving phosphorus bioavailability and uptake [143]. Therefore, based on the above findings, it is interpretable that utilization of this spent adsorbent to agricultural growing media was very successful for facilitating horticultural plant conditions in attempts of its recycling as a fertilizer and the recommended application amount of P-BC-LDHs 6 was 2.5% (w/w). Additionally, phosphorus available in the spent composite would

offer an attractive alternative as a slow-release fertilizer since both biochar and LDHs have become an increasingly investigated strategy for enhancing nutrient utilization [144,145]. Moreover, visual differences among lettuce crops from the controls and treatments are illustrated in Figure 33.

7.3.2 Effect of application rates of P-LDHs on early plant growth

Lettuce was also cultured in realistic growing systems in combination with various application rates of P-LDHs and multiple vegetative growth indices among individual treatments and the control were compared. Among the treatments studied, P-LDHs applied at 1.0% (w/w) (t6) showed excellent performances for the improvement of both plant shoot and root length (Figure 34(a)). The average shoot length of lettuce from non-amended growing media was approximately 167 mm, whereas that from t6 was enhanced by approximately 9%. Nonetheless, the other three cases slightly reduced plant growth compared to the control. As presented thereafter in Figure 34(a), t6 still maximized the vegetable roots with 71.26 mm in length; however, statistical analysis reveals that there were no substantial differences among lettuce planted in the substrate with and without P-LDHs.

The yield responses of lettuce in each pot were also measured, and the results are illustrated in Figure 34(b). The progressive enhancement in fresh weight coincided with a rise in P-LDH concentrations, but P-LDHs at dosages higher than 1.0% (w/w) caused a decline in fresh biomass. Specifically, the fresh weight of lettuce was lowest in t8 (1.457 g) and was greatest in t6 (1.723 g), which was also remarkably higher than that of lettuce grown without P-LDH addition (1.422 g) ($p < 0.05$). When it comes to a dry matter production, a similar trend was noticed. A P-LDH dose of 1.0% (w/w) produced the best productivity with 0.072 g of dry matter, compared to 0.055 g when P-LDHs were not used. Nonetheless, there were no significant differences in this parameter among the test groups and the control group ($p > 0.05$).

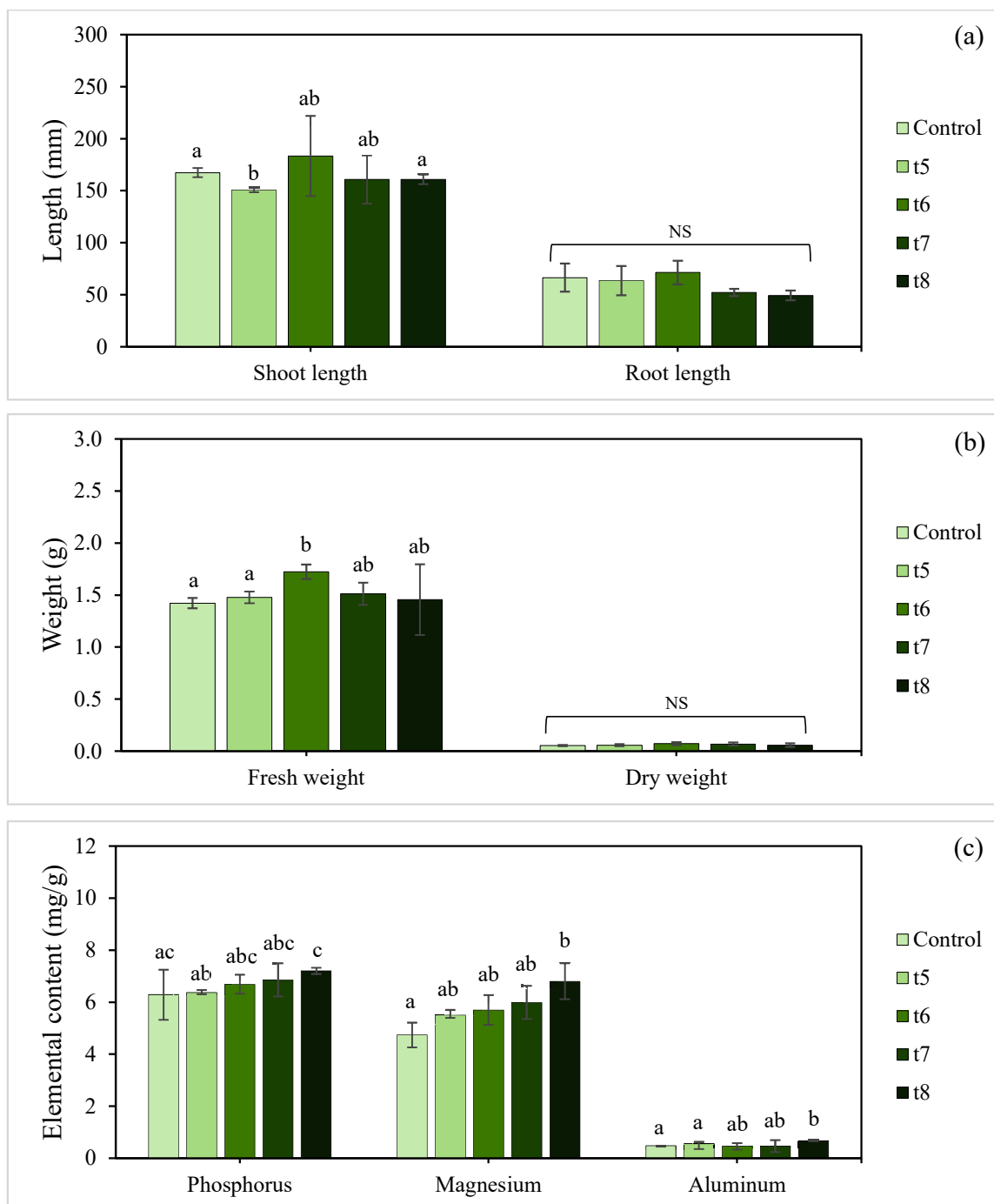


Figure 34. Effect of P-LDHs at different dosages on growth parameters and elemental composition of lettuce from early plant growth experiments: (a) shoot and root length (b) fresh and dry weight (c) elemental analysis. Different letters indicate statistically significant differences. NS indicates no significance.

The elemental values of lettuce leaves after 21 d of cultivation are presented in Figure 34(c). The P-LDHs supplied a larger amount of phosphorus and magnesium for plants by a factor of approximately 1.0 to 1.4 than those cultivated without P-LDHs. Serious concerns about aluminum issues, which are highly toxic to plants, have been raised as to whether aluminum in P-LDHs would be released when it is in contact with growing media and is not acceptable for the plant growth process. However, most of the P-LDH dosages applied and non-treatment groups did not show any significant differences ($p > 0.05$), disclosing their aluminum contents ranging from 0.452 to 0.680 mg/g.

In fact, aluminum is the most abundant metal on earth, and it is the third most abundant element (after oxygen and silicon) in the earth's crust; however, its availability depends on soil pH [138]. At pH values lower than 4.3, trivalent aluminum (Al^{3+}) is the most abundant form and has a powerful impact on plant growth [138]. Fortunately, increased pH of substrate cultures was observed after fertilization of P-LDHs. pH measurements were carried out after 21 d of treatment with P-LDHs, and the pH for all cases was in the range of 4.3 to 5.8, which could therefore alleviate aluminum accumulation in plants. It is well known that aluminum toxicity is more pronounced in seedlings than in more adult plants [139], which could explain why lettuce in these experiments did not show any toxicity symptoms even at high levels of P-LDH supply in comparison with those from the seed germination assay. It has been proposed that aluminum transport is frequently insufficient in the mature stage of plants because of their much lower efficiency of translocating aluminum to their upper parts via transpiration, which can mediate aluminum distribution in plant leaves. This will, therefore, compromise the potential for a high concentration of aluminum to be stored in adult crops [130,146].

Hence, from the results obtained, it can be presumed that the application of P-LDHs with 1.0% (w/w) in growing media was sufficient for lettuce growth. A possible explanation is that P-LDHs with high pH property could provide consistent positive benefits for reducing the acidity of the substrate, leading to favorable plant growth conditions. The increased pH in P-LDHs-treated growing media could decisively influence the microbial population and enzymatic activities in the system, which might be related to growth stimulation in lettuce [147]. Particularly, a rich source of the majority of essential nutrients, including phosphorus and magnesium contained in P-LDHs

was reflected in best plant growth attributes since they were able to remedy the nutrient deficiency of the growing media used in this study, and those nutrients were also actively absorbed by plants in slightly acidic to near-neutral pH [148]. On the other hand, the restricted growth behaviors from high intakes of this material might be due to the critical toxic limit of magnesium. Despite the fact that magnesium is well described as one of the most important nutrients playing integral roles in many plant functions, the administration of an improper high amount of magnesium can be involved in the prevention of plant development due to osmotic stress. According to Venkatesan and Jayaganesh [149], tea plants established in soil containing 5,000 mg/kg of magnesium showed toxicity symptoms on day 12 and died on day 45 after magnesium treatment. In this experiment, substantial input of P-LDHs (t7 and t8) was observed in the undesirable feedback in plants, especially the reduction of shoot and root lengths in comparison with the control and the rest of treatments. In detail, the calculated magnesium content in the substrate cultures for t7 and t8 accounted for 5,000 and 10,000 mg/kg, respectively, so this evidence could partly be responsible for such phenomena. Thus, 2.5% and 5.0% (w/w) of P-LDH application were proposed to be inappropriate for lettuce growth in this study. A comparison of lettuce plants among the control and different P-LDH treatment groups is displayed in Figure 35.



Figure 35. Comparison of lettuce plants among the control and different treatments of P-LDHs.

7.3.3 Comparison of plant growth performance derived from P-BC-LDH 6 and P-LDH treatments

In search of effective dosage with multiple plant growth promoting traits, the fertilizer supply of 2.5% (T7) and 1.0% (t6) of P-BC-LDHs 6 and P-LDHs, respectively, showed a far greater potential to improve plant productivity when compared to the control and other treatments. Therefore, values of growth parameters from both treatments were primarily compared and the data is presented in Table 6.

Table 6. Comparison of plant growth performance from P-BC-LDH 6 and P-LDH treatments

Growth parameters	Treatments	
	P-BC-LDHs 6 (T7)	P-LDHs (t6)
Shoot length (mm)	231 ^a (18.30)	183 ^a (38.48)
Root length (mm)	101 ^a (6.05)	71 ^b (11.28)
Fresh weight (g)	2.229 ^a (0.37)	1.723 ^a (0.07)
Dry weight (g)	0.105 ^a (0.01)	0.072 ^b (0.02)

Values represented in the table are the average data with standard deviations in parentheses and different letters indicate statistically significant differences between different groups.

The results from Table 6 highlight the positive effects on plant growth parameters caused by the fertilization of P-BC-LDHs 6 during the initial lettuce development, which contributed to a much more obvious stimulatory growth response compared to P-LDH application. Shoot length measured from lettuce cultured in P-BC-LDHs 6 (231 mm) was longer than that from P-LDH treatment (183 mm), representing a great improvement of approximately 26% in this parameter. However, statistical analysis revealed insignificant differences among those samples ($p > 0.05$). In addition, significant root promotion also correlated to P-BC-LDH 6 administration, by which root

length was substantially enhanced by approximately 42% in comparison with that from the other treatment ($p < 0.05$). The findings also showed that P-BC-LDHs 6 induced higher biomass accumulation, both in fresh and dry matter, compared to P-LDHs. Those lettuce traits after amendment with P-BC-LDHs 6 considerably increased up to about 1.5-fold compared to ones with P-LDHs ($p < 0.05$). These observations clearly indicate that P-BC-LDHs 6 allowed the stimulation of plant growth over P-LDHs. According to the physicochemical properties of materials in Table 4, the EC of P-BC-LDHs 6 (1.36 dS/m), which is within the range of optimal levels for lettuce cultivation (1.2-1.6 dS/m) [150], could be related to the outstanding quality of lettuce crops in this study. Meanwhile, the EC of P-LDHs is relatively low (0.00365 dS/m), which may severely affect plant health and yield. The author also assumed that biochar added in the composite was partially responsible for favorable plant attributes. As stated earlier, a high surface area and large pore volume of biochar resulted in greater water holding capacity of this composite, which could have direct and indirect effects on the retention of water in growing media. Its extreme surface and porosity directly raised the water holding capacity and reduced water evaporation of substrates. On the other hand, an indirect effect was the improvement of growing media aggregation, which might positively contribute to its capacity to conserve water [151]. The higher CEC was also found for the biochar composite and the utilization of this material would increase the ability of growing media to adsorb exchangeable cations available for plants and resist nutrient leaching during watering [152]. Therefore, these favorable characteristics of the composite directly attributed to its higher efficiency in lettuce growth promotion than that of P-LDHs.

7.4 Conclusions

P-BC-LDHs 6 and P-LDHs were sequentially assessed for their further application possibility as phosphate fertilizers by using an early plant growth assay, where lettuce was separately grown in the growing media with 0.5, 1.0, 2.5, and 5.0% (w/w) of those fertilizers. The results indicated that vegetables cultivated under the mixtures with high P-BC-LDHs 6, particularly at application rate of 2.5%, possessed superb growth quality. The length of lettuce shoots and roots from such optimal dosage was increased by at least 24% compared to untreated samples; meanwhile, a reduction in biomass yield of 17% was attained for those from non-supplemented substrates. On the other hand, high input of P-LDHs could be detrimental to plants. In this experiment, P-LDHs applied at 1.0%

outperformed other treatments and the control in stimulating plant improvement. Moreover, findings of comparison of plant growth performance from the optimal levels of these two materials verified that P-BC-LDHs 6 caused a significant enhancement of plant development over P-LDHs. An increase of at least 26% in all growth indices was attained for P-BC-LDHs 6-amended plants. This study pointed to the conclusion that BC-LDHs 6 after phosphate remediation could be reused as an agricultural fertilizer to encourage crop quality cultivated under substrate or soil conditions, where an application rate of 2.5% (w/w) was recommended.

Chapter 8 – Key summaries and recommendations

Phosphate removal and recovery have attracted growing interest due to two issues of aquatic eutrophication and global phosphate rock scarcity. Herein, rice straw-derived biochar functionalized with layered double hydroxides (BC-LDHs) was developed for abatement of excess phosphate in water bodies and the spent BC-LDHs was sequentially assessed for their application possibility as an agricultural fertilizer.

Firstly, the difference in phosphate adsorption capacity by several BC-LDHs prepared with varying amounts of biochar and different modification routes, including precipitation of LDHs on pristine biochar and pyrolysis of rice straw loaded with LDHs was simultaneously compared. The most excellent adsorption capability was obtained in the composite, namely BC-LDHs 6, which was synthesized from the highest feedstock dosing quantity through the latter method. In this technique, the structural evolution of thermally treated LDHs contributed to the adsorption improvement of BC-LDHs 6. Moreover, the abundant mesoporous structure of biochar in this material could serve as an effective matrix to support LDHs, thereby increasing active sites for the phosphate removal reaction. Currently, plant-based feedstock is widely used to produce biochar as presented in the present study and most existing research. Hence, greater emphasis on developing composites from varied biochar sources, such as sewage sludge and industrial biowastes should be placed on the synthesis of biochar-based composites.

Secondly, the performance of selected BC-LDHs 6 was extensively investigated under several adsorption-influencing parameters, including solution pH, coexisting anions, reaction time, and initial concentrations of phosphate. The adsorption behavior and interaction mechanisms of phosphate with this propitious adsorbent were also evaluated through a comparison with pure LDHs using various adsorption isotherm and kinetic models. The optimized removal of phosphate on both samples was obtained at pH of 3.0. The kinetic performance of BC-LDHs 6 (24 h) was slower than that of pure LDHs (3 h); however, a maximum adsorption capacity of the composite of up to 192 mg/g was achieved, which exceeded that of pure LDHs by nearly 1.2 times. In both cases, the kinetics of phosphate adsorption followed the pseudo-second-order model, whereas adsorption isotherms were consistent with the Freundlich model. The composite also exhibited

specific selectivity toward phosphate over highly competing anions and pH changes. The prevalent mechanisms of this composite included electrostatic interaction, inner-sphere surface complexation, pore diffusion, precipitation, and reconstruction. The results obtained demonstrate that the amalgamation of both starting materials, biochar and LDHs, has allowed the development of an innovative adsorbent for phosphate removal, the advantages of which are its high potentiality and cost effectiveness. As this study was conducted based on batch adsorption experiments with synthetic phosphate solutions, hence, more investigations should be further extended in order to assess the applicability of this BC-LDH composite in real wastewater under actual environmental conditions. Furthermore, more comprehensive characterization should be performed with the composite before and after phosphate adsorption to further fully understand such proposed mechanisms of this adsorbent to remove phosphate.

Thirdly, the desorption characteristics of previously adsorbed phosphate ions on both adsorbents were tested with different NaOH alkalinity (0.01, 0.1, and 1.0 M). Among concentrations studied, 1.0 M NaOH solution showed the highest desorption efficiency in the range of 73-85%. Meanwhile, the amounts of phosphate desorbed ranged between 61-77% and 67-81% by 0.01 M and 0.1 M NaOH, respectively. However, there were no statistically significant differences in desorption performance of adsorbents from the two greatest concentration solutions. Therefore, the exhausted adsorbents were then regenerated by 0.1 M NaOH for up to four sequences. The recycled BC-LDHs 6 significantly maintained their higher removal efficiency beyond 20 mg/g even after three consecutive cycles. In comparison with pure LDHs, they achieved noticeably lower adsorption capacity throughout the experiments. The regeneration study indicates the desirable suitability of BC-LDHs 6 to be utilized repeatedly without significant reduction in the adsorption capacity that will further improve its adsorption economy and possibility for the practical wastewater treatment application. Nonetheless, extensive investigations are required in order to establish optimal operational conditions for phosphate desorption on BC-LDHs 6, which will offer a great opportunity to effectively enhance the phosphate recovery efficiency of this composite.

Finally, seed germination and early growth assays of lettuce were employed for the evaluation of agronomic effectiveness of phosphate-loaded BC-LDHs 6 (P-BC-LDHs 6) in order to verify the

feasibility of using this composite after its usage in phosphate treatment as a fertilizer, and its performance was also compared to that of phosphate-adsorbed LDHs (P-LDHs). Of these two experiments, results from the former showed that aluminum contained in both samples diminished seed germination and seedling development. On the contrary, beneficial effects were obtained in the successive experiment. Lettuce was less sensitive toward aluminum because of the fact that the alkalinity of these materials would reduce the possibility of a high concentration of aluminum being stored in crops. Furthermore, it was found that high input of P-BC-LDHs 6 was reflected in best nutrient accumulation within plant tissues and their growth features, especially root characteristic, where its length was significantly improved by up to 45% in the treatment of 2.5% compared with that of the control. Moreover, P-BC-LDHs 6 also completely outperformed P-LDHs in stimulating plant productivity, by which all growth indices tested were enormously increased of up to 46%.

The fact that plants have distinct nutrient requirements at different growth stages and that differential metal tolerance also varies depending on plant species and growth stages were also the reasons for the contradictory P-BC-LDH 6 reaction on plant responses in both experiments. In this regard, it is important to know a certain concentration range, in which beneficial elements in the P-BC-LDHs 6 may become antagonistic with respect to its use as a fertilizer. The results of this study suggest that 2.5% of P-BC-LDHs 6 supplied under growing media or soil conditions was sufficient and produced positive advantages in horticultural plant development since this composite could improve nutrition and desirable conditions for lettuce growth. Indeed, based on characterization analyses, harmful substances were not detected in this material, ensuring their safe and sustainable use for agricultural purposes. However, future research should concentrate on assessing the possible mechanisms, by which P-BC-LDHs 6 influences various plant growth parameters, which will provide a more in-depth and nuanced insight into the application of this composite in phosphate fertilization practices. Additionally, longer term studies and evaluation under natural field conditions are required in order to validate its practical application.

Overall, not only will the transformation of used adsorbents into fertilizers provide a new pathway for phosphate recovery from contaminated water bodies, but it also offers an attractive strategy for environmental waste disposal and nutrient recycling in agricultural fields. The present study

provides a helpful guide for fabricating high-efficiency adsorbents and confirms that rice straw-derived biochar can be designed as promising and high value-added adsorbent materials for phosphate removal. Furthermore, post-adsorption products are able to offer an available source of essential nutrients for plants, which were validated to be advantageous in stimulating plant improvement.

References

- [1] Lee SY, Choi J-W, Song KG, Choi K, Lee YJ, Jung K-W. Adsorption and mechanistic study for phosphate removal by rice husk-derived biochar functionalized with Mg/Al-calcined layered double hydroxides via co-pyrolysis. *Compos Part B Eng* 2019;176:107209. doi:10.1016/j.compositesb.2019.107209.
- [2] Mustafa S, Zaman MI, Khan S. pH effect on phosphate sorption by crystalline MnO₂. *J Colloid Interface Sci* 2006;301:370–5. doi:10.1016/j.jcis.2006.05.020.
- [3] Duan, X., Evans DG. Layered double hydroxides. *Appl. Clay Sci.*, vol. 36, 2007, p. 103–21. doi:10.1016/j.clay.2006.06.010.
- [4] Kameda T, Yoshiok T. Hybrid inorganic/organic composites of layered double hydroxides intercalated with organic acid anions for the uptake of hazardous substances from aqueous solution. *Met Ceram Polym Compos Var Uses* 2011. doi:10.5772/17518.
- [5] Ulibarri MA, Hermosin MDC. Layered double hydroxides in water decontamination. In: Rives V, editor. *Layer Double Hydroxides Present Futur.*, vol. 66, New York: Nova Science Publishers; 2012, p. 37–9.
- [6] Yan L guo, Yang K, Shan R ran, Yan T, Wei J, Yu S jun, et al. Kinetic, isotherm and thermodynamic investigations of phosphate adsorption onto core-shell Fe₃O₄@LDHs composites with easy magnetic separation assistance. *J Colloid Interface Sci* 2015;448:508–16. doi:10.1016/j.jcis.2015.02.048.
- [7] Tan X, Liu Y, Zeng G, Wang X, Hu X, Gu Y, et al. Application of biochar for the removal of pollutants from aqueous solutions. *Chemosphere* 2015;125:70–85. doi:10.1016/j.chemosphere.2014.12.058.
- [8] Tan X, Liu S, Liu Y, Gu Y, Zeng G, Cai X, et al. One-pot synthesis of carbon supported calcined-Mg/Al layered double hydroxides for antibiotic removal by slow pyrolysis of biomass waste. *Sci Rep* 2016;6:1–12. doi:10.1038/srep39691.
- [9] Wang S, Gao B, Li Y, Ok YS, Shen C, Xue S. Biochar provides a safe and value-added solution for hyperaccumulating plant disposal: A case study of *Phytolacca acinosa* Roxb. (*Phytolaccaceae*). *Chemosphere* 2017;178:59–64. doi:10.1016/j.chemosphere.2017.02.121.
- [10] Adekiya AO, Agbede TM, Olayanju A, Ejue WS, Adekanye TA, Adenusi TT, et al. Effect of Biochar on Soil Properties, Soil Loss, and Cocoyam Yield on a Tropical Sandy Loam Alfisol. *Sci World J* 2020;2020. doi:10.1155/2020/9391630.

- [11] Zhang M, Riaz M, Zhang L, El-Desouki Z, Jiang C. Biochar induces changes to basic soil properties and bacterial communities of different soils to varying degrees at 25 mm rainfall: More effective on acidic soils. *Front Microbiol* 2019;10. doi:10.3389/fmicb.2019.01321.
- [12] Benício LPF, Silva RA, Lopes JA, Eulálio D, dos Santos RMM, De Aquino LA, et al. Layered double hydroxides: Nanomaterials for applications in agriculture. *Rev Bras Cienc Do Solo* 2015;39:1–13. doi:10.1590/01000683rbc20150817.
- [13] Touloupakis E, Margelou A, Ghanotakis DF. Intercalation of the herbicide atrazine in layered double hydroxides for controlled-release applications. *Pest Manag Sci* 2011;67:837–41. doi:10.1002/ps.2121.
- [14] Smit AL, Bindraban PS, Shroeder JJ, Conijin JG, G VDMH. Phosphorus in agriculture: global resources, trends and developments. Wageningen, Plant Res Int BV 2009;282:36.
- [15] UNESCO. The united nations world water development report 2018: Nature-based solutions for water. Unesco 2018:1–139.
- [16] Plum D, Xufei F. A rock and a hard place. *Int Water Power Dam Constr* 1996;48:30–3.
- [17] Marjolein de Ridder, Sijbren de Jong JP and SL. Risks and opportunities in the global phosphate rock market. Hague: The Hague Centre for Strategic Studies; 2012.
- [18] Volterra L, Boualam M, Menesguen A, Duguet JP, Duchemin J, Bonnefoy X. Eutrophication and health. 2002.
- [19] Janus LL, Vollenwelder RA. OECD Cooperative program on eutrophication 1981.
- [20] Richardson CJ, King RS, Qian SS, Vaithiyanathan P, Qualls RG, Stow CA. Estimating ecological thresholds for phosphorus in the Everglades. *Environ Sci Technol* 2007;41:8084–91. doi:10.1021/es062624w.
- [21] Carvalho L, McDonald C, de Hoyos C, Mischke U, Phillips G, Borics G, et al. Sustaining recreational quality of European lakes: Minimizing the health risks from algal blooms through phosphorus control. *J Appl Ecol* 2013;50:315–23. doi:10.1111/1365-2664.12059.
- [22] González EJ, Roldán G. Eutrophication and phytoplankton: Some generalities from lakes and reservoirs of the Americas. In: Vítová M, editor. *Microalgae*, Rijeka: IntechOpen; 2020. doi:10.5772/intechopen.89010.
- [23] Addy K, Green L. *Natural resources facts* 1996;4.
- [24] US Environmental Protection Agency. *Nutrient criteria technical guidance manual* 2000.
- [25] Michael RP, Boyce A and, Walsh G. Identification and evaluation of phosphorus recovery

- technologies in an Irish context. 2012.
- [26] Luengo C V., Volpe MA, Avena MJ. High sorption of phosphate on Mg-Al layered double hydroxides: Kinetics and equilibrium. *J Environ Chem Eng* 2017;5:4656–62. doi:10.1016/j.jece.2017.08.051.
- [27] Richard Sedlak. Phosphorus and nitrogen removal from municipal wastewater: Principals and practice. New York: The Soap and Detergent Association; 1991.
- [28] Xing L, Ren L, Tang B, Wu G, Guan Y. Dynamics of intracellular polymers in enhanced biological phosphorus removal processes under different organic carbon concentrations. *Biomed Res Int* 2013;2013. doi:10.1155/2013/761082.
- [29] Blackall LL, Crocetti GR, Saunders AM, Bond PL. A review and update of the microbiology of enhanced biological phosphorus removal in wastewater treatment plants. *Antonie Van Leeuwenhoek* 2002;81:681–91. doi:10.1023/A:1020538429009.
- [30] Zuthi MFR, Guo WS, Ngo HH, Nghiem LD, Hai FI. Enhanced biological phosphorus removal and its modeling for the activated sludge and membrane bioreactor processes. *Bioresour Technol* 2013;139:363–74. doi:10.1016/j.biortech.2013.04.038.
- [31] Chan Pacheco CR. Integrating enhanced biological phosphorus removal (EBPR) in a resource recovery scenario. Universitat Autònoma de Barcelona, 2019.
- [32] Welles L. Enhanced biological phosphorus removal: Metabolic insights and salinity effects. Delft University of Technology, 2016.
- [33] Setiadi W. Antimicrobial resistance in a membrane enhanced biological phosphorus removal process. University of British Columbia, 2018.
- [34] Tomei MC, Stazi V, Daneshgar S, Capodaglio AG. Holistic approach to phosphorus recovery from urban wastewater: Enhanced biological removal combined with precipitation. *Sustain* 2020;12. doi:10.3390/su12020575.
- [35] Lamb JC, Hill C. Biological phosphorus removal: Current status and future prospects 1984.
- [36] Kamika I, Coetzee M, Mamba BB, Msagati T, Momba MNB. The impact of microbial ecology and chemical profile on the enhanced biological phosphorus removal (EBPR) process: A case study of northern wastewater treatment works, Johannesburg. *Int J Environ Res Public Health* 2014;11:2876–98. doi:10.3390/ijerph110302876.
- [37] Menar AB, Jenkins D. Calcium phosphate precipitation in wastewater treatment. Washington, D.C.: United States Environmental Protection Agency; 1972.

- [38] Ruzhitskaya O, Gogina E. Methods for removing of phosphates from wastewater. *MATEC Web Conf* 2017;106:1–7. doi:10.1051/mateconf/201710607006.
- [39] Qin H. Investigation of direct-reduced iron as a filter media for phosphorus removal in wastewater applications 2019.
- [40] U.S. Environmental Protection Agency. Wastewater technology fact sheet chemical precipitation. *Environ Prot Agency* 2000:1–7.
- [41] Farzadkia M, Bazrafshan E. Lime stabilization of waste activated sludge. *Heal Scope* 2014;3:1–5. doi:10.17795/jhealthscope-16035.
- [42] Zarrouk SJ, McLean K. Chapter 5 - Advanced analytical pressure-transient analysis relevant to geothermal wells. In: Zarrouk SJ, McLean K, editors. *Geotherm. Well Test Anal.*, Academic Press; 2019, p. 89–111. doi:https://doi.org/10.1016/B978-0-12-814946-1.00005-0.
- [43] Pasarín MM. Phosphate adsorption onto laterite and laterite waste from a leaching process 2012.
- [44] Kumar PS, Korving L, van Loosdrecht MCM, Witkamp GJ. Adsorption as a technology to achieve ultra-low concentrations of phosphate: Research gaps and economic analysis. *Water Res X* 2019;4:100029. doi:10.1016/j.wroa.2019.100029.
- [45] Mitchell SM, Ullman JL. Removal of phosphorus, BOD, and pharmaceuticals by rapid rate sand filtration and ultrafiltration systems. *J Environ Eng* 2016;142:06016006. doi:10.1061/(asce)ee.1943-7870.0001137.
- [46] Luo X, Wang X, Bao S, Liu X, Zhang W, Fang T. Adsorption of phosphate in water using one-step synthesized zirconium-loaded reduced graphene oxide. *Sci Rep* 2016;6:1–13. doi:10.1038/srep39108.
- [47] Gu AZ, Saunders A, Neethling JB, Stensel HD, Blackall LL. Functionally relevant microorganisms to enhanced biological phosphorus removal performance at full-scale wastewater treatment plants in the United States. *Water Environ Res a Res Publ Water Environ Fed* 2008;80:688–98. doi:10.2175/106143008x276741.
- [48] Clark T, Stephenson T, Pearce PA. Phosphorus removal by chemical precipitation in a biological aerated filter. *Water Res* 1997;31:2557–63. doi:10.1016/S0043-1354(97)00091-2.
- [49] Zubair M, Ihsanullah I, Abdul Aziz H, Azmier Ahmad M, Al-Harathi MA. Sustainable wastewater treatment by biochar/layered double hydroxide composites: Progress, challenges, and outlook. *Bioresour Technol* 2021;319:124128. doi:10.1016/j.biortech.2020.124128.

- [50] Vithanage M, Ashiq A, Ramanayaka S, Bhatnagar A. Implications of layered double hydroxides assembled biochar composite in adsorptive removal of contaminants: Current status and future perspectives. *Sci Total Environ* 2020;737:139718. doi:10.1016/j.scitotenv.2020.139718.
- [51] Micháleková-Richveisová B, Frišták V, Pipíška M, Ďuriška L, Moreno-Jimenez E, Soja G. Iron-impregnated biochars as effective phosphate sorption materials. *Environ Sci Pollut Res* 2017;24:463–75. doi:10.1007/s11356-016-7820-9.
- [52] Wu H, Zhang H, Yang Q, Wang D, Zhang W, Yang X. Calcined chitosan-supported layered double hydroxides: An efficient and recyclable adsorbent for the removal of fluoride from an aqueous solution. *Materials (Basel)* 2017;10. doi:10.3390/ma10111320.
- [53] Cai P, Zheng H, Wang C, Ma H, Hu J, Pu Y, et al. Competitive adsorption characteristics of fluoride and phosphate on calcined Mg-Al-CO₃ layered double hydroxides. *J Hazard Mater* 2012;213–214:100–8. doi:10.1016/j.jhazmat.2012.01.069.
- [54] Iftekhhar S, Küçük ME, Srivastava V, Repo E, Sillanpää M. Application of zinc-aluminium layered double hydroxides for adsorptive removal of phosphate and sulfate: Equilibrium, kinetic and thermodynamic. *Chemosphere* 2018;209:470–9. doi:10.1016/j.chemosphere.2018.06.115.
- [55] Prasad C, Tang H, Liu W. Magnetic Fe₃O₄ based layered double hydroxides (LDHs) nanocomposites (Fe₃O₄/LDHs): recent review of progress in synthesis, properties and applications. *J Nanostructure Chem* 2018;8:393–412. doi:10.1007/s40097-018-0289-y.
- [56] Xu ZP, Stevenson G, Lu CQ, Lu GQ. Dispersion and size control of layered double hydroxide nanoparticles in aqueous solutions. *J Phys Chem B* 2006;110:16923–9. doi:10.1021/jp062281o.
- [57] Zhang M, Gao B, Yao Y, Inyang M. Phosphate removal ability of biochar/MgAl-LDH ultra-fine composites prepared by liquid-phase deposition. *Chemosphere* 2013;92:1042–7. doi:10.1016/j.chemosphere.2013.02.050.
- [58] Zhang Z, Yan L, Yu H, Yan T, Li X. Adsorption of phosphate from aqueous solution by vegetable biochar/layered double oxides: Fast removal and mechanistic studies. *Bioresour Technol* 2019;284:65–71. doi:10.1016/j.biortech.2019.03.113.
- [59] He H, Zhang N, Chen N, Lei Z, Shimizu K, Zhang Z. Efficient phosphate removal from wastewater by MgAl-LDHs modified hydrochar derived from tobacco stalk. *Bioresour*

- Technol Reports 2019;8:100348. doi:10.1016/j.biteb.2019.100348.
- [60] Wan S, Wang S, Li Y, Gao B. Functionalizing biochar with Mg–Al and Mg–Fe layered double hydroxides for removal of phosphate from aqueous solutions. *J Ind Eng Chem* 2017;47:246–53. doi:https://doi.org/10.1016/j.jiec.2016.11.039.
- [61] Meili L, Lins P V, Zanta CLPS, Soletti JI, Ribeiro LMO, Dornelas CB, et al. MgAl-LDH/Biochar composites for methylene blue removal by adsorption. *Appl Clay Sci* 2019;168:11–20. doi:https://doi.org/10.1016/j.clay.2018.10.012.
- [62] Li S, Dong L, Wei Z, Sheng G, Du K, Hu B. Adsorption and mechanistic study of the invasive plant-derived biochar functionalized with CaAl-LDH for Eu(III) in water. *J Environ Sci (China)* 2020;96:127–37. doi:10.1016/j.jes.2020.05.001.
- [63] Tan X fei, Liu Y guo, Gu Y ling, Liu S bo, Zeng G ming, Cai X, et al. Biochar pyrolyzed from MgAl-layered double hydroxides pre-coated ramie biomass (*Boehmeria nivea* (L.) Gaud.): Characterization and application for crystal violet removal. *J Environ Manage* 2016;184:85–93. doi:10.1016/j.jenvman.2016.08.070.
- [64] Buates J, Imai T. Biochar functionalization with layered double hydroxides composites: Preparation, characterization, and application for effective phosphate removal. *J Water Process Eng* 2020;37:101508. doi:10.1016/j.jwpe.2020.101508.
- [65] Fidel RB, Laird DA, Spokas KA. Sorption of ammonium and nitrate to biochars is electrostatic and pH-dependent. *Sci Rep* 2018;8:1–10. doi:10.1038/s41598-018-35534-w.
- [66] Park JH, Ok YS, Kim SH, Cho JS, Heo JS, Delaune RD, et al. Evaluation of phosphorus adsorption capacity of sesame straw biochar on aqueous solution: influence of activation methods and pyrolysis temperatures. *Environ Geochem Health* 2015;37:969–83. doi:10.1007/s10653-015-9709-9.
- [67] Greenberg AE, Clesceri LS, Eaton AD. Phosphorus. *Stand. Methods Exam. Water Wastewater* 18th Ed. 1992, Washington: American Public Health Association; 1992, p. 4.108-4.117.
- [68] Sing KSW, Haul RAW, Pierotti RA, Siemieniewska T. Reporting physisorption data for gas/solid systems with special reference to the determination of surface area and porosity. *Pure Appl Chem* 1985;57:603–19.
- [69] Starukh GM, Oranska OI, Levytska SI. Reconstruction of calcined Zn-Al layered double hydroxides during tetracycline adsorption. *Odesa Natl Univ Herald Chem* 2015;20:82–93.

- doi:10.18524/2304-0947.2015.3(55).56248.
- [70] Triantafyllidis KS, Peleka EN, Komvokis VG, Mavros PP. Iron-modified hydrotalcite-like materials as highly efficient phosphate sorbents. *J Colloid Interface Sci* 2010;342:427–36. doi:10.1016/j.jcis.2009.10.063.
- [71] Peng X, Yan Z, Cheng X, Li Y, Wang A, Chen L. Quaternary ammonium-functionalized rice straw hydrochar as efficient adsorbents for methyl orange removal from aqueous solution. *Clean Technol Environ Policy* 2019;21:1269–79. doi:10.1007/s10098-019-01703-2.
- [72] Alagha O, Manzar MS, Zubair M, Anil I, Mu'azu ND, Qureshi A. Comparative adsorptive removal of phosphate and nitrate from wastewater using biochar-MgAl LDH nanocomposites: Coexisting anions effect and mechanistic studies. *Nanomaterials* 2020;10. doi:10.3390/nano10020336.
- [73] Cui Q, Jiao G, Zheng J, Wang T, Wu G, Li G. Synthesis of a novel magnetic: Caragana korshinskii biochar/Mg-Al layered double hydroxide composite and its strong adsorption of phosphate in aqueous solutions. *RSC Adv* 2019;9:18641–51. doi:10.1039/c9ra02052g.
- [74] Xie Q, Li Y, Lv Z, Zhou H, Yang X, Chen J. Effective adsorption and removal of phosphate from aqueous solutions and eutrophic water by Fe-based MOFs of MIL-101 2017:1–15. doi:10.1038/s41598-017-03526-x.
- [75] Mahmood T, Saddique MT, Naeem A, Westerhoff P, Mustafa S, Alum A. Comparison of different methods for the point of zero charge determination of NiO. *Ind Eng Chem Res* 2011;50:10017–23. doi:10.1021/ie200271d.
- [76] Bakatula EN, Richard D, Neculita CM, Zagury GJ. Determination of point of zero charge of natural organic materials. *Environ Sci Pollut Res* 2018;25:7823–33. doi:10.1007/s11356-017-1115-7.
- [77] Rey C, Combes C, Drouet C, Grossin D. Bioactive ceramics: Physical chemistry. In: Ducheyne P, editor. *Compr. Biomater.*, Oxford: Elsevier; 2011, p. 187–221. doi:https://doi.org/10.1016/B978-0-08-055294-1.00178-1.
- [78] Lucena GL, De Lima LC, Honório LMC, De Oliveira ALM, Tranquilim RL, Longo E, et al. CaSnO₃ obtained by modified Pechini method applied in the photocatalytic degradation of an azo dye. *Ceramica* 2017;63:536–41. doi:10.1590/0366-69132017633682190.
- [79] Lǔ J, Liu H, Liu R, Zhao X, Sun L, Qu J. Adsorptive removal of phosphate by a nanostructured Fe-Al-Mn trimetal oxide adsorbent. *Powder Technol* 2013;233:146–54.

- doi:10.1016/j.powtec.2012.08.024.
- [80] Li R, Wang JJ, Zhou B, Awasthi MK, Ali A, Zhang Z, et al. Enhancing phosphate adsorption by Mg/Al layered double hydroxide functionalized biochar with different Mg/Al ratios. *Sci Total Environ* 2016;559:121–9. doi:10.1016/j.scitotenv.2016.03.151.
- [81] Awual MR, Jyo A, El-Safty SA, Tamada M, Seko N. A weak-base fibrous anion exchanger effective for rapid phosphate removal from water. *J Hazard Mater* 2011;188:164–71. doi:10.1016/j.jhazmat.2011.01.092.
- [82] Awual MR. Efficient phosphate removal from water for controlling eutrophication using novel composite adsorbent. *J Clean Prod* 2019;228:1311–9. doi:10.1016/j.jclepro.2019.04.325.
- [83] Tomar V, Kumar D. A critical study on efficiency of different materials for fluoride removal from aqueous media. *Chem Cent J* 2013;7:1. doi:10.1186/1752-153X-7-51.
- [84] Awual MR, Yaita T, Kobayashi T, Shiwaku H, Suzuki S. Improving cesium removal to clean-up the contaminated water using modified conjugate material. *J Environ Chem Eng* 2020;8:103684. doi:10.1016/j.jece.2020.103684.
- [85] Jiang D, Chu B, Amano Y, Machida M. Removal and recovery of phosphate from water by Mg-laden biochar: Batch and column studies. *Colloids Surfaces A Physicochem Eng Asp* 2018;558:429–37. doi:10.1016/j.colsurfa.2018.09.016.
- [86] Mi X, Li G, Zhu W, Liu L. Enhanced adsorption of orange II using cationic surfactant modified biochar pyrolyzed from cornstalk. *J Chem* 2016;2016. doi:10.1155/2016/8457030.
- [87] Cheung CW, Porter JF, McKay G. Elovich equation and modified second-order equation for sorption of cadmium ions onto bone char. *J Chem Technol Biotechnol* 2000;75:963–70.
- [88] Mezenner NY, Bensmaili A. Kinetics and thermodynamic study of phosphate adsorption on iron hydroxide-eggshell waste. *Chem Eng J* 2009;147:87–96. doi:10.1016/j.cej.2008.06.024.
- [89] Kumar D, Gaur JP. Chemical reaction- and particle diffusion-based kinetic modeling of metal biosorption by a *Phormidium* sp.-dominated cyanobacterial mat. *Bioresour Technol* 2011;102:633–40. doi:10.1016/j.biortech.2010.08.014.
- [90] Xu Q, Chen Z, Wu Z, Xu F, Yang D, He Q, et al. Novel lanthanum doped biochars derived from lignocellulosic wastes for efficient phosphate removal and regeneration. *Bioresour Technol* 2019;289:121600. doi:10.1016/J.BIORTECH.2019.121600.
- [91] Yan H, Chen Q, Liu J, Feng Y, Shih K. Phosphorus recovery through adsorption by layered

- double hydroxide nano-composites and transfer into a struvite-like fertilizer. *Water Res* 2018;145:721–30. doi:10.1016/j.watres.2018.09.005.
- [92] Li M, Liu J, Xu Y, Qian G. Phosphate adsorption on metal oxides and metal hydroxides: A comparative review. *Environ Rev* 2016;24:319–32. doi:10.1139/er-2015-0080.
- [93] Yang F, Zhang S, Sun Y, Tsang DCW, Cheng K, Ok YS. Assembling biochar with various layered double hydroxides for enhancement of phosphorus recovery. *J Hazard Mater* 2019;365:665–73. doi:10.1016/j.jhazmat.2018.11.047.
- [94] Vikrant K, Kim KH, Ok YS, Tsang DCW, Tsang YF, Giri BS, et al. Engineered/designer biochar for the removal of phosphate in water and wastewater. *Sci Total Environ* 2018;616–617:1242–60. doi:10.1016/j.scitotenv.2017.10.193.
- [95] Ibrahim EH, Tajuddin NA, Hamzah N. Synthesis and characterization of alkali free Mg-Al layered double hydroxide for transesterification of waste cooking oil to biodiesel: Effect of Mg-Al ratio. *Int J Eng Technol* 2019;7:154–7. doi:10.14419/ijet.v7i4.14.27518.
- [96] Zhang M, Gao B, Fang J, Creamer AE, Ullman JL. Self-assembly of needle-like layered double hydroxide (LDH) nanocrystals on hydrochar: Characterization and phosphate removal ability. *RSC Adv* 2014;4:28171–5. doi:10.1039/c4ra02332c.
- [97] Ownby M, Desrosiers DA, Vaneeckhaute C. Phosphorus removal and recovery from wastewater via hybrid ion exchange nanotechnology: a study on sustainable regeneration chemistries. *Npj Clean Water* 2021;4:1–8. doi:10.1038/s41545-020-00097-9.
- [98] Gulyas A, Genc S, Can ZS, Semerci N. Phosphate recovery from sewage sludge supernatants using magnetic nanoparticles. *J Water Process Eng* 2020:101843. doi:10.1016/j.jwpe.2020.101843.
- [99] Luo Y, Liu M, Chen Y, Wang T, Zhang W. Preparation and regeneration of iron-modified nanofibres for low-concentration phosphorus-containing wastewater treatment. *R Soc Open Sci* 2019;6. doi:10.1098/rsos.190764.
- [100] Sun J, Xiu YF, Huang K, Yu JT, Alam S, Zhu HM, et al. Selective recovery of phosphorus from acid leach liquor of iron ore by garlic peel adsorbent. *RSC Adv* 2018;8:22276–85. doi:10.1039/c8ra03203c.
- [101] Pitakteeratham, Niti; Hafuka, Akira; Satoh, Hisashi; Watanabe Y. High efficiency removal of phosphate from water by zirconium sulfate-surfactant micelle mesostructure immobilized on polymer matrix. *Water Res* 2020;47:3583–90.

doi:<https://doi.org/10.1016/j.watres.2013.04.006>.

- [102] Maiti, Bidinger. Phosphate adsorption onto granular ferric hydroxide (GFH) for wastewater reuse. *J Chem Inf Model* 1981;53:1689–99.
- [103] Zach-Maor A, Semiat R, Shemer H. Adsorption–desorption mechanism of phosphate by immobilized nano-sized magnetite layer: Interface and bulk interactions. *J Colloid Interface Sci* 2011;363:608–14. doi:<https://doi.org/10.1016/j.jcis.2011.07.062>.
- [104] Ajmal Z, Muhmood A, Usman M, Kizito S, Lu J, Dong R, et al. Phosphate removal from aqueous solution using iron oxides: Adsorption, desorption and regeneration characteristics. *J Colloid Interface Sci* 2018;528:145–55. doi:10.1016/j.jcis.2018.05.084.
- [105] Azimzadeh Y, Najafi N, Reyhanitabar A, Oustan S, Khataee A. Effects of phosphate loaded LDH-biochar/hydrochar on maize dry matter and P uptake in a calcareous soil. *Arch Agron Soil Sci* 2020;0:1–16. doi:10.1080/03650340.2020.1802012.
- [106] Yan H, Chen Q, Liu J, Feng Y, Shih K. Phosphorus recovery through adsorption by layered double hydroxide nano-composites and transfer into a struvite-like fertilizer. *Water Res* 2018;145:721–30. doi:10.1016/j.watres.2018.09.005.
- [107] Food and Agricultural Organization of the United Nations. Procedures for soil analysis. Wageningen: International Soil Reference and Information Center; 2002.
- [108] Dias MAN, Obara FEB, Arruda N, Cursi PR, Gonçalves NR, Christoffoleti PJ. Germination test as a fast method to detect glyphosate-resistant sourgrass. *Bragantia* 2015;74:307–10. doi:10.1590/1678-4499.0089.
- [109] Morrison DA, Morris EC. Pseudoreplication in experimental designs for the manipulation of seed germination treatments. *Austral Ecol* 2000;25:292–6. doi:10.1046/j.1442-9993.2000.01025.x.
- [110] Sanchez PL, Chen M kuang, Pessaraki M, Hill HJ, Gore MA, Jenks MA. Effects of temperature and salinity on germination of non-pelleted and pelleted guayule (*Parthenium argentatum* A. Gray) seeds. *Ind Crops Prod* 2014;55:90–6. doi:10.1016/j.indcrop.2014.01.050.
- [111] Katembe WJ, Ungar IA, Mitchell JP. Effect of salinity on germination and seedling growth of two *Atriplex* species (Chenopodiaceae). *Ann Bot* 1998;82:167–75. doi:10.1006/anbo.1998.0663.
- [112] Pauzaitė G, Malakauskienė A, Nauciene Z, Zukiene R, Filatova I, Lyushkevich V, et al. Changes in Norway spruce germination and growth induced by pre-sowing seed treatment with cold plasma and electromagnetic field: Short-term versus long-term effects. *Plasma*

- Process Polym 2018;15. doi:10.1002/ppap.201700068.
- [113] Raipure PA V, Dhande AP. Design of control system for measurement of pH and EC of fertilizer solution 2015:2290–6.
- [114] Masís-Meléndez F, Segura-Chavarría D, García-González CA, Quesada-Kimsey J, Villagra-Mendoza K. Variability of physical and chemical properties of TLUD stove derived biochars. *Appl Sci* 2020;10:1–20. doi:10.3390/app10020507.
- [115] Luo Y, Wu L, Liu L, Han C, Li Z. Heavy metal contamination and remediation in Asian agricultural land. *Natl Institutes Agro-Environmental Sci* 2009;1(1):1–9.
- [116] Lehmann J, Joseph S. *Biochar for environmental management: Science, technology and implementation*. Taylor & Francis; 2015.
- [117] Chibueze F. U, E. A, Kingsley N A, Nnanna A. L, Nwokocha J. N, Ekekwe D N. Appraisal of heavy metal contents in commercial inorganic fertilizers blended and marketed in nigeria. *Am J Chem* 2012;2:228–33. doi:10.5923/j.chemistry.20120204.07.
- [118] Nursyamsi D., Osaki M., Tadano T. Effect of aluminum on plant growth, phosphorus and calcium uptake of tropical rice (*Oryza sativa*), maize (*Zea mays*), and soybean (*Glycine max*). *Indones J Agric Sci* 2000;1:51–62. doi:10.21082/ijas.v1n2.2000.p51-62.
- [119] Malik B, Pirzadah TB, Tahir I, Hakeem KR, Rather IA, Sabir JSM, et al. Lead and aluminium-induced oxidative stress and alteration in the activities of antioxidant enzymes in chicory plants. *Sci Hortic (Amsterdam)* 2020:109847. doi:10.1016/j.scienta.2020.109847.
- [120] Tammam AA, Khalil SM, E. Hafez E, M. Elnagar A. Impacts of aluminum on growth and biochemical process of wheat plants under boron treatments. *Curr Agric Res J* 2018;6:300–19. doi:10.12944/carj.6.3.09.
- [121] Osman HE, Al-Jabri M, El-Ghareeb DK, Al-Maroi YA. Impact of aluminum and zinc oxides on morphological characters, germination, metals accumulation and DNA in fenugreek (*Trigonella foenum-graecum*). *J Saudi Soc Agric Sci* 2020. doi:10.1016/j.jssas.2020.09.004.
- [122] Dixon M, Simonne E, Obreza T, Liu G. Crop response to low phosphorus bioavailability with a focus on tomato. *Agronomy* 2020;10:1–26. doi:10.3390/agronomy10050617.
- [123] Ramzi E, Asghari A, Khomari S, Chamanabad HM. Determination of aluminum stress tolerance threshold during seed germination of wheat. *J Plant Physiol Breed* 2016;6:19–30.
- [124] Scheffer-Basso SM, Prior BC. Aluminum toxicity in roots of legume seedlings assessed by

- topological analysis. *Acta Sci - Agron* 2015;37:61–8. doi:10.4025/actasciagron.v37i1.18362.
- [125] Silva P, Matos M. Assessment of the impact of Aluminum on germination, early growth and free proline content in *Lactuca sativa* L. *Ecotoxicol Environ Saf* 2016;131:151–6. doi:10.1016/j.ecoenv.2016.05.014.
- [126] Brito DS, Neri-Silva R, Ribeiro KVG, Peixoto PHP, Ribeiro C. Effects of aluminum on the external morphology of root tips in rice. *Rev Bras Bot* 2020;43:413–8. doi:10.1007/s40415-020-00620-9.
- [127] Shetty R, Prakash NB. Effect of different biochars on acid soil and growth parameters of rice plants under aluminium toxicity. *Sci Rep* 2020;10:1–10. doi:10.1038/s41598-020-69262-x.
- [128] Singh NB, Yadav K, Amist N. Phytotoxic effects of aluminium on growth and metabolism of *Pisum sativum* L. *Int J Innov Biol Chem Sci* 2011;2:10–21.
- [129] Eisenmenger WS. Toxicity of aluminum on seedlings and action of certain ions in the elimination of the toxic effects 1935;10.
- [130] Neenu S, Karthika KS. Aluminium toxicity in soil and plants. *Har Dhara* 2019;2:15–9.
- [131] Macedo CEC, Jan VVS. Effect of aluminum stress on mineral nutrition in rice cultivars differing in aluminum sensitivity 2008;12:363–9.
- [132] Sotta Machado J, Steiner F, Zoz T, Bento Honda G, Leminski Neto de Oliveira B. Effects of aluminum on seed germination and initial growth of physic nut seedlings. *J Neotrop Agric* 2015;02:24–31. doi:10.32404/rean.v2i1.248.
- [133] Wenzl P, Mayer JE, Rao IM. Aluminum stress inhibits accumulation of phosphorus in root apices of aluminum-sensitive but not aluminum-resistant *Brachiaria* cultivar. *J Plant Nutr* 2002;25:1821–8. doi:10.1081/PLN-120006059.
- [134] Cavusoglu K, Kabar K. Effects of hydrogen peroxide on the germination and early seedling growth of barley under NaCl and high temperature stresses. *EurAsian J Biosci* 2010;79:70–9. doi:10.5053/ejobios.2010.4.0.9.
- [135] Nguyen TTN, Xu CY, Tahmasbian I, Che R, Xu Z, Zhou X, et al. Effects of biochar on soil available inorganic nitrogen: A review and meta-analysis. *Geoderma* 2017;288:79–96. doi:10.1016/j.geoderma.2016.11.004.
- [136] Mukherjee A, Lal R. The biochar dilemma. *Soil Res* 2014;52:217–30. doi:10.1071/SR13359.
- [137] Jahan N, Zhang Y, Lv Y, Song M, Zhao C, Hu H, et al. QTL analysis for rice salinity

- tolerance and fine mapping of a candidate locus qSL7 for shoot length under salt stress. *Plant Growth Regul* 2020;90:307–19. doi:10.1007/s10725-019-00566-3.
- [138] Bojorquez-Quintal E, Escalante-Magaña C, Echevarría-Machado I, Martínez-Estévez M. Aluminum, a friend or foe of higher plants in acid soils. *Front Plant Sci* 2017;8:1–18. doi:10.3389/fpls.2017.01767.
- [139] Merino-Gergichevich C, Alberdi M, Ivanov AG, Reyes-Díaz M. Al³⁺-Ca²⁺ interaction in plants growing in acid soils: Al-phytotoxicity response to calcareous amendments. *J Soil Sci Plant Nutr* 2010;10:217–43.
- [140] Gentili R, Ambrosini R, Montagnani C, Caronni S, Citterio S. Effect of soil pH on the growth, reproductive investment and pollen allergenicity of ambrosia artemisiifolia l. *Front Plant Sci* 2018;9:1–12. doi:10.3389/fpls.2018.01335.
- [141] Liang JF, An J, Gao JQ, Zhang XY, Song MH, Yu FH. Interactive effects of biochar and AMF on plant growth and greenhouse gas emissions from wetland microcosms. *Geoderma* 2019;346:11–7. doi:10.1016/j.geoderma.2019.03.033.
- [142] Kerkeni L, Ruano P, Delgado LL, Picco S, Villegas L, Tonelli F, et al. Biochar and soil physical health. *Intech* 2016:13.
- [143] Chen H, Yang X, Wang H, Sarkar B, Shaheen SM, Gielen G, et al. Animal carcass- and wood-derived biochars improved nutrient bioavailability, enzyme activity, and plant growth in metal-phthalic acid ester co-contaminated soils: A trial for reclamation and improvement of degraded soils. *J Environ Manage* 2020;261. doi:10.1016/j.jenvman.2020.110246.
- [144] Benicio LPF, Eulálio D, de Moura Guimarães L, Pinto FG, Da Costa LM, Tronto J. Layered double hydroxides as hosting matrices for storage and slow release of phosphate analyzed by stirred-flow method. *Mater Res* 2018;21. doi:10.1590/1980-5373-mr-2017-1004.
- [145] Chen L, Chen Q, Rao P, Yan L, Shakib A, Shen G. Formulating and optimizing a novel biochar-based fertilizer for simultaneous slow-release of nitrogen and immobilization of cadmium. *Sustain* 2018;10. doi:10.3390/su10082740.
- [146] Shen R, Jian Feng Ma. Distribution and mobility of aluminium in an Al-accumulating plant, *Fagopyrum esculentum* Moench. *J Exp Bot* 2001;52:1683–7. doi:10.1093/jxb/52.361.1683.
- [147] Trupiano D, Coccozza C, Baronti S, Amendola C, Vaccari FP, Lustrato G, et al. The effects of biochar and its combination with compost on lettuce (*Lactuca sativa* L.) growth, soil properties, and soil microbial activity and abundance. *Int J Agron* 2017;2017.

doi:10.1155/2017/3158207.

- [148] Soti PG, Jayachandran K, Koptur S, Volin JC. Effect of soil pH on growth, nutrient uptake, and mycorrhizal colonization in exotic invasive *Lygodium microphyllum*. *Plant Ecol* 2015;216:989–98. doi:10.1007/s11258-015-0484-6.
- [149] Venkatesan S, Jayaganesh S. Characterisation of magnesium toxicity, its influence on amino acid synthesis pathway and biochemical parameters of tea. *East* 2009;3:101–12. doi:10.3923/rjphyto.2010.234.241.
- [150] Huh Y, Jang S, Choo Y, Chung S, Kim Y. Basic tests of pH and EC probes for automatic real time nutrient control in protected crop production. 15th Int. Conf. Precis. Agric., International Society of Precision Agriculture; 2014.
- [151] Batista EMCC, Shultz J, Matos TTS, Fornari MR, Ferreira TM, Szpoganicz B, et al. Effect of surface and porosity of biochar on water holding capacity aiming indirectly at preservation of the Amazon biome. *Sci Rep* 2018;8:1–9. doi:10.1038/s41598-018-28794-z.
- [152] Maher M, Prasad M, Raviv M. Organic soilless media components. In: Raviv M, Lieth JH, editors. *Soil. Cult.*, Amsterdam: Elsevier; 2008, p. 459–504. doi:https://doi.org/10.1016/B978-044452975-6.50013-7.
- [153] Buates J, Imai T. Assessment of plant growth performance and nutrient release for application of phosphorus-loaded layered double hydroxides as fertilizer. *Environ Technol Innov* 2021;22:101505. doi:10.1016/j.eti.2021.101505.
- [154] Buates J, Imai T. Application of Biochar Functionalized with Layered Double Hydroxides: Improved Plant Growth Performance after Use as Phosphate Adsorbent. *Appl Sci* 2021;11:6489. doi:10.3390/app11146489.
- [155] Salomao R, Milena LM, Wakamatsu MH, Pandolfelli VC. Hydrotalcite synthesis via co-precipitation reactions using MgO and Al(OH)₃ precursors. *Ceramics International* 2011; 37: 3063-3070. doi.org/10.1016/j.ceramint.2011.05.034.

Appendices

Appendix A. Physicochemical characteristics of rice straw used in this study

Table A1. Chemical and physical properties of rice straw

	Characteristics	Rice straw
pH		6.66
Proximate analysis (wt.%, dry basis)	Moisture content	5.83
	Ash content	12.64
	Volatile matter content	73.26
	Fixed carbon content (by difference)	8.27
Elemental analysis (wt.%, dry basis)	Carbon	39.38
	Hydrogen	5.55
	Nitrogen	0.95
	Oxygen (by difference)	41.48
	H/C ratio	1.68
	O/C ratio	0.79
Textural properties	BET surface area (m ² /g)	1.54
	Total pore volume (cm ³ /g)	0.01
	Average pore diameter (nm)	26.74

Appendix B. Determination of optimal conditions for synthesis of BC-LDHs by using the second technique

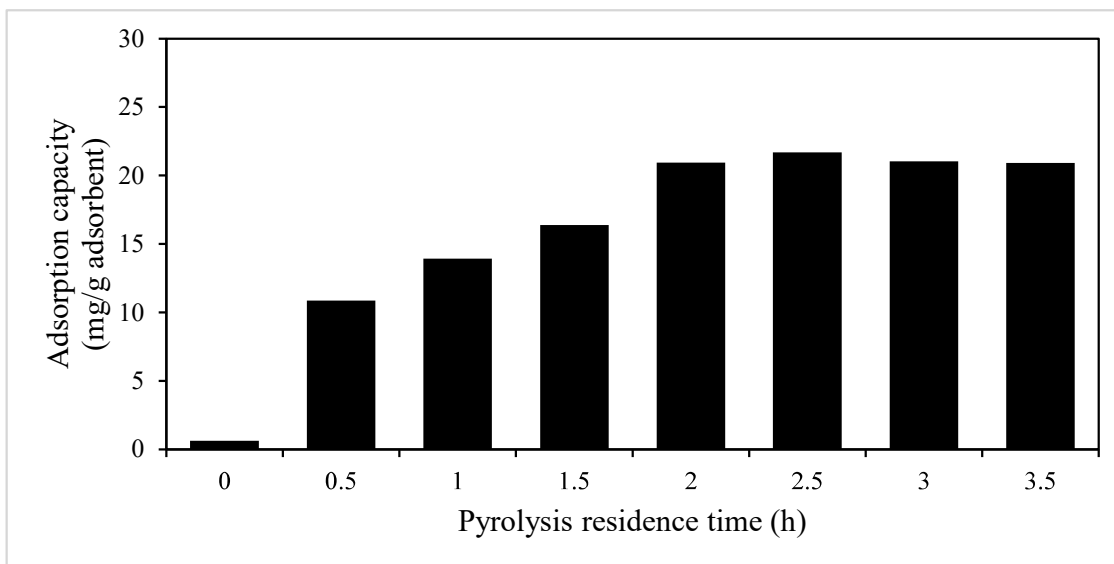


Figure B1. Effect of pyrolysis residence time on phosphate adsorption of BC-LDHs

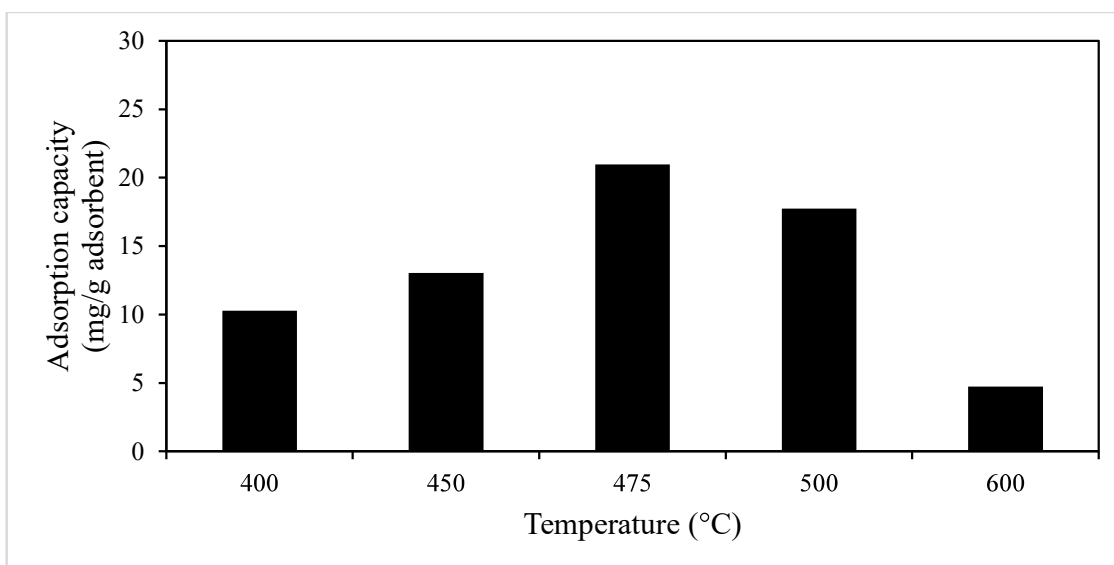


Figure B2. Effect of pyrolysis temperature on phosphate adsorption of BC-LDHs

Appendix C. List of equations used in the study

Table C1. Kinetic and isotherm models and other equations used in this study

Equations	Description
<p>Adsorption capacity</p> $q_e = \frac{V(C_i - C_e)}{M}$	<p>q_e: adsorption capacity (mg/g)</p> <p>R: removal efficiency (%)</p> <p>C_i: initial concentration of phosphate solution (mg/L)</p>
<p>Removal efficiency</p> $R = \frac{(C_i - C_e)}{C_i} \times 100$	<p>C_e: final concentration of phosphate solution (mg/L)</p> <p>V: volume of phosphate solution (L)</p> <p>M: mass of adsorbent (g)</p>
<p>Desorption efficiency</p> $D = \frac{q_{des}}{q_e} \times 100$	<p>D: desorption efficiency (%)</p> <p>q_{des}: amount of phosphate desorbed in solution (mg/g)</p>
<p>Kinetic models:</p> <p>Pseudo-first-order</p> $\ln(q_e - q_t) = \ln q_e - k_1 t$	<p>k_1: pseudo-first-order rate constant (1/h)</p> <p>k_2: pseudo-second-order rate constant (g/mg/h)</p> <p>q_t: adsorption capacity at time t (mg/g)</p>
<p>Pseudo-second-order</p> $\frac{t}{q_t} = \frac{1}{k_2 q_e^2} + \frac{t}{q_e}$	<p>q_e: adsorption capacity at equilibrium (mg/g)</p> <p>α: rate of chemisorption at zero coverage (mg/g/h)</p> <p>β: extent of surface coverage and activation energy for chemisorption (g/mg)</p>
<p>Elovich model</p> $q_t = \frac{1}{\beta} \ln \alpha \beta + \frac{1}{\beta} \ln t$	<p>k_i: intraparticle diffusion rate constant</p> <p>C: intercept</p>
<p>Intraparticle diffusion</p> $q_t = k_i t^{0.5} + C$	<p>t: time (h)</p>
<p>Isotherm models:</p> <p>Langmuir</p> $q_e = \frac{K_L Q_m C_e}{1 + K_L C_e}$	<p>K_L: Langmuir bonding term related to interaction energies (L/mg)</p> <p>K_F: Freundlich affinity coefficient ((mg/g)(L/mg)^{1/n})</p> <p>Q_m: Langmuir maximum capacity (mg/g)</p>
<p>Freundlich</p> $q_e = K_F C_e^{\frac{1}{n}}$	<p>C_e: phosphate concentration at equilibrium (mg/L)</p> <p>n: Freundlich linearity constant</p>

